# Response to the Reviews

We would like to thank all three anonymous referees for their challenging, but constructive comments that helped considerably improving the manuscript. The referees pointed to the need for a more representative title, improved clarity in text and figures, including a separate discussion section, additional comparison of some model estimates with observations and literature beyond what is already presented, and additional analyses for the justification of some conclusions, in several instances harmoniously. We agree with most comments, and followed the suggestions of the referees as documented below, but we believe some of the suggested extensions require more elaborate analysis than can be included here. As now more prominently placed in the introduction, the objectives of the current study are; *i*)exemplifying the integration of a fully dynamic physiological regulation model in a 3D framework for the first time to the best of our knowledge, and (now with the additional analysis), gaining some first insight into the relevance of acclimation *ii*) evaluating the skill of the new model system at various spatial and temporal scales, which requires consideration of an extremely diverse array of observation sets. These objectives lead to a wide scope, and generation of a number of research questions that are better treated separately.

We have a remark relevant to all three referees, therefore placed once again here: upon further examination of our model simulation presented in our original manuscript, we found out that the performance of the hydrodynamical model could be improved by not specifying the momentum fluxes at the open boundaries, and a re-parameterization of the bottom friction. We also realized that, due to a wrong configuration file, the atmospheric nitrogen deposition was not correctly registered during the model initialization in the simulation presented in the original manuscript. A new simulation run for the entire simulation period with the improvements in hydrodynamical model and inclusion of atmospheric nitrogen deposition results in better model performance overall, although not qualitatively affecting our conclusions based on the original manuscript. Therefore, in the revised version of the manuscript, we presented the results obtained with this new simulation run.

## Referee #1

*Title: I have two problems with the title: 1) as the acclimatisation scheme has been published previously, I would advise against using the word 'novel'; 2) 'implementation' suggests the presentation and discussion of how the acclimatisation method is implemented in the biogeochemical model, which is included in the manuscript, but not related to the application to the SNS. So I would suggest reformulating to, eg., The application of an acclimative biogeochemical model to the southern North Sea.*
We would like to thank the referee for this careful observation and thoughtful suggestions. We changed the title to 'The acclimative biogeochemical model of the southern North Sea'.

*Structure: The authors should introduce a separate discussion section.*
A separate discussion section was included in the revised manuscript.

*Comparison: In comparing model results with observations, the text is too qualitative, using expressions such as 'compare well', 'reasonable match', and so on, without defining what these are. This should be tightened up and quantified throughout. The same holds for comparison with previous work in the literature: a small subset of earlier biogeochemical modelling work is referenced, and it is suggested that the current model performs better, but without providing the evidence and quantifying the differences. It is also unclear why these studies were selected, and not others.*

More precise formulations were used throughout the revised text for the evaluation of the model. Moreover, the correlation coefficients and normalized bias values for the biogeochemical variables are additionally presented in a color-coded table with colors indicating model performance, such that at least the internal consistency can be improved. When referring to literature, we attempted to cover most recent work on the modelling of a relevant model domain. In the revised version, we included a few additional relevant work. A detailed and precise comparison of the performance of our model with other models is not in the scope of our study: such a comparison requires a dedicated effort with standardized benchmarking data and tools as mentioned in the discussion.

*Logic/interpretation: The logic and interpretation tend to be hand-waving at best, flawed in some cases, and don't always consider multiple options. Examples are listed in the details section below. This needs to be improved. Separating the discussion will help.*
In the revised manuscript, the discussion section was separated and in many cases, interpretations were extended and supported by additional material (please see the '**List of All Relevant Changes**' at the end of our response letter).

*Is it really 'better'? The authors state at several points in the paper that their acclimative phytoplankton growth method is better what's used in more traditional biogeochemical models. However, unfortunately, they fail to provide any proof of this. In the very least, there should be an in-depth, quantified discussion comparing the current results with those of a suitably wide range of 'traditional' models.*
As explained above, we did not intend to claim that our model performs better than the others, and mentioned in the manuscript that such would require some dedicated effort and is out of the scope of the current work. As also explained in the relevant discussion, different methodologies and datasets used in different studies make even a qualitative comparison difficult. However, we still claim that the estimates for chlorophyll 'can argued to be at least comparable' to those of the earlier studies. We leave however the final judgment to the reader.

*I get the impression from the manuscript that the 'novel' biogeochemical model was constructed by stripping an existing 'traditional' biogeochemical model of the relevant parts, and replacing these with the acclimative methods. If this is indeed the case, the authors would strengthen the manuscript immensely by providing and discussing a comparison with a similar run with the earlier model version.*
Referee #3 also suggested a comparison with a non-acclimative model version. We did not start from a traditional model and upgrade to an acclimative one, so we do not have such an earlier model version. However, in the revised version, two alternative parameterizations of the non-acclimative version of the model was considered (explained in appendix B3), and the resulting horizontal (Fig.14) and vertical (Fig.B4) distributions were compared with those of the full model.

*The authors will also need to discuss the following in a systematic way. More traditional biogeochemical models may lack (to various extents depending on the model) the full suite of acclimatisation as presented here, but they make up for that at least to some extent by representing several types of phytoplankton. This allows for spatial and temporal changes/patterns in phytoplankton composition. One could argue that the new model reflects this with one type with a range of traits, but it presumably has more flexibility in changing these traits over time for the same biomass than could happen in nature (one type of plankton can not change into another).*
The plankton functional type (PFT) models might make up for the unrepresented acclimation processes to some extent, but we are not aware of any study which tested this idea rigorously. We do not really see why our model is presumably more flexible than reality: consider the case of the competition of two species, where the first species, dominant at the beginning, is being gradually

replaced by the second until it completely vanishes by the end of the experiment. Throughout this plausible experiment, representation of the traits may completely change, possibly without considerable changes in total biomass. A hypothetically perfect simulation of this experiment by our model in terms of biomass and the average trait representation in the system, might seem to suggest that one plankton type changed into another, which is however just an interpretation and not a limitation inherent to our approach. In conclusion, a comparison of the intracellular Chl:C:N:P ratios observed, e.g., in chemostat experiments, and estimations by a PFT model and our acclimation model might provide valuable insights in this direction, however such a comparison would be beyond the scope of the current study. Nevertheless, in the new discussion section, we discuss how the PFT models may represent some physiological acclimation.

*Also, the authors are suggesting that they plan the inclusion of additional phytoplankton types. That would require curtailing the ranges of acclimatisation. Would that throw the baby out with the bath water, or have they already done so and would this be an attempt to get it back in?*
The plastic response simulated by our model can already be seen at the species level as shown by Wirtz and Kerimoglu (2016). Introduction of further plankton groups for resolving other ecophysiological traits such as silicate limitation and edibility will also allow taxa-specific parameterization of resource utilization traits, which is expected to further improve the representation spatio-temporal distribution of the overall cellular composition of the phytoplankton. This is further discussed in the new discussion section.

*Figures: Not all of the figures are clearly readable, and some information is missing.*
*Fig 3: I suspect that the colour scale is truncated, both at the high and low end, resulting in artificial saturation of the figure. This must be addressed. Also this figure would benefit from using a wider range of colours.*
The scale was truncated (from the lower range) on purpose, as doing so helps emphasizing the salinity front. This is now mentioned in the caption of the figure. We also used the color scheme used in also other contour plots and discrete color levels to facilitate comparing the location of certain value ranges in the measured and simulated data.

*Fig 4. S and T are partly obscured by the dots, the cursive eta and n are barely visible on my printout*
In the revised version, the spacing between labels and markers were increased, the text annotation were moved outside the scatter plots, larger font size were used and layout was changed to a single-column format for better visibility and reduced space requirement.

*Fig 5-7. These are all too small. I can hardly read the axis legends and legends. Names on maps are cluttered.*
The plots were improved by 1) using larger fonts, 2) carrying the text annotation outside the panels 3) and reworking the maps, such that names do not overlap.

*Fig 8. Does ICES store chlorophyll? If so it would help if this were included.*
Referee #2 raised the same question. We included chlorophyll in the figure.

*Fig 9. Re-plot in colour. I can't work out the route taken from the cruise track figure.*
We re-plotted the Figure in color. Moreover, we used 'cumulative distance' as the position indicator for a more accurate representation of spatial scales.

*Fig 10, 11, 14. The black contours are partially obscured by the dark blue.*
In the revised version we used light-gray contour lines for all contour plots.

*Fig 11. I understand that these are surface values. Please also provide the bottom values.*
The winter concentrations of DIN and DIP at the bottom are almost identical to the values at the surface, which is now indicated in the revised manuscript. In this plot, we now provided the growing season averages due to their relevance.

*Fig. 12. The colour scale is symmetrical around the centre, making it impossible to distinguish spring and autumn values. Please re-plot.*
This figure was removed from the revised manuscript.

*Grammar and language: Please check the grammar. There are quite a few anomalies that even a grammar checker would pick up (I'm not going to list them all). Also use past tense to describe the results throughout.*
We attempted to improve the language throughout the text.

*Further detailed comments*
*p. 8 - l. 6. Other explanations could be that: 1) the river-runoff is too high, or 2) the set of open boundary conditions used for the hydrodynamics and disolved components restricts the amount of flushing, leading to an accumulation of fresh water, nutrients, etc. Or a combination. Please discuss.*
We thank the referee for this insightful comment. As explained at the beginning of this response letter, we found out not specifying the momentum fluxes led to a better representation of the tidal dynamics, hence, the residual currents and as a consequence, spatial distribution of salinity and other transported variables. Accordingly, such a critical discussion is not necessary anymore.

*p. 9 - Fig 4. There seems to be a 1:1 relationship, but with an anomaly on top. Does the anomaly in T correspond to the low values of S that bend away from the 1:1 line? Does this cluster represent a particular geographic area (front?)? Or a particular event/year (2010?)?*
Now a 1:1 line is included in the scatter plots. In the new model run, that deviation from the 1:1 relationship is largely resolved. We found out that a majority of these events are located within the western portion of the model domain, as indicated in the text.

*p. 15 - l. 29-34. This seems a rediculous over-interpretation of a potential contribution by estuarine overturning circulation. There's no evidence of overall higher nutrient concs in bottom waters (fig 8). Providing bottom values in fig 11 will likely support this. What's happening is that the nutrient-rich riverine waters enter/mix with the coastal waters, which are trapped by the coastal density(salinity) front.*
The dynamic effect of horizontal density gradients on residual transport of particulate organic matter, which we refer to, is a known feature of shallow, tidal seas, as elaborated in detail with observational and modelling approaches in the cited literature. However the referee is right, that the estuarine-type circulation does not explain the gradients during winter. We therefore updated our interpretation accordingly. Realizing also that nutrient concentrations during growing season is more important for the discussion of the chlorophyll gradients, we now expanded this figure by including the growing-season nutrient concentrations, and mention the estuarine-type circulation as a passing reference.

*p. 17 - l. 9-12. This is an unfair comparison. The observations in fig 5 are instantaneous, whereas the satellite composites are 3-monthly averaged. It's obvious that the satellite values presented in this way should be lower! This statement requires a proper*

*comparison.*
Both other referees raised relevant questions. This sentence was actually based on such a point-to-point comparison of the raw satellite (not-averaged) and station data, which revealed a bias in the form of low concentrations by the satellite data (Fig. R1 in our earlier response letter). However, upon a contact with one of the leading researchers of the Ocean Color Climate Change Initiative, Dr. Shubha Sathyendranath, we were informed that a newer version (v.3.1) of the dataset was recently published, which is particularly improved with respect to the coastal waters with complex optical properties. Furthermore, we were also informed that bias estimates are available for chlorophyll. Therefore in the revised version of the manuscript, this more suitable and bias-corrected product was used, estimates of which agrees with the station data better than the earlier version, although some deviations still exist (Fig.R1). Moreover, the upper range of chlorophyll concentrations predicted by the updated simulation is now much lower than the older model version. As a result of the improvements in both the observation dataset and simulations, the comparison is much better (Fig.R2 below shows the match for the early and later growing season as were shown in the previous version of the manuscript. Fig.12 in the revised manuscript shows the match for non-growing (months 1-3,10-12) and growing (months 4-9) seasons, for the sake of presenting the full annual coverage, but the skill scores for the early and late growing seasons, as well as for the annual average are shown in the new Table 1. There are however still systematic deviations, which are discussed in the text, now with a more balanced account of source of errors.

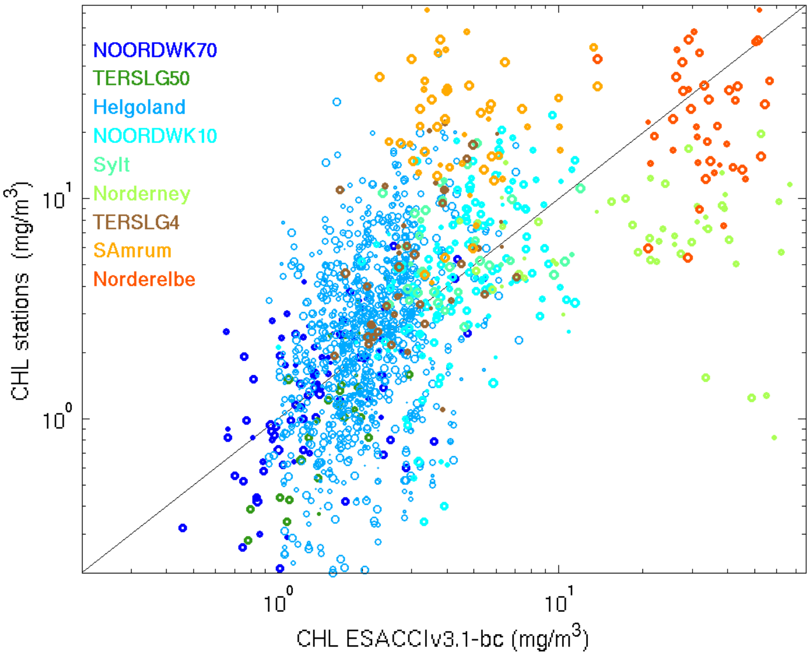

**Fig. R1**: Chlorophyll concentrations measured at the stations (x-axis) vs. estimated by the Ocean Color v.3.1 product.

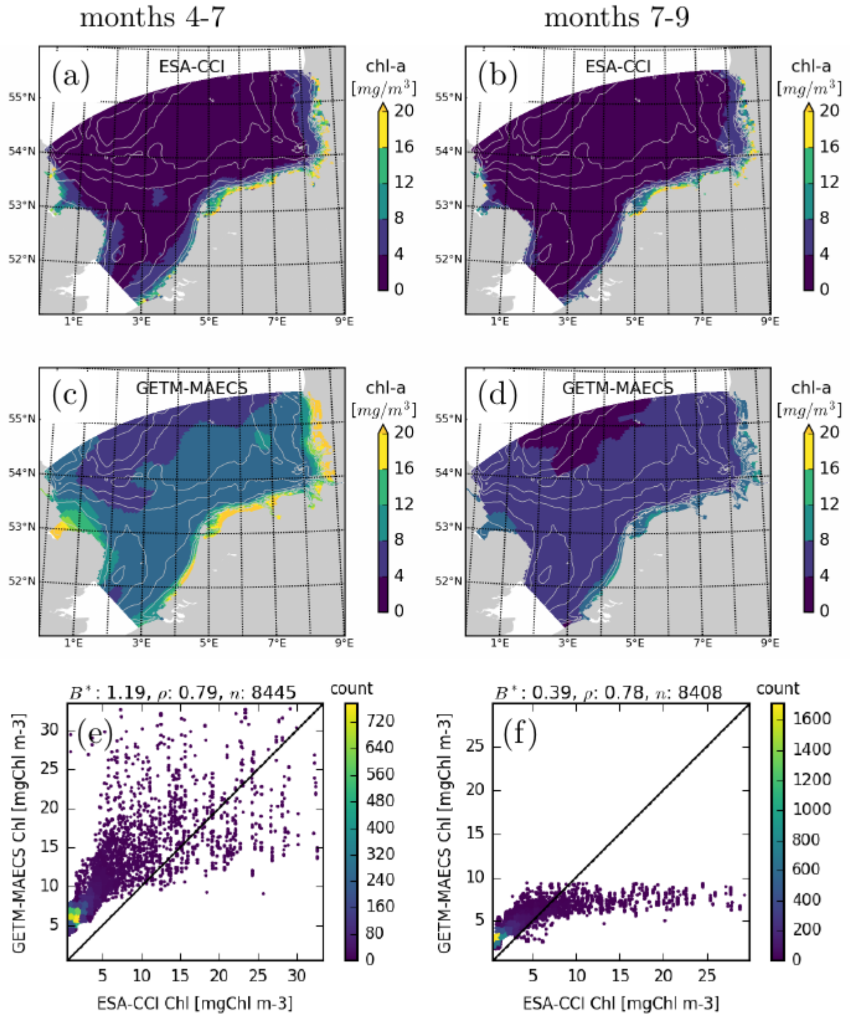

**Fig. R2**: as in Figure 12 in the revised text, but for months 4-6 and 7-9. Comparison of satellite (ESA-CCI, a,b) and MAECS (c,d) estimates of surface chlorophyll concentrations averaged over 2008-2010 and for different seasonal intervals of the year. 2-D histograms (e,f) show the number of occurrence of simulation-satellite data pairs. Gray lines in a-d show the isobaths. Normalized bias (B*), Pearson correlation coefficients (ρ), and corresponding number of data points (n) are shown on top of scatter plots.

Minor issues:

*p. 1 - l. 1. autotroph: autotrophic?*

A: Done

*p. 1 - l. 5. is based on novel concepts*

A: Replaced with ‘based on a set of novel concepts’

*p. 1 - l. 11 ’sparce measurements’. Not clear what these are.*

A: Expanded.

*p. 1 - l. 13. delete prevalently*

A: Done

*p. 1 - l. 14 shows significant seasonal and spatial variability*

A: Entire sentence was modified.

*p. 1 - l. 14-16. not clear what is meant here*

A: The sentence was expanded.

*Section 2.1, title. ’Data’ can originate from anywhere, including models. Use ’Observations’, apply throughout.*

A: Done

*p. 2 - l. 18 monitoring stations used here(?)*

A: Done

*p. 3 - l. 11 in the benthos*

A: Done

*p. 3 - l. 14 and rivers considered*

A: Done

*p. 3 - l. 19 accessory: access to?*

A: Entire sentence was reworded

*p. 3 - l. 24 give value for flexibility constant. Give rang of i, and values for q_i*

A: Done

*p. 3 - l. 29 why use 'B' for phytoplankton (most models use P, and B for bacteria)?*

A: Symbols were chosen to keep the notation consistent with Wirtz and Kerimoglu 2016.

*p. 8 - l. 15 Now the rivers do come up, but the sentence is unclear, and I don't understand the link to grid resolution.*

A: This sentence was removed, as with the updated model version, the discussion became obsolete.

*p. 8 - l. 18. Trends. These figures are not suitable to identify trends.*

A: Here the intention is not to identify trends, but we are merely pointing to the fact that there are no 'obvious' trends, which we believe is important to mention, as generation of trends by the model could have been indicative of problems regarding the balance of source-sink terms and/or flawed fluxes at the open boundaries.

*p. 8 - l. 19. 'in general well reproduced': this too qualitative, I list it here to present an example, but the paper is littered with these kinds of statements (I will not list them all).*

A: removed.

*p. 8 - l. 20/21. 'rather realistically represented': another one.*

A: removed.

p. 9 - l. 2-3. this should be easy to test?

A: Elaboration of various assumptions regarding the composition of organic loads desires a study on its own.

*p. 9 - l. 5. Earlier. Than what?*

A: The sentence continues: 'replenishment of phosphrous relative to nitrogen'.

*p. 9 - l. 5. 'mostly well reproduced': difficult to see on the small graphs; quantify.*

A: These section is re-written.

*p. 9 - l. 6. 'probably'. other potential causes?*

A: This is what we think is the most likely explanation. There are other potential causes, but a discussion of them all is not likely to be beneficial.

*p. 9 - l. 10. 'is entirely reversed': I don't see this…*

A: This discussion was removed from the revised manuscript.

*p. 9 - l. 11-p10 - l. 3: this is discussion*

A: moved to the new discussion section.

*p. 11 - l. 1. 'easier': than what?*

A: sentence was removed

*p. 11 - l. 3. variability matches very well: I don't see this/quantify.*

A: Quantified.

*p. 11 - l. 6. 'might be': why?*

A: Sentence was removed.

*p. 11 - l. 8. 'typical': give numbers*

A: Numbers greatly vary, and depend on the processing (eg., binning, as mentioned in the discussion) so giving specific numbers would be misleading.

p. 14 - l. 2. grammatically incorrect.

A: Corrected

*p. 15 - l. 6. 'were not able to ... observations': but this model doesn't do this, either…*

A: We do not agree with this comment. The referee should note that the emphasis here is the diversity of the deep chlorophyll structures, and the fact that our model can reproduce this diversity.
*p. 15 - l. 6-13. Please provide evidence for this.*
A: A new appendix section (B2) is now included to provide evidence for this paragraph.
*p. 15 - l. 28. 'intuitively predictable': this is a contradiction in terms.*
A: Sentence was removed
*p. 16 - l. 8-p17 l. 5: It's not very clear what the function and message of this section are.*
A: Considering quite a number of additions to the manuscript, we indeed decided to remove this discussion.
*p. 17 - l. 7. higher chlorophyll concentrations*
A: Done
*p. 17 - l. 13-14. this sentence trips over the various averages. Reformulate/clarify.*
A: we reworded the sentence.
*p. 18 - l. 8. nutrient and turbidity gradients?*
A: the turbidity gradients are aligned with, therefore oppose the observed chlorophyll gradient (high at the coastal zone). Therefore the main driver should be high nutrient concentrations.
p. 19 - l. 11-14. Please provide evidence for this.
A: This section was re-written.
*p. 20 - l. 5. ignorance of: ignoring*
A: Done.
*fig 2. Fe-P is not in the figure. Explain bAP in the caption.*
A: Done.
*fig 4. delete 'abbreviated' (2x)*
A: Done.
*fig 5. Observations (circles) and model estimates (lines) ... correlation coefficients (r),... data points (n)*
A: Done.
*Fig 10, 11, 14. Specify what the black contour lines represent.*
A: Done
*fig 13. Mention that this is a log scale. Explain rho and eta.*
A: Done

**Referee #2**

*- The time series comparison of chlorophyll results with in-situ data suggest that chlorophyll concentrations are systematically over-predicted in spring at many monitoring stations. The validation plots with in-situ data are only presented for other model variables and not for chlorophyll.*
The updated model (please see the preamble of the response letter) predicts lower spring blooms in all problematic stations. The Referee #1 also pointed to the need to include the chlorophyll in the validation plots. We included chlorophyll from the ICES dataset in validation plots.

*- The validation with satellite data shows also that chlorophyll is systematically overpredicted throughout the model domain during spring. The authors conclude that the satellite data are wrong. This is not supported by any comparison with in-situ data, but the above comparison with time series suggests that the model over-predicts chlorophyll in spring.*
This is an issue mentioned by both other referees. As we responded to the Referee#1 above, a comparison of the raw satellite data (v.2.0) with station data clearly revealed a bias (Fig.R1 in our previous response letter). The updated (v.3.1) and bias-corrected product agrees better with the station data especially at the upper range (Fig.R1). Moreover, as mentioned above, chlorophyll

estimates of the updated model are also much lower now. Overall, the updated model and updated data set suggest a much better agreement now (Fig.R2 for the early and late growing seasons as previously shown in the manuscript, and Fig.12 for the newly chosen non-growing and the entire growing season in the manuscript). Comparison of the model and satellite estimates do not any longer point to an overestimation problem at the upper range but at the rather lower range, which we discuss in the manuscript.

*- It is unclear what trait effects are included in the model, which are not included in existing models. On page 4, line 20 a few traits are listed (very brief) but in the discussion at page 15 and 17 other effects are mentioned, such as effects on chlorophyll to carbon ratio and sinking rates.*
Model description in section 2.2.1 is extended with explanations of the novel and relevant aspects of the model.

*- A critical discussion of the novel aspects of the phytoplankton model is lacking. For example: are the chlorophyll to carbon ratios in spring in a realistic range for spring conditions? How do sinking rates change over the year and how does that relate to observations?*
The agreement between the coastal pattern displayed by the chlorophyll to carbon ratios estimated by the model and that reported by Alvarez-Fernandez and Riegman (2014) was already pointed out in the manuscript, but we now refer to the values and show that the estimations by the model are in a realistic range. In the new Appendix B2, we show the average sinking rates estimated at the surface and bottom layer of the model (Fig.B3), and compare these values with literature.

*- There is no validation of the light climate (as Kd) included in the manuscript. This would be helpful in explaining differences between the model and observed data.*
The largest source of errors for the representation of the light climate in our study is already known: shading by suspended particulate matter (SPM) was incorporated as a climatological model forcing, which has a rather coarse horizontal resolution (about 20km), and does not represent the vertical heterogeneities as well as inter-annual and sub-daily variations. Therefore, a through evaluation of the light field should encompass various spatio-temporal scales, which is therefore better treated in a separate study, possibly dedicated to improving the representation of the light climate. However, we recognize that the issue is relevant for the spatial distribution of the chlorophyll concentrations and chlorophyll:carbon ratios, which is one of the core findings of this study, therefore we included a new appendix section (B1) where we compared the attenuation of the downwelling irradience estimated by the satellite product and by the model. Moreover, at one station (Noordwijk-10), where the model estimates for chlorophyll are particularly biased and poorly correlated with the observations, we compare the measured SPM concentrations with those from the static forcing dataset and mention these results in the discussion.

*Specific comments:*
*-Page 4, line 20 and equation 1. This part needs to give a complete list of acclimation effects included in the model. It should also describe in words how it works. Like it is written on page 17: " sinking speed of algae in MAECS is inversely related to nutrient quota of cells.". So there are not only effects of nutrients on growth rate (as suggested by eq 1) but also on other aspects. And there are effects of light on chlorophyll to carbon ratio. And does a flexibility constant represent?*
In the revised manuscript, the novel aspects of the model are now explained in the main text. Considering its relevance, description of sinking as a function of nutrient quotas was moved from the appendix to the Section 2.2.1. Please see below for the particular case of sinking speed-nutrient quota relationship.

*- Page 5, caption of Figure 2 mentions Fe-P:P adsorbed in iron-phosphorus complexes. I don't see*

*this in the figure. Or you should refer to bAP in the caption.*
Corrected.

*- Page 7: Could you please clarify in more detail the source of the ESA-CCI dataset. Is there a website where these data can be downloaded and where we can find validation reports of this dataset?*
We have included the requested additional information in the revised version. Validation reports are available on-line from the provided website.

*- Figure 4: the T and S are too small to read and overlap with the dots.*
A: Larger fonts were used, layout was changed for better visibility and spacing between the markers the labels were adjusted.

*- Page 9, line 10. I don't see that the classical seasonal pattern of phosphorus is entirely reversed in the data. This may be partly due to the small size of the figure. But also it may be that phosphorus concentrations in shallow muddy areas of the Wadden Sea are higher during the summer than during winter due to release of phosphorus from anoxic sediments. This does not reverse the seasonal pattern, because there is a classical drop in phosphorus concentrations during the spring bloom*
We removed the discussion of this issue from the revised manuscript, considering the increasing relevance of other issues.

*- Page 9: line 15: "potentially inadequate description of certain processes". Here a more thorough discussion of model functioning is needed. Now the validation data is more critically discussed than the model. I would expect that at location with a measurement frequency of several weeks to months, there is not much smoothing effect in monthly averages. Anyway such effect cannot explain structural differences between model and in-situ data, as shown in Figure 5a: DIN is consistently underpredicted and DIP overpredicted by the model.*
In the revised manuscript, the limitations of the model are discussed more systematically in the new discussion section. However, some of the issues pointed out in the previous version such as this discussion about the success of model at this particular station lost their relevance, partially due to the better model performance, but also considering the amount and weight of the new material included in the manuscript.

*- Page 10, Figure 5: the Pearson coefficients in the figures are too small to read. It would be clearer to present them in a table.*
The text annotations (now including the normalized bias) were moved outside the panels with a larger font size. These numbers are additionally presented in a color-coded table (Table 1), where the colors indicate the skill level.

*- Page 13, Figure 8: Please also include similar figures for chlorophyll. Chlorophyll is the only model variable that is relevant to judge the validity of the novel modeling approach.*
We included chlorophyll in the analysis.

*- Page 15, lines 5 – 13. The reader has no information to judge whether the sinking speeds in MAECS are more realistic than in other models. I would expect that the variability in the physical model underlying the ecosystem model is the main driver of vertical variability in phytoplankton concentrations. I don't see any information to convince me that "intracellular regulation of nutrient storages and pigmentory material" plays any role in this.*
We did not intend to claim that the sinking speeds in MAECS are more realistic than other models,

and full assessment of such a claim is again beyond the scope of the current study. We argued however, that the formation of thin chlorophyll layers is captured better than some other recent modelling attempts, citing one of those as an example. The reproduction of these structures is sensitive to the dependency of sinking rates on nutrient quotas, which is now supported by Fig.B4a. Description of this dependency in our model is based on earlier literature as was previously described in the appendix, but now in Section 2.2.1 of the revised manuscript. As also mentioned there, similar relationships have been employed in previous work. The quoted sentence is based on the fact that the internal quotas in our model scheme is affected by the allocation of resources to light harvesting (as proxied by pigmentory material) and nutrient acquisition (as proxied by nutrient stores), although we recognize that the sentence was possibly misleading, therefore we expanded it (relevant paragraph is now in the discussion section). Moreover, comparisons of the vertical phytoplankton concentrations with a model with quota-independent sinking rates (Fig.B4a), and two fixed-trait (i.e., non-acclimative) parameterizations (Fig.B4c) now provide evidence for this paragraph.

*- Page 17, lines 3-5. This is not an entirely open question. There are some interesting papers about this effect, such as: Burson, Amanda, et al. "Unbalanced reduction of nutrient loads has created an offshore gradient from phosphorus to nitrogen limitation in the North Sea." Limnology and Oceanography (2016) and references therein.*
Realizing that spatio-temporal variations in the N:P ratios requires more detailed elaboration, we decided to remove the figure (previously Fig.12) that was relevant to this comment. However, we still refer to this interesting phenomena, and refer to the relevant paper pointed out by the referee.

*- Page 17, line 10: If you use a data source for validation of the model you cannot conclude that the data are wrong instead of the model. Also the reason that some in-situ measurements in Figure 5 are above 50 is not valid. Figure 5 shows that the majority of the in-situ data is well below 50. So to make a fair comparison between in-situ data and satellite data, you should compare the seasonal averages, also at the offshore stations.*
Although we agree that our sentence here was misleading, the 'bias' implied in this sentence was based on a pointwise comparison of the in-situ data with the satellite estimates (Fig.R1 in the previous response letter). Nevertheless, such tedious discussion will not be necessary in the revised version. With the newer satellite product more suitable for the coastal waters (Fig. R1 above)and the updated model, the comparison now is much metter (see also Fig. R2 above for the periods considered in the previous version)

*- Page 17: lines 13 – 18. Here you only compare patterns in chlorophyll-c ratios with literature, but not the actual ranges. The numbers in Figure 14 are too small to read so I cannot judge whether the overprediction in chlorophyll in spring (figure 13) is caused by too much phytoplankton biomass or too high chlorophyll to carbon ratios.*
The over-prediction was caused by high phytoplankton concentrations, which is largely resolved in the new model run while the range of chlorophyll to carbon concentrations remains the same, which is between 0.015-0.045 gChl/gC for the seasonal averages as shown in this figure. We improved the clarity of this figure (now Fig.13, previously Fig.14) by using larger font sizes and discrete color levels and adding the previously omitted units.

*- Page 20: Lines 3 – 4. This is an interesting conclusion, but it is not well supported by the results presented in this paper.*
In the revised version, the new Fig.14 now provides direct evidence for the stronger gradients in phytoplankton concentrations in the acclimative model in comparison to the fixed-trait parameterizations (described in appendix B3), and how these gradients are further strengthened by

the higher chlorophyll:carbon ratios at the turbid, coastal sites.

*Technical comments*
*The text is too small to read in most figures.*
In the renewed figures larger font sizes were used, and layouts were changed for better visibility.

**Referee #3**

*1) Model formulation: The authors consider a grazing rate function of prey biomass whatever the phytoplankton species represented. There are potential issues with this hypothesis as Phaeocystis colonies (that can dominate the spring bloom in some of the coastal stations of the studied area) is not grazed by copepods. This should be modified or/and discussed.*
Our model indeed does not resolve the differences between phytoplankton taxa. Extension of the model at this stage to resolve such differences is not feasible. In the new discussion section, we extensively discuss the limitations of the model, including the necessity of resolving the ecological traits of various plankton groups, such as the grazing resistance of *Phaeocystis.*

*2) Model validation: In general, the model reasonably well reproduced available data. However, it is not clear which criteria is used to determine when observed data are realistically represented or not (e.g. p9 L1). This needs to be clarified.*
Referee #1 also raised concerns about subjective statements regarding the assessment of the model skill. Now the performance metrics are explicitly referred to, correlation coefficient and relative bias (now provided also for the station comparisons). Moreover, the new Table 1, listing the skill scores for DIN, DIP and chlorophyll for all stations and ices data is color-coded, where the colors indicate model skill.

*3) Model exploitation: The mechanistic description of the regulation of phytoplankton composition is pointed as an important process and an improvement compared to other existing models to correctly describe primary producers but also nutrient cycling. However, this is not directly evidenced in the paper based on model results. A comparison of results obtained with and without taking into account for these processes is needed to support this conclusion.*
Referee #1 also suggested a comparison with a non-acclimative version. In the revised manuscript, we considered a model with fixed-trait parameterizations (appendix B3) and compared the horizontal (Fig.14) and vertical distributions (Fig.B4c) resulting from this model with those from the fully acclimative one.

*Specific comments:*
*Figure 4: legend 'T' and 'S' on the dots: not clear*
The spacing between labels and markers were adjusted and larger font sizes were used

*P9 L1: How determine 'realistic' and 'not realistic' results ? (see general comment 2)*
As explained above, by often referring explicitly to the skill scores, and providing the color-coded table we at least hope to have improved the internal consistency for evaluating the model performance.

*P15 L6-8: This is an important result and could be developed and evidenced based on model results (Figure with different parameterization of under-water light climate and sinking rate of phytoplankton for example).*
The suggested sensitivity runs were performed and reported (appendix B2,Fig.B4)

*Figure 12: Why N:P variability of model results is always lower than the one observed?*
Considering the increasing content of the manuscript, and realizing that the variability in N:P requires a more detailed elaboration, we decided to leave this topic out.

*P17 L10-11: This is not so clear for me: Fig 5 also shows an important overestimation of simulated Chl a compared to observation.*
Both other referees raised similar questions about this issue. As can be seen in Fig.R2 above, the agreement between the satellite and model estimates is much improved. The improvement was a result of 1) lower chlorophyll concentrations estimated by the updated model; 2) using a newer version of the satellite product (v3.1 instead of v2.0), which is more suitable for coastal waters with complex optical properties, and indeed shows a better agreement with the station data (Fig. R1). Moreover, at many stations in Fig.5, chlorophyll estimates are also lower by the updated model.

*P 18 L5: The variability of Chl:C can also partly result from the overestimation of Chl a in the model (see previous comment).*
A similar concern was raised by the Referee #2 too. With the updated model results, we obtained lower chlorophyll concentrations overall, although the degree of variability in Chl:C ratios was not affected.

*P20 L 3-10: This should be evidenced based on comparison of two simulations (with and without taking account for photoacclimation) (see general comment 3)*
In the revised version of the manuscript, we considered a fixed-trait (non-acclimative) model (appendix B3), and compare the horizontal and vertical distributions.

## List of All Relevant Changes

1. With the approval of Editor, Rolf Riethmüller was included as a co-author.
2. Simulation results were repeated with an updated model:
   i. more realistic bottom roughness parameterization (constant, $z_0$=1mm) was employed.
   ii. at the open ocean boundaries, only the surface heights were nudged, while the momentum fluxes were relaxed.
   iii. configuration for atmospheric deposition fluxes were fixed.
3. A figure was removed (formerly Fig.12).
4. A new figure (Fig.14) was introduced.
5. A new table is included for summarizing model skill scores.
6. A new Discussion section was included.
7. A new appendix section (B), with 3 subsections were included:
   i. (B1): validation of light climate, (includes 2 new figures, B1,2).
   ii. (B2): phytoplankton sinking, (includes 2 new figures, B3,4) .
   iii. (B3): description of the non-acclimative model version .
8. A newer version of the ESA CCI-oceancolor data was used in Fig. 12 (which formerly used to be Fig.13).
9. In Fig.9, ‘cumulative distance’ is used instead of the ‘cast-id’ in the previous version and the figure was colored.
10. Layout of Fig.4, Fig.8, Fig.10 were changed for better visibility and overall consistency.
11. In Figures 3,4,8,9 color scheme was changed for improved overall consistency.
12. 2 new panels were added both to Fig.10 (March and October values) and Fig.11 (averages for months 4-9).

# The acclimative biogeochemical model of the southern North Sea

Onur Kerimoglu[1], Richard Hofmeister[1], Joeran Maerz[1,2], Rolf Riethmüller[1], and Kai W. Wirtz[1]

[1]Institute of Coastal Research, Helmholtz-Zentrum Geesthacht, Geesthacht, Germany
[2](present) Max Planck Institute for Meteorology, Hamburg, Germany

*Correspondence to:* Onur Kerimoglu (kerimoglu.o@gmail.com)

**Abstract.** Ecosystem models often rely on heuristic descriptions of ~~autotroph~~ autotrophic growth that fail to reproduce various stationary and dynamic states of phytoplankton cellular composition observed in laboratory experiments. Here, we present the integration of an advanced phytoplankton growth model within a coupled 3-dimensional physical-biogeochemical model, and the ~~implementation~~ application of the model system to the Southern North Sea (SNS) defined on a relatively high resolution ($\sim$ 1.5-4.5 km) curvilinear grid. The autotrophic growth model, recently introduced by Wirtz and Kerimoglu (2016), is ~~built up~~ based on a set of novel concepts for the allocation of internal resources and operation of cellular metabolism. The coupled model system consists of the general estuarine transport model (GETM) as the hydrodynamical driver, a lower trophic level model and a simple sediment diagenesis model. We force the model system with realistic atmospheric and riverine fluxes, background turbidity caused by suspended particulate matter and open ocean boundary conditions. For a simulation for the period 2000-2010, we show that the model system satisfactorily reproduces the physical and biogeochemical states of the system within the German Bight characterized by steep salinity, nutrient and chlorophyll gradients, as inferred from comparisons against observation data from long-term monitoring stations, sparse in-situ measurements, continuous transects, and ~~remote sensing data. In particular, the model shows high skill both in coastal and off shore waters, and captures the steep gradients in nutrient and chlorophyll concentrations observed prevalently across the coastal transition zone. We show that the~~ satellites. The model displays skill also in capturing the formation of thin chlorophyll layers at the pycnocline, frequently observed within the stratified regions during summer. A sensitivity analysis reveals that the vertical distributions of phytoplankton concentrations estimated by the model can be qualitatively sensitive to the description of the light climate and dependence of sinking rates on the internal nutrient reserves. A non-acclimative (fixed-physiology) version of the model predicted entirely different vertical profiles, suggesting that accounting for physiological flexibility might be relevant for a consistent representation of the vertical distribution of phytoplankton biomass. Our results point to significant variability in cellular chlorophyll to carbon ratio ~~show significant seasonal and lateral variability, the latter amplifying~~ (Chl:C) across seasons and the coastal to offshore transition. Up to 3 fold higher Chl:C at the coastal areas in comparison to those at the offshore areas contribute to the steepness of the ~~transitional chlorophyll gradient, thus, pointing to~~ chlorophyll gradient. The model predicts also much higher phytoplankton concentrations at the coastal areas in comparison to its non-acclimative equivalent. Hence, findings of this study provide evidence for the relevance of ~~resolving the physiological acclimation processes for an accurate~~ the physiological flexibility, here reflected by spatial and seasonal variations in Chl:C, for a realistic description of biogeochemical fluxes, particularly in the environments displaying strong resource gradients.

Wirtz, K.W. and Kerimoglu, O.: Optimality and variable co-limitation controls autotrophic stoichiometry, Frontiers in Ecology and Evolution, doi:10.3389/fevo.2016.00131, 2016.

## 1 Introduction

Modelling the biogeochemistry of coastal and shelf systems requires the representation of a multitude of interacting processes, not only within the water but also at the adjacent earth system components such as the atmosphere (e.g., nitrogen deposition), land (e.g., ~~rivers~~riverine inputs), sediment (e.g., diagenetic processes), and biochemical processes in water (see., e.g., Cloern et al., 2014; Emeis et al., 2015). For being able to reproduce the large scale spatial and temporal distribution of biogeochemical variables in coastal systems, a realistic representation of hydrodynamical processes is often critically important, at least those relevant to the circulation patterns and stratification dynamics: the former is needed to describe the spread of nutrient-rich river plumes and exchange at the open ocean boundaries, and the latter for being able to capture the vertical gradients in the light and nutrient conditions for primary productivity. Representation of biological processes and the two way interactions between biological, chemical and benthic compartments in models are particularly challenging, given the complexity of physiological processes displayed by individual organisms, e.g., regarding the regulation of their internal stoichiometries (e.g., see Bonachela et al., 2016) and the differences in functional traits of species constituting communities (e.g., see Litchman et al., 2010).

3-D ecosytem models often describe the processes relevant to primary production, e.g., the nutrient and light limitation of phytoplankton, using heuristic formulations that have been shown to be inadequate in reproducing patterns obtained in laboratory experiments. For instance, light limitation is determined not only by the instantaneously available irradiance, but also by the amount of light harvesting apparatus, i.e., chlorophyll pigments maintained by the phytoplankton cells, which can change considerably through a process referred to as photoacclimation. However, photoacclimation is often completely ignored in 3-D model applications, or its effects are mimicked heuristically, for instance, by describing the chlorophyll to carbon ratio as a function of irradiance (Blackford et al., 2004; Fennel et al., 2006), which cannot capture the dependence of chlorophyll synthesis on nutrient availability ~~(e.g., Pahlow and Oschlies, 2009; Smith et al., 2011)~~(e.g., Pahlow and Oschlies, 2009; Smith et al., 2011; Wirtz and K
Similarly, interaction of limitation by different nutrient elements is described by heuristic formulations, dichotomously either by a product rule or a threshold function, which, again, cannot reproduce complex patterns observed in laboratory conditions, such as the asymmetric cellular N:C and P:C ratios emerging under N- and P- limited conditions (Bonachela et al., 2016; Wirtz and Kerimoglu, 2016). Such simplifications in the description of primary production processes, in turn, potentially lead to flawed representations of nutrient cycling. Despite the recently revived theoretical work on stoichiometric regulation and photoacclimation (e.g., Klausmeier et al., 2004; Pahlow and Oschlies, 2009; Wirtz and Pahlow, 2010; Bonachela et al., 2013; Daines et al., 2014), an implementation of a model with a mechanistic description of the regulation of phytoplankton composition at a full ecosystem scale in a coupled physical-biological modeling framework remains to be lacking. In this study, we therefore present a 3-D application of the Model for Adaptive Ecosytems for Coastal Seas (hereafter MAECS), to the Southern North Sea (SNS), for a decadal hindcast simulation. MAECS features an photoacclimative autotrophic growth model that has

been recently introduced by Wirtz and Kerimoglu (2016), which resolves the regulation of the stoichiometry and composition of autotrophs employing an innovative suit of adaptive and optimality based approaches.

The SNS is part of a shallow shelf system (Fig. 1). Especially the south eastern portion of the SNS, known as the German Bight surrounded by the inter-tidal Wadden Sea, is characterized by steep gradients with respect to both nutrients (Hydes et al., 1999; Ebenhöh, 2004) and turbidity. The latter is largely determined by suspended particulate matter (SPM) concentrations (Tian et al., 2009; Su et al., 2015). These gradients are driven by a complex interplay of riverine and atmospheric fluxes, complex topography, residual tidal currents, density gradients, biological processing of organic matter, benthic-pelagic coupling and sedimentation/resuspension dynamics ~~(Postma, 1961; Puls et al., 1997; van Beusekom and de Jonge, 2002; Burchard et al., 2008; Hofmeis~~

A number of modelling studies previously addressed the biogeochemistry of the North Sea, including the German Bight. In a majority of these studies, such as ECOHAM-HAMSOM (Pätsch and Kühn, 2008), NORWECOM (Skogen and Mathisen, 2009), ECOSMO-HAMSOM (Daewel and Schrum, 2013), HAMOCC-MPIOM (Gröger et al., 2013), ERSEM-NEMO ~~(de Mora et al., 2013; Ford~~

(Edwards et al., 2012; Ford et al., 2017), ERSEM-POLCOMS (de Mora et al., 2013; Ciavatta et al., 2016) and ERSEM-BFM-GETM ~~(van Leeuwen et al., 2015; Ford et al., 2017) and HAMOCC-MPIOM (Gröger et al., 2013)~~(van Leeuwen et al., 2015; van der Mole

large domains and relatively coarse grids were employed ($\geq$ 7 km). While showing good skill in reproducing ~~off-shore~~ offshore dynamics, these models seemed to have a relatively limited performance at the shallow, near-coast regions (when reported). The BLOOM-Delft3D (Los et al., 2008) on the other hand, is one of the rare examples with a finer grid (down to 1 km at the Dutch coasts) at the cost of a relatively smaller domain, similar to ours. Although this model system performs decently at both coastal and ~~off-shore~~ offshore areas, its performance within the German Bight has not been fully assessed. Moreover, none of these models provide elaborate descriptions of the stoichiometric regulation of autotrophs, as mentioned above. Therefore, our new model system is expected to fill two important gaps by; ~~1) exemplifying~~

1. Exemplifying for the first time to the best of our knowledge, implementation of a highly complex phytoplankton growth model at an ecosystem scale, coupled to a hydrodynamic model and other biogeochemical compartments~~; 2) establishing~~ , and gain some first insight into the relevance of acclimation to the modelling of coastal biogeochemistry.

2. Establishing the capacity to reproduce the biogeochemistry of the German Bight both at coastal and ~~off-shore~~ offshore regions with a single parameterization and model setup.

For a 11 year hindcast simulation of the period 2000-2010, we show that the model can adequately capture the spatio-temporal variability of the physical and biogeochemical features of the SNS based on comparisons against various data sources. Importantly, the model can reproduce the steep chlorophyll and nutrient gradients prevalently observed across the ~~Waddensea-German~~ Wadden Sea-German Bight continuum. We show that the chlorophyll gradients are linked with nutrient, hence, productivity gradients, ~~but also~~ and further amplified by acclimation capacity of the phytoplankton, and particularly by the high chlorophyll to carbon ratios at the ~~shallower regionsowed to the high turbidity~~coastal regions.

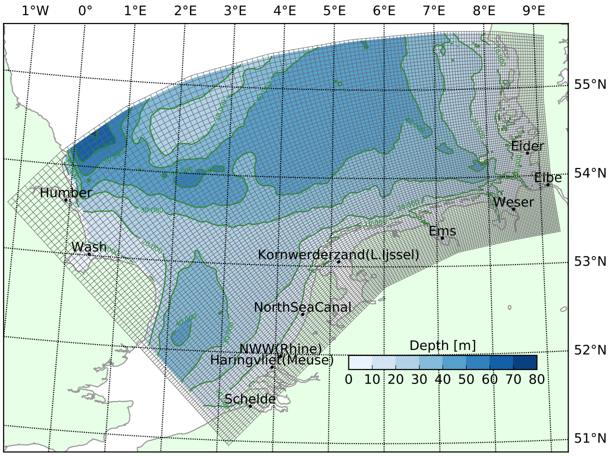

**Figure 1.** Bathymetry of the model domain and the location of rivers considered in this study. Gray lines display the model grid.

## 2 Methods

### 2.1 ~~Data~~Observations

~~Data from monitoring stations all reflect surface measurements~~Observation data from Helgoland Roads, Sylt and 17 other monitoring stations reflect surface measurments. Extensive analyses of the data from Helgoland Roads have been ~~provided~~ previously performed by Wiltshire et al. (2008) and from Sylt by Loebl et al. (2007). ~~Temperature~~Sparse measurements of temperature, salinity, dissolved inorganic nitrogen~~and phosphorus data~~, phosphorus and chlorophyll were obtained from the online database of International Council for the Exploration of the Sea (ICES, www.ices.dk)~~were used for the validation of the physical and biogeochemical model, by means of point-wise comparisons within the surface and bottom layers, i.e., upper and lower 5 meters~~.

~~Vertically resolved Scanfish data and continuous Ferrybox measurements were all gathered within the~~ Continuous Scanfish and FerryBox measurements were performed within the operation of the Coastal Observing System for Northern and Arctic Seas ~~(COSYNA, Baschek et al., 2016, and references therein). Satellite data employed here are provided by the European Space Agency (ESA), Ocean Color~~ (COSYNA, Baschek et al., 2016). Data collection, processing and quality control of the Scanfish data are described by Maerz et al. (2016) and of the FerryBox data by Petersen (2014). Satellite dataset used here is the Ocean Colour Climate Change Initiative~~version 2.0, where the NASA OC4.V6 algorithm had been applied to the MERIS, MODIS and SeaWiFS products for the estimation of chlorophyll concentrations(Grant et al., 2015)~~, Version 3.1, European Space Agency, available online at http://www.esa-oceancolour-cci.org/. Chlorophyll estimates of the satellite product were bias-corrected according to the product user guide (Grant et al., 2017): $C_{bc} = 10^{\log_{10}(C)+\delta}$, where $C_{bc}$, $C$ and $\delta$ are, respectively, the bias-corected, raw, and log10 bias estimates for chlorophyll concentrations.

## 2.2 Model

Major processes taken into account by the model are the lower trophic food web dynamics, phytoplankton ecophysiology and basic biogeochemical transformations in the water, and the transformation of N- and ~~P- species in~~ P-species in the benthos (Fig. 2 and Section 2.2.1). Physical processes are resolved by the coupled 3-D hydrodynamical model, GETM (Section 2.2.2). Turbidity caused by suspended particulate matter (SPM), nutrient loading by rivers and atmospheric nitrogen deposition were considered as model forcing (Section 2.2.3). The model grid and ~~riverine fluxes~~ rivers considered in this study are shown in Fig. 1.

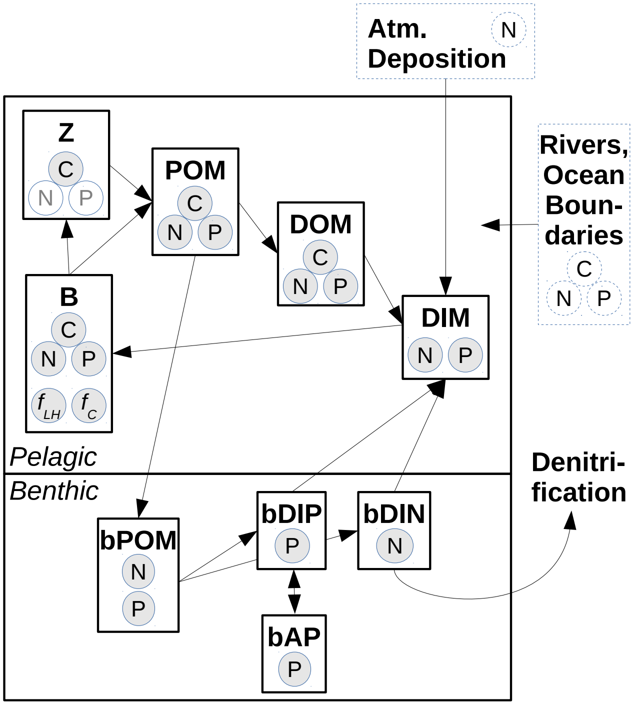

**Figure 2.** Structure of the biogeochemical model. Model components (rectangles) comprise; B: phytoplankton, Z: zooplankton, POM and DOM: particulate and dissolved organic matter, DIM(N,P): dissolved inorganic matter (nitrogen,phosphorus), ~~Fe-P~~b-AP: P adsorbed in iron-phosphorus complexes (See Section 2.2.1 and ~~supplementary material~~ Appendix A for further details). C, N, P in small circles refer to carbon, nitrogen and phosphorus bound to each component, respectively, whereas $f_{LH}$ and $f_C$ are the allocation coefficients for light harvesting and carboxylation (Section 2.2.1). Boxes in dashed lines indicate model forcing.

### 2.2.1 Biogeochemical model

The pelagic module, the Model for Adaptive Ecosystems in Coastal Seas (MAECS), is a lower trophic level model that resolves cycling of carbon, nitrogen (N) and phosphorus (P), and importantly, acclimation processes ~~of phytoplankton , a detailed description of which is provided by Wirtz and Kerimoglu (2016) and in the supplementary material (A). The acclimation~~

~~module features a whole set of physiological traits (~~involved in phytoplankton growth. In MAECS, the acclimation of phytoplankton is resolved by a scheme recently introduced by Wirtz and Kerimoglu (2016), which describes the instantaneous or transient optimization of physiological traits, $x$ ~~), which control accessory and assimilation of multiple resources in autotrophs. These comprise, affinity for DIN and DIP, protein pools invested to nutrient uptake and light harvesting, and specific P- and N-uptake activities. Their instantaneous or transitory acclimation follows an~~ by the extended optimality principle~~,~~

:

$$\frac{\mathrm{d}}{\mathrm{d}t}x = \delta_x \cdot \left[\frac{\partial V_\mathrm{C}}{\partial x} + \sum_i \frac{\partial V_\mathrm{C}}{\partial q_i}\frac{\partial q_i}{\partial x}\right] \tag{1}$$

where $\delta_x$ corresponds to ~~a flexibility constant~~the flexibility of traits (Eq.A18), $i$ expands to N and P, and the two terms in brackets describe the direct effects of trait changes on the specific phytoplankton growth rate $V_\mathrm{C}$ (in units of cellular C) and the indirect effects through changes in the Chl:C:N:P stoichiometry, expressed by the quotas $q$, respectively~~(Wirtz and Kerimoglu, 2016). As a result of trait variations formulated in Eq~~. ~~1~~Specifically, three-levels of acclimative regulations are considered (see Fig. 2 in Wirtz and K

1. Machinery allocation: we describe the changes in allocations to light harvesting, carbon fixation and nutrient acquisition machineries, as also in (Wirtz and Pahlow, 2010). These allocations correspond to synthesis of cellular structures like chloroplasts for absorbing light, Rubisco enzyme involved in carboxylation process and proteins for gathering nutrient molecules, therefore we track these fractional allocations with two dynamic state variables, $f_{LH}$ and $f_C$, that describe the allocations for light harvesting and carboxylation, while the allocations for nutrient uptake, $f_V$ is assumed to be the rest $1 - f_{LH} - f_C$. Here, the flexibility term, set to $\delta_x = f_x \cdot (1 - f_x)$, regulates the speed of optimization as determined by the differential terms in Eq.1.

2. Nutrient affinity-processing optimality: we assume that there is a trade-off between nutrient affinity and processing, and the optimal affinity fractions for each nutrient, $f_i^A$, are instantaneously optimized, such that $d_x/d_t = 0$ and $f_i^A$ are algebraically found by setting $\frac{\partial V_\mathrm{C}}{\partial x} = 0$ (Pahlow, 2005; Smith et al., 2009).

3. Nutrient uptake activity: (down-) regulation of the uptake rate of nutrients, which is often formulated as a linear function of nutrient quotas (Morel, 1987) in traditional models, is in our approach, described by the instantaneously optimized uptake activity trait, $a_i$. Assuming that energy expenditure for taking up of each nutrient depends on the metabolic needs, values of $a_i$ are found by scaling their marginal growth benefits (Eq.A17).

Driven by the variations of these physiological traits, Chl:C:N:P stoichiometry ~~is continuously varied~~ varies continuously depending on ambient light and nutrient conditions and on the metabolic demands of autotrophic cells. As a further novel aspect of the acclimation model, multiple limitation is described as a queuing function, which allows formulating the co-limitation strength as a function of internal nitrogen reserve $q_N$, instead of prescribing it to be either high as by a product rule, or low as by a threshold (Liebig) function (Wirtz and Kerimoglu, 2016). A detailed description of the phytoplankton growth module can be found in Wirtz and Kerimoglu (2016). Equations and parameters of the model are provided in Appendix A1.

Other components of the pelagic module are similar to standard descriptions in state-of-the-art ecosystem models. Phytoplankton take up nutrients in the form of dissolved inorganic material (DIM). Losses of phytoplankton (B) and zooplankton (Z) due to mortality are added to the particulate organic matter (POM) pool, which degrades into dissolved organic material (DOM), before becoming again DIM and closing the cycle (Appendix A1). As a relevant aspect of the model, while the sedimentation speed of POM ($w_{POM}$) prescribed as a constant value, that of the phytoplankton, $w_B$ is assumed to be modified by its nutrient (quota) status. As decreased internal nutrient quotas likely affect the cells ability to regulate buoyancy and lead to faster migration towards deeper, potentially nutrient rich waters (Boyd and Gradmann, 2002), we assume that maximum sinking rates realized at fully depleted quotas converge to a small background value with increasing quotas as has been observed especially for, but not limited to, diatoms (Smayda and Boleyn, 1965; Bienfang and Harrison, 1984). Although the phytoplankton sinking is often parameterized as a constant rate in 3-D modelling applications, similar formulations of increasing sinking rates under nutrient stress have been also used (e.g., Vichi et al., 2007).

The benthic module describes only the dynamics of macronutrients N and P. Degradation of OM to DIM is described as a one step, first order reaction. Denitrification is described as a proportion of POM degradation, limited by DIN and dissolved oxygen (DO) availability in benthos. As DO is not directly modeled, it is estimated from temperature in order to mimic the seasonality of the hypoxia-driven denitrification. The model accounts for the sorption-desorption dynamics of phosphorus as an instantaneous process also as a function of temperature based on the correlation observed in the field (Jensen et al., 1995). Further details are provided in Appendix ~~A~~A2.

### 2.2.2 Hydrodynamic model and model coupling

The General Estuarine Transport Model (GETM) was used to calculate various hydrodynamic processes, as well as the transport of the biogeochemical variables. A detailed description of GETM is provided by ~~Burchard and Bolding (2002); Stips et al. (2004)~~Burchard Stips et al. (2004). GETM utilizes the turbulence library of the General Ocean Turbulence Model (GOTM) to resolve vertical mixing of density and momentum profiles with a k-$\varepsilon$ two equation model (Burchard et al., 2006). GETM was run in baroclinic mode, resolving the 3-D dynamics of temperature, salinity and currents and 2-D dynamics of sea surface elevation and flooding-drying of cells at the Wadden Sea. Following Gräwe et al. (2016), we assumed the bottom roughness length to be constant through out the domain, and $z_0$=$10^{-3}$m. We used 20 terrain-following layers and a curvilinear grid of 144x98 horizontal cells~~with~~ , providing a horizontal resolution of approximately 1.5 km at the south-east corner and 4.5 km at the north-west corner (Fig. 1). The curvilinear grid focuses on the German Bight, and roughly follows the coastline (Fig. 1) for an optimal representation of along- and across- shore processes. Similar gridding strategies were applied successfully in other coastal setups with the GETM model ~~(Hofmeister et al., 2013; Hetzel et al., 2015)~~(Hofmeister et al., 2013; Hetzel et al., 2015). We employed integration time steps of 5 and 360 seconds for the 2-D and 3-D processes, respectively.

Integration of model forcing was realized through the Modular System for Shelves and Coasts (MOSSCO, http://www.mossco.de), which, among others, provides standardized data representations (Lemmen et al., 2017). Meteorological forcing originated from an hourly-resolution hindcast by COSMO-CLM (Geyer, 2014). Boundary conditions for surface elevations ~~and currents~~ are extracted from an hourly resolution hindcast by TRIM-NP (Weisse et al., 2015). For temperature and salinity, daily climatologies from HAMSOM (Meyer et al., 2011) are used, all of which are available through coastDat http://www.coastdat.de.

Two-way coupling of the biological model with GETM was achieved via the Framework for Aquatic Biogeochemical Models (FABM, Bruggeman and Bolding, 2014)~~as one of the coupling standards adopted in MOSSCO~~. The pelagic module is defined in the 3-D grid of the hydrodynamic model, whereas the benthic module is defined in 0-D boxes for each water column across the lateral grid of the model domain (Fig. 1). Each benthic box interacts with the bottom-most pelagic box of the corresponding water column in terms of a uni-directional flux of POM from the pelagic to the benthic states, and a bi-directional flux of DIM depending on the concentration gradients.

For the integration of the source terms, a fourth order explicit Runge-Kutta scheme was used with an integration time step of 360 seconds, as for the 3-D fields in GETM. Exchange between pelagic and benthic variables was integrated with a first order explicit scheme at a time step identical to that of the biological model.

### 2.2.3 Model forcing and boundary conditions

Light extinction is described according to:

$$I(z) = I_0 a e^{-\frac{z}{\eta_1}} + I_0(1-a)e^{-\frac{z}{\eta_2} - \int_z^0 \sum_i k_{c,i} c_i(z')dz'} \tag{2}$$

where, $I_0$ is the photosynthetically available radiation at the water surface, and the first and second terms describe the attenuation at the red and blue-green portions of the spectrum. We assume that the partitioning of the two ($a$) and the attenuation length scale of the red light ($\eta_1$) are constant over space and time as in Burchard et al. (2006), and that the attenuation of blue-green light is due to SPM (as described by $\eta_2$) and organic matter (sum term). We chose $a = 0.58$ and $\eta_1 = 0.35$, which correspond to Jerlov class-I type water, thus clear water conditions (Paulson and Simpson, 1977), given that the attenuation by SPM and organic matter is explicitly taken into account. For calculating attenuation due to SPM, a daily climatology of SPM concentrations defined over the model domain was utilized, like in ECOHAM (Große et al., 2016). The SPM field was constructed by multiple linear regression of salinity, tidal current speed and depth for each Julian day (Heath et al., 2002). Then, $\eta_2$, or the inverse of SPM caused attenuation coefficient was calculated according to:

$$1/\eta_2 = k_{SPM} = \underline{K_w +} \epsilon_{SPM} * SPM \tag{3}$$

where, the attenuation for background turbidity, $K_w = 0.16$ m$^{-1}$ and specific attenuation coefficient for SPM, $\epsilon_{SPM} = 0.02$ m$^2$ g$^{-1}$ according to Tian et al. (2009). For calculating the attenuation due to organic matter in Eq.(2), phytoplankton, POC and DOC were considered (Table A3).

Freshwater and nutrient influxes were resolved for eleven major rivers along the German, Dutch, Belgian and British coasts (Fig. 1). For eight of these rivers, Radach and Pätsch (2007) and Pätsch and Lenhart (2011) ~~present~~ presented a detailed quantitative analysis of nutrient fluxes. Besides the fluxes in inorganic form based on direct measurements, fluxes in organic form have been accounted for, first by calculating the total organic material concentration by subtracting dissolved nutrient concentrations from total nitrogen and total phosphorus, then by assuming 30 % of the organic material to be in particulate form (i.e., POM; Amann et al., 2012). Further, 20 % of POM is assumed to describe phytoplankton biomass (Brockmann, 1994), C:N:P ratio of which was assumed to be in Redfield proportions. Finally, no estuarine retention/enrichment was assumed, following Dähnke et al. (2008). All river data except for the river Eider were available in daily resolution, however with gaps. Short gaps (<28 days) were filled by linear interpolation. Loadings from the river Eider were calculated first by merging the data measured at the stations on two upstream branches, Eider and Treene, then by filling the short gaps (<28 days) by linear interpolation, replacing the larger gaps with daily climatology, and extending for 2000-2003 by using the climatology as well. To describe DIN deposition at the water surface, sum of annual average atmospheric deposition rates of $NO_x$ and $NH_3$ provided by EMEP (European Monitoring and Evaluation Programme, http://www.emep.int) were used. At the open boundaries in the north and west of the model domain (Figure 1), all state variables belonging to the phytoplankton and zooplankton compartments are assumed to be at zero-gradient. For DIM, DOM and POM, monthly values of ECOHAM (Große et al., 2016), interpolated to 5m depth intervals are used as clamped boundary conditions.

### 2.3 Quantification of Model Performance

For the comparisons with the ~~station data for DIN, DIP and Chl concentrations~~data at monitoring stations, sparse in-situ measurements from the ICES database, and with the satellite (ESA-CCI oceancolor) dataset, Pearson correlation coefficients~~were calculated for all temporal matches~~, $\rho$, and mean normalized bias, $B^* = (\langle S\rangle - \langle O\rangle)/\langle O\rangle$, where $\langle S\rangle$ and $\langle O\rangle$, respectively, are the average simulated and observed values) were calculated. For the ~~evaluation of model performance against the ICES~~ DIN, DIP and chlorophyll comparisons with the station and ICES data, these skill scores are reported in a color-coded table, where the 4 color levels indicate low (red: $|B*|$ $\geq$0.75 and $\rho$ <0.25), moderate-low (yellow: 0.5$\geq$ $|B*|$ <0.75 and 0.25$\leq$ $\rho$ <0.5), moderate-high (green: 0.25$\geq$ $|B*|$ <0.5 and 0.5$\leq$ $\rho$ <0.75) and high (blue $|B*|$ $\leq$0.25 and $\rho$ $\geq$0.75) model performance. For the comparisons against the sparse ICES and ESA-CCI data~~for temperature, salinity, DIN and DIP~~, correlation scores and model standard deviations normalized to measured standard deviations are displayed as Taylor diagrams, where the correlation score and the normalized standard deviation correspond to the angle and distance to the center (Jolliff et al., 2009). For ~~this purpose~~the comparisons against the ICES and ESA-CCI data, only the middle-99 percentile of simulated and measured values were considered (i.e., leaving out the first and last 0.5th percentiles).

For the ICES data, temporal matching was identified at daily resolution, vertical matching ~~were~~ was obtained by comparing the measurements within the upper 5 meters from the sea surface and within the 5 meters above the sea floor with the model estimates at the top-most and bottom-most layers, and finally ~~lateral~~ horizontal matching by calculating the average of the values from four nearest cells surrounding the measurement location, inversely weighted ~~with respect to the~~ by their Cartesian distance. ~~Finally, comparison of the spatial structure of the model estimates to that of the satellite (~~For the ESA-CCI ~~) datawas achieved also through Taylor Diagrams. For this purpose,~~ data, the temporal matching was obtained by averaging the data from both sources for the period 2008-2010 for particular seasons of the year, and ~~lateral~~ horizontal matching by performing a 2-dimensional linear interpolation of the satellite data to the model grid. ~~For the comparisons against the ICES and ESA-CCI data , only the middle-99 percentile of model and measurements were considered (i.e., leaving out the first and last 0.05th percentiles)~~Extraction of the hourly model temporally matching to the Scanfish data was based on the hourly-binned average time for each cast (defined as a full downward and upward undulation cycle) and 3-D spatial matching was obtained by constructing an average vertical profile from the 4 closest cells to the average coordinate of each cast. For facilitating the qualitative comparison of the simulated chlorophyll and the Scanfish measurements of fluorescence, which have different units and signal strengths, normalized anomalies were used, according to $\hat{p}_i = (p_i - \langle p \rangle)/\sigma_p$, where $\hat{p}_i$ and $p_i$ are the normalized anomaly and raw value of a given data point, and $\langle p \rangle$ and $\sigma_p$ are the mean and standard deviation of all data points.

## 3 Results~~and Discussion~~

### 3.1 Evaluation of Model Performance by in-situ Data

A comparison of simulated salinities with the FerryBox measurements along the cruise between Cuxhaven (at the mouth of river Elbe) and Immingham (at the mouth of river Humber)~~(Petersen, 2014)~~, demonstrates that the model captures the ~~general salinity patterns~~ horizontal salinity distribution (Fig. 3). ~~However, the freshwater plume in the German Bight as simulated by GETM seems to extend further from the coast than observed, which suggests moderate over-estimation of horizontal mixing~~ In particular, the contrast between the north-western model domain characterized by the rapid flushing of the coastal freshwater input and the south-eastern model domain (i.e., German Bight) characterized by a strong and permanent salinity gradient is well captured. Confinement of the salinity front during winter towards the coast and its seaward intrusion especially during early spring, and the smaller scale modulations that appear to be controlled by the spring-neap cycle are both reproduced by the model.

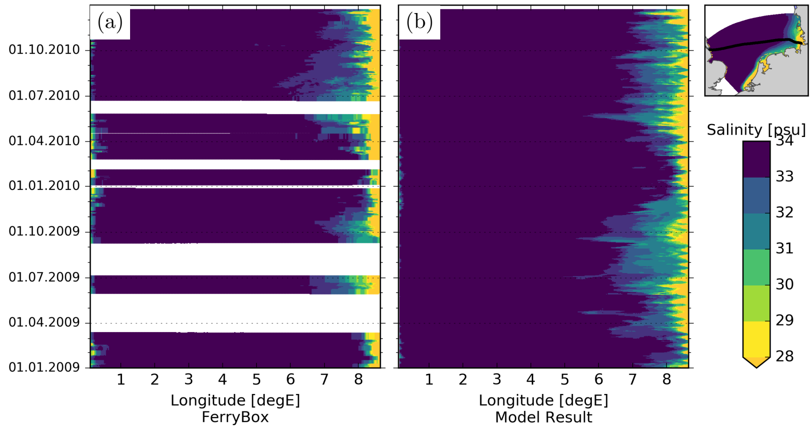

**Figure 3.** Salinity [PSU] measured by ~~ferry-box~~ FerryBox (a) and estimated by the model (b) along the route shown in the inset. Note that the lower range of salinity was truncated

Comparison of simulated surface and bottom temperatures with those extracted from the ICES ~~data set~~ dataset for the period 2006-2010 are provided in Fig. 4. High correlation scores ~~($\geq$0.85 for surface and >0.9 for bottom layers)~~ and low bias attained for water temperature and salinity suggest that the model can ~~generally~~ reproduce the seasonal warming, spread of freshwater discharges and ~~stratification dynamics driven by temperature and salinity gradients~~thermohaline stratification dynamics. However, in a relatively small number of instances, surface temperatures are ~~in part~~ underestimated and bottom temperatures are overestimated, which indicates that not all stratification events were captured. ~~Most of the mismatch in salinity occur at the lower range, in the form of a systematic underestimation in both surface and bottom layers, resulting in a higher standard deviation of the model estimates relative to the measurements. Further analysis (not shown) revealed that this problem was most pronounced in 2010, which was a relatively wet year, indicating again that the model overestimates the transport of freshwater from rivers especially during high-discharge events, which points to the deficiency of the grid resolution to capture such events realistically.~~ Almost all of these instances are found to be located either at the north-eastern margin ($> 4$°E & $> 55$°N) and at the north-western corner ($< 4$°E & $> 54$°N) of the model domain, i.e., close to the open ocean boundary (Fig. 1).

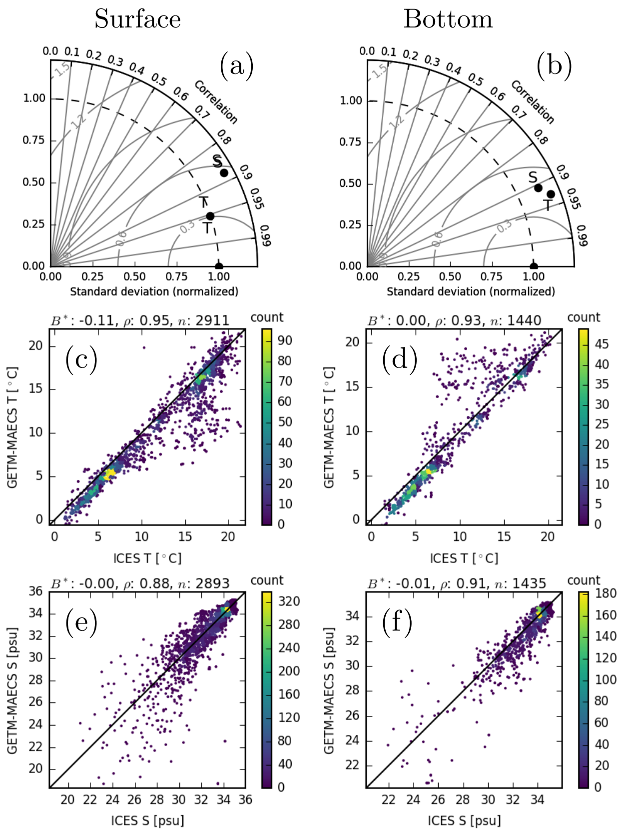

**Figure 4.** Comparison of modeled and measured (ICES) temperature (abbreviated T in panels a,~~d,~~b,~~e~~c,d) and salinity (~~abbreviated~~ S in a,~~d~~b,~~e~~e,f) at the surface (~~a-e~~left) and bottom (~~d-f~~right) layers for the period 2006-2010. 2-D histograms show the number of occurrence of simulation-measurement pairs. Normalized bias ($B^*$), Pearson correlation coefficients ($\rho$), and corresponding number of data points ($n$) are shown on top of scatter plots.

Comparisons of ~~model-estimated~~ surface chlorophyll, DIN and DIP concentrations estimated by the model with the measurements in 19 stations scattered across the southern North Sea ~~(~~are shown in Fig. 5~~-Fig.7) yields following: *i*) there are no obvious decadal trends neither in observations, nor in simulated values. *ii*) Average and peak nutrient and chlorophyll concentrations are in general well reproduced. In some coastal stations, like Sylt, chlorophyll concentrations seem to be overestimated although the nutrient concentrations are rather realistically represented. In a few other stations like Norderelbe and Noordwijk, nutrient concentrationsare not very realistic: given the proximity of these stations to major rivers Elbe, North Sea Canal and Rhine (Fig.1), these mismatches are likely to be related with our assumption that the non-dissolved fractions of the total nitrogen and total phosphorus to be all in labile form (Sect. 2.2.3). *iii*) Timing of spring blooms, nutrient draw-down and regeneration are mostly well reproduced, as also reflected by high correlation coefficients in general. Earlier replenishment of phosphorus relative to nitrogen is often reproduced, although with delays in some coastal stations like Norderney, which probably reflects the oversimplification of the benthic processes with respect to the description of oxygen-driven iron-phosphorus complexation kinetics (Sect. A), which has been suggested to be the main driver for the phenomena in the coastal areas (Jensen et al., 1995; van Beusekom et al., 1999; Grunwald et al., 2010). Finally, measurements from S.Amrum suggest that the classical summer-low-~~7, ~~winter-high phosphorus pattern, as also predicted by our model in general, is entirely reversed, calling for a more detailed investigation.~~and the corresponding skill scores are listed in Table 1. Estimates of average nutrient concentrations, and the timing of their depletion and regeneration in a majority of stations agree well with the observations, as indicated by the frequency of ‘high’ and ‘moderate-high’ scores (Table 1). Notably, at several stations (e.g., Sylt,T8,T36,T26,T22,T11,T12) the difference between the relative bias for DIP and DIN (i.e., $B^*_{DIP} - B^*_{DIN}$) was relatively large (with 55% being highest at T22), suggesting a tendency for underestimating the DIN:DIP ratio, although this was not the case for the comparison against ICES measurements (see below). Relative to the nutrients, performance of the model in estimating the chlorophyll is lower, especially at the stations located along the Dutch coast (Fig. 6, Table 1). However, for about half of the 10 stations where data is available, the model performance is at moderate levels.

~~There are a number of caveats when using coastal time-series data for model validation, which start from the sampling problem: short term fluctuations common for near-shore waters can only be tentatively represented by measurement frequencies of several weeks or months. For the special case of Sylt,for example,data reflect the average monthly concentrations,which naturally smooths out the short-lived blooms. However,we acknowledge the potentially inadequate description of certain processes that might have led to the overestimation of chlorophyll concentrations at Sylt,such as the grazing formulation of zooplankton and the representation of the light climate. In reality, effects of temperature on mesozooplankton occurs through phenological shifts (e.g., Greve et al., 2004) that might have a determining role on the maximum chlorophyll concentrations (van Beusekom et al., 2009), which can probably be only partially reflected by the simple Q10 rule we applied for grazing rates (Sect. A1). Light climate on the other hand, especially in the shallow regions in the German Bight, is largely influenced by SPM concentrations (Tian et al., 2009), which is here provided to the model as a daily climatological forcing (Sect. 2.2.3), hence, neglecting any potential inter-annual variability.~~

~~Taylor diagrams for DINand DIP~~ Comparison of model results with the DIN, DIP and chlorophyll measurements available at the ICES database at the surface and bottom layers ~~(Fig. 12) indicate a reasonable match to the ICES data for the period~~

~~Observations and model estimates of surface chlorophyll, DIN and DIP concentrations at the stations located along the coasts of the German Bight, operated by Alfred Wegener Institute (Helgoland and Sylt), Landesamt für Landwirtschaft, Umwelt und ländliche Räume des Landes Schleswig-Holstein (S. Amrum, Norderelbe) and Niedersächsichser Landesbetrieb für Wasserwirtschaft, Küsten- und Naturschutz (Norderney). Pearson correlation coefficients, and corresponding number of data points are shown at the top-right corner.~~

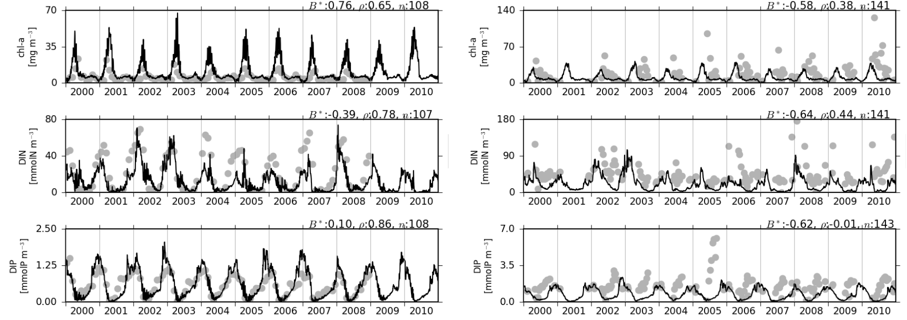
(a) Sylt
(b) S. Amrum

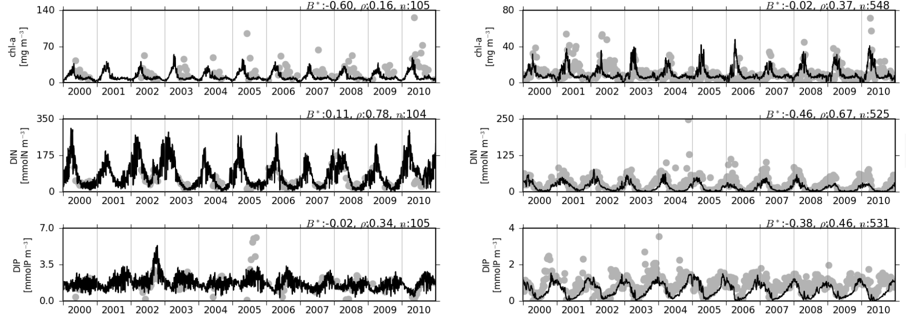
(c) Norderelbe
(d) Norderney

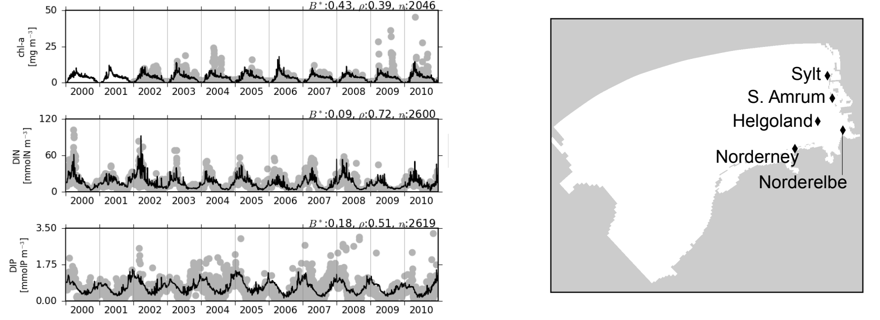
(e) Helgoland
(f) Location of stations

**Figure 5.** Observations (gray dots) and model estimates (lines) of surface chlorophyll, DIN and DIP concentrations at the stations located along the coasts of the German Bight, operated by Alfred Wegener Institute (Helgoland and Sylt), Landesamt für Landwirtschaft, Umwelt und ländliche Räume des Landes Schleswig-Holstein (S. Amrum, Norderelbe) and Niedersächsichser Landesbetrieb für Wasserwirtschaft, Küsten- und Naturschutz (Norderney). Normalized bias ($B^*$), Pearson correlation coefficients ($\rho$), and corresponding number of data points ($n$) are shown on top of each panel.

(a) Noordwijk-2 (b) Noordwijk-10

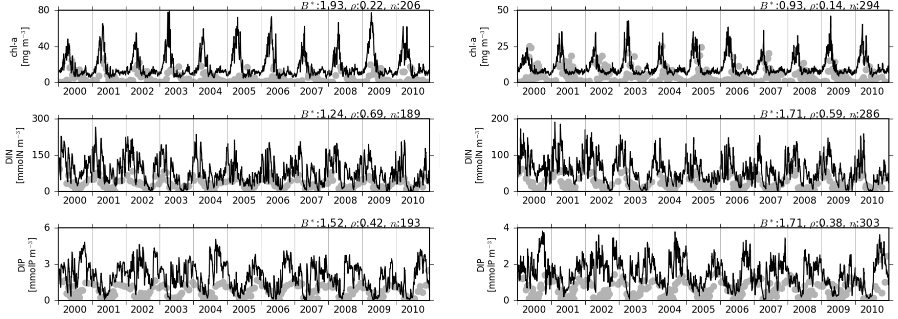

(c) Noordwijk-70 (d) Terschelling-4

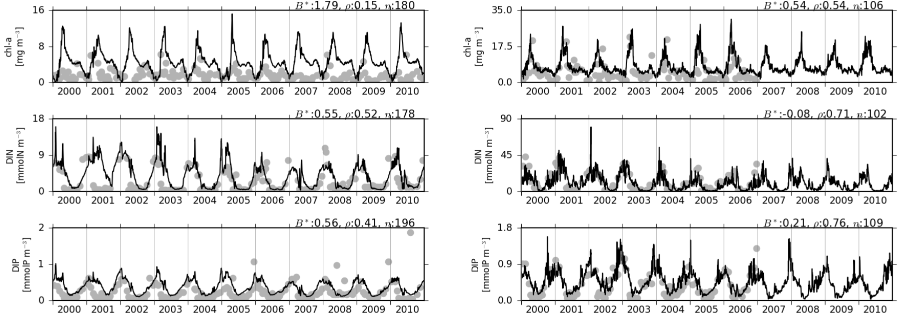

(e) Terschelling-50 (f) Location of stations

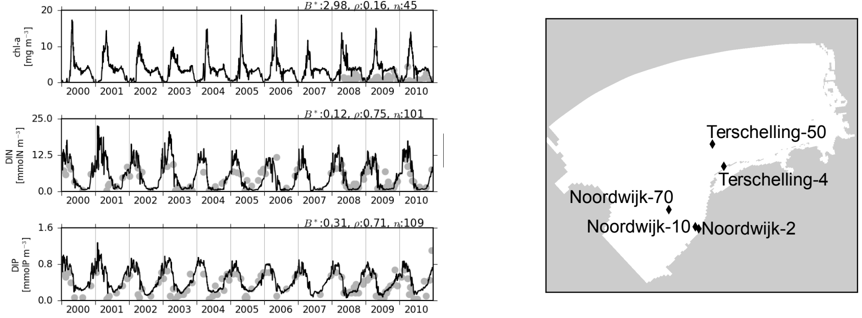

**Figure 6.** As in Fig. 5, but for the stations located along the coasts of the Netherlands, operated by Rijkswaterstaat.

~~2000-2010. Comparison of surface and bottom data separately prevents the domination of the performance statistics by strong differences between the surface and bottom layers which are relatively easier to reproduce, as would be captured by the correlation scores. Therefore, the comparison with the ICES data rather reflects the ability of model to capture the lateral and temporal (at seasonal and inter-annual scales)variability of DIN and DIP~~for the entire simulation period indicate negligible normalized mean bias and correlation coefficients at around 0.6%–0.7% for nutrients and about 60% overestimation and correlation coefficients of about 0.3 for chlorophyll (Fig. 8, Table 1). Modeled variability ~~matches very well to the observed variability for both DIN and DIP at the surface and DIN at the bottom layer. However, the variability of DIP at the bottom layer is overestimated, which seems to be caused by the occasional overestimation of the values at the higher~~

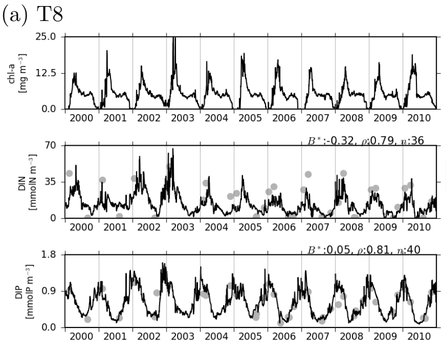
(a) T8

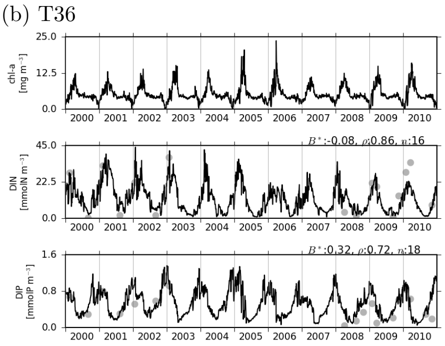
(b) T36

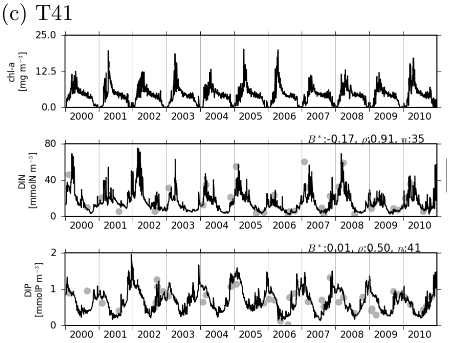
(c) T41

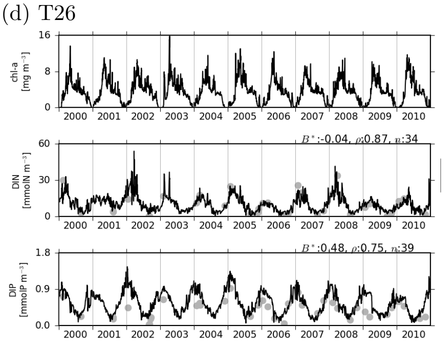
(d) T26

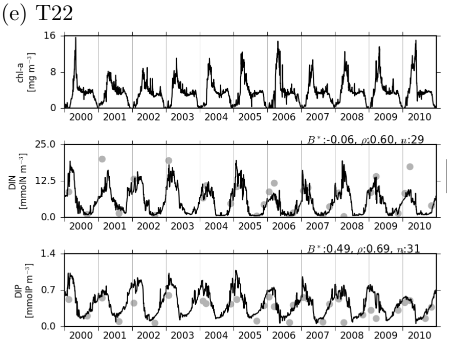
(e) T22

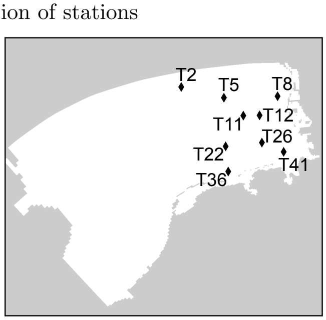
(f) Location of stations

(continued on the next page)

~~range (1-2 mmolP/m$^3$), which, again, might be related with the oversimplified representation of phosphorus dynamics in the sediment. Correlation coefficients obtained for DIN and DIP both at the surface and bottom layers seem to be relatively high, considering the typical skill level of coupled physical-biogeochemical models in estimating nutrient concentrations for the North Sea (e.g., Radach and Moll, 2006; Daewel and Schrum, 2013; de Mora et al., 2013), noting, however that a conclusive model inter-comparison would require standardized benchmarking data set and procedures~~for all three bigeochemical state variables is within an approximately 50% envelope of the observed variability (Fig. 8).

For an assessment of the accuracy of the simulated vertical distributions, water density (expressed as $\sigma_T$) and fluorescence captured by a Scanfish cruise (Heincke-331) obtained during 13-19 July 2010 were compared to those estimated by the model (chlorophyll for fluorescence) averaged over the same time period (Fig. 9). This period was characterized by significant thermal

(continues from the previous page)

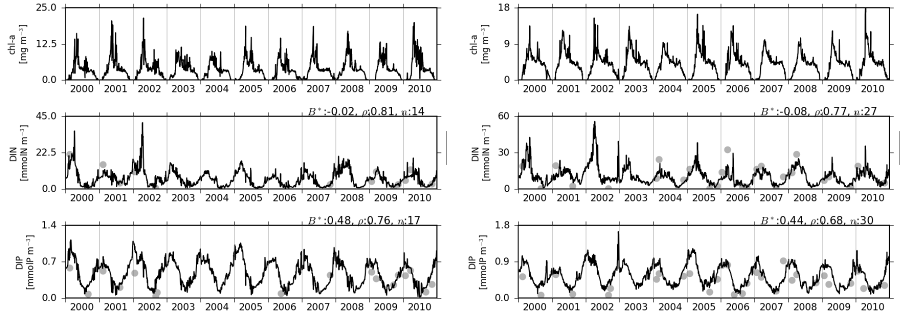
(a) T11 (b) T12

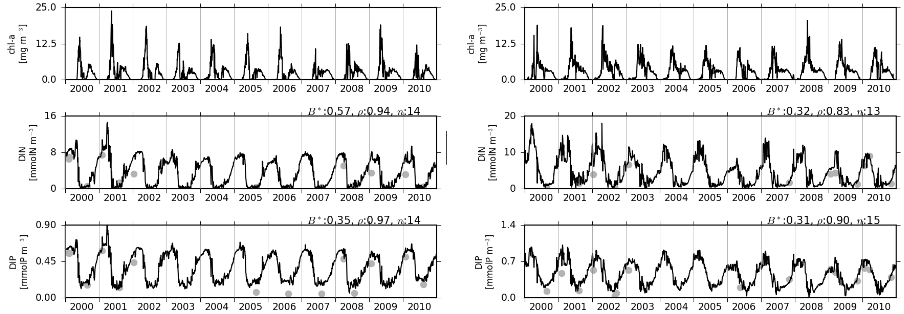
(c) T2 (d) T5

**Figure 7.** As in Fig. 5, but for the ~~off-shore~~ offshore monitoring stations operated by Bundesamt für Seeschifffahrt und Hydrographie.

summer stratification reaching deep into the near coastal regions of the German Bight. Thus, $\sigma_T$ ~~transect~~ reflects two major mechanisms that control the distribution of phytoplankton: first is the vertical gradients characterized by denser water at the bottom layers, which is mainly driven by thermal stratification as suggested by temperature profiles (not shown). Second is the horizontal gradients characterized by lighter water at the coasts, driven by low salinity due to the freshwater flux from the rivers. The model can accurately reproduce both vertical and horizontal density gradients, ~~except small discrepancies~~ although some discrepancies exist, such as slightly ~~overestimated densities at the bottom layers~~ underestimated depth of the pycnocline and steepness of lateral gradients at around the coastal section.

~~$\sigma_T$ (a) and fluorescence (c) measured by Scanfish recorded during 13-19 July 2010 compared to $\sigma_T$ (b) and chlorophyll concentration (d) estimated by the model averaged throughout the same period. Black line indicates the sea floor. Cruise track shown in (e).~~

Fluorescence measurements along the Scanfish track in July 2010 indicate frequent occurrences of ~~deep-chlorophyll~~ subsurface chlorophyll maxima (Fig. 9)~~, in accordance with previous observations (Weston et al., 2005; Fernand et al., 2013). These deep-chlorophyll maxima~~. These are in some cases in the form of higher concentrations below the pycnocline but in some others, appear as thin layers at around the pycnocline. While the deep chlorophyll maxima are ~~visible in stratified waters that occur in deeper regions,~~ prevalently found in stratified offshore regions, the well-mixed shallower regions mostly show ~~vertically~~ homogeneously distributed high chlorophyll concentrations throughout the water column due to higher dissipation rates (Maerz et al., 2016). The

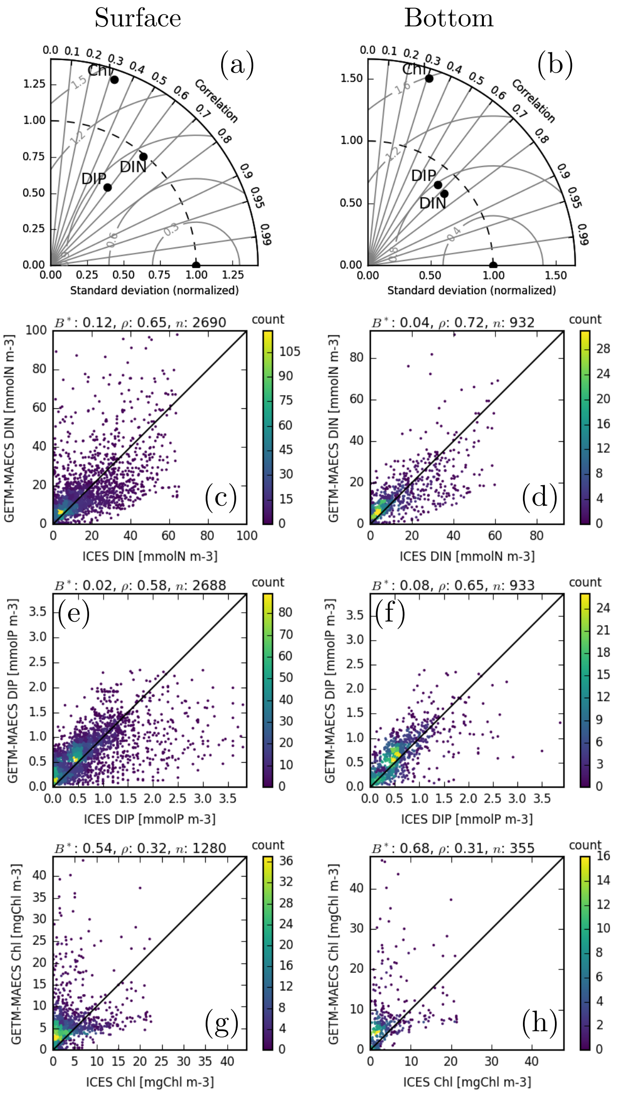

**Figure 8.** Comparison of simulated and measured (ICES) DIN (a,b,c,d), DIP (a,b,e,f) and ~~DIP~~ chlorophyll (a,~~d~~b,~~e~~g,~~f~~h) at the surface (~~a-e~~left) and bottom (~~d-f~~right) layers for the period 2000-2010. 2-D histograms show the number of occurrence of simulation-measurement pairs. Normalized bias ($B^*$), Pearson correlation coefficients ($\rho$), and corresponding number of data points ($n$) are shown on top of scatter plots.

MAECS simulation agrees qualitatively ~~very~~ well with these patterns and captures the spatial variability of the observed vertical chlorophyll distribution (Fig. 9). ~~Former 3-D modeling studies, such as that of van Leeuwen et al. (2013), apart from capturing the presence of a deep chlorophyll maximum, were not able to reproduce the rich variability revealed by the observations. Our model-based analysis indicates that the formation and maintenance of such structures are critically dependent on the parametrization of the underwater light climate and sinking rate of phytoplankton. Sinking speed of algae in the MAECS is inversely related to the nutrient quota of the cells, which mimics the internal buoyancy regulation ability of algae depending~~

**Table 1.** Skill scores obtained at each station ($B^*$ normalized bias, $\rho$: Pearson correlation coefficients, and $n$: number of matching data points), against ICES and ESA-CCI data shown in Fig.5-8 and Fig.12 partially (for the averages of months 1-3,10-12 and 4-9). Colors indicate skill level, with red: low, yellow: moderate-low, green: moderate-high, blue: high (see Section 2.3).

| | DIN | | | DIP | | | Chl | | |
|---|---|---|---|---|---|---|---|---|---|
| **Station** | $B^*$ | $\rho$ | $n$ | $B^*$ | $\rho$ | $n$ | $B^*$ | $\rho$ | $n$ |
| Sylt | -0.39 | 0.78 | 107 | 0.10 | 0.86 | 108 | 0.76 | 0.65 | 108 |
| S. Amrum | -0.64 | 0.44 | 141 | -0.62 | -0.01 | 143 | -0.58 | 0.38 | 141 |
| Norderelbe | 0.11 | 0.78 | 104 | -0.02 | 0.34 | 105 | -0.60 | 0.16 | 105 |
| Norderney | -0.46 | 0.67 | 525 | -0.38 | 0.46 | 531 | -0.02 | 0.37 | 548 |
| Helgoland | 0.09 | 0.72 | 2600 | 0.18 | 0.51 | 2619 | 0.43 | 0.39 | 2046 |
| Noordwijk-2km | 1.22 | 0.69 | 189 | 1.50 | 0.42 | 193 | 1.92 | 0.22 | 206 |
| Noordwijk-10km | 1.70 | 0.59 | 286 | 1.71 | 0.38 | 303 | 0.94 | 0.14 | 294 |
| Noordwijk-80km | 0.49 | 0.54 | 178 | 0.53 | 0.42 | 196 | 1.82 | 0.17 | 180 |
| Terschelling-4km | -0.10 | 0.70 | 102 | 0.19 | 0.77 | 109 | 0.47 | 0.54 | 106 |
| Terschelling-50km | 0.12 | 0.76 | 101 | 0.31 | 0.72 | 109 | 3.01 | 0.17 | 45 |
| T36 | -0.08 | 0.86 | 16 | 0.32 | 0.72 | 18 | - | - | 0 |
| T26 | -0.04 | 0.87 | 34 | 0.48 | 0.75 | 39 | - | - | 0 |
| T41 | -0.17 | 0.91 | 35 | 0.01 | 0.50 | 41 | - | - | 0 |
| T8 | -0.32 | 0.79 | 36 | 0.05 | 0.81 | 40 | - | - | 0 |
| T2 | 0.57 | 0.94 | 14 | 0.35 | 0.97 | 14 | - | - | 0 |
| T22 | -0.06 | 0.60 | 29 | 0.49 | 0.69 | 31 | - | - | 0 |
| T5 | 0.32 | 0.83 | 13 | 0.31 | 0.90 | 15 | - | - | 0 |
| T12 | -0.08 | 0.77 | 27 | 0.44 | 0.68 | 30 | - | - | 0 |
| T11 | -0.02 | 0.81 | 14 | 0.48 | 0.76 | 17 | - | - | 0 |
| ICES–surface | 0.12 | 0.65 | 2690 | 0.02 | 0.58 | 2688 | 0.54 | 0.32 | 1280 |
| ICES–bottom | 0.04 | 0.72 | 932 | 0.08 | 0.65 | 933 | 0.68 | 0.31 | 355 |
| ESA–CCI M1-3+10-12 | - | - | - | - | - | - | 0.10 | 0.75 | 8542 |
| ESA–CCI M4-9 | - | - | - | - | - | - | 0.79 | 0.81 | 8502 |
| ESA–CCI M4-6 | - | - | - | - | - | - | 1.19 | 0.79 | 8445 |
| ESA–CCI M7-9 | - | - | - | - | - | - | 0.39 | 0.78 | 8408 |
| ESA–CCI M1-12 | - | - | - | - | - | - | 0.43 | 0.81 | 8515 |

~~on internal nutrient reserves (see section A1) but also indirectly emulates chemotactic migration as typical for dinoflagellates (Durham and Stocker, 2012). The critical dependence of the formation and maintenance of vertical chlorophyll structures on the functional representation of sinking underlines the relevance of an accurate description of the intracellular regulation of nutrient storages and pigmentory material.~~

### 3.2 Coastal Gradients

Temperature stratification is one of the key drivers of biogeochemical processes through its determining role on the resource environment, i.e., light and nutrient availability experienced by the primary producers. The comparison against Scanfish transect (Fig. 9) ~~indicated that our model can capture density stratification quite accurately~~showed that the physical model has the potential to realistically capture the density stratification. Using the temperature difference between surface and bottom layers as an indicator of temperature stratification (Schrum et al., 2003; Holt and Umlauf, 2008; van Leeuwen et al., 2015), and using monthly averages across all simulated years (2000-2010), ~~we illustrate~~ the areal extent and seasonality of stratification within the SNS is shown in Fig. 10. This analysis suggests that a large portion of the model domain deeper than ∼30 m becomes

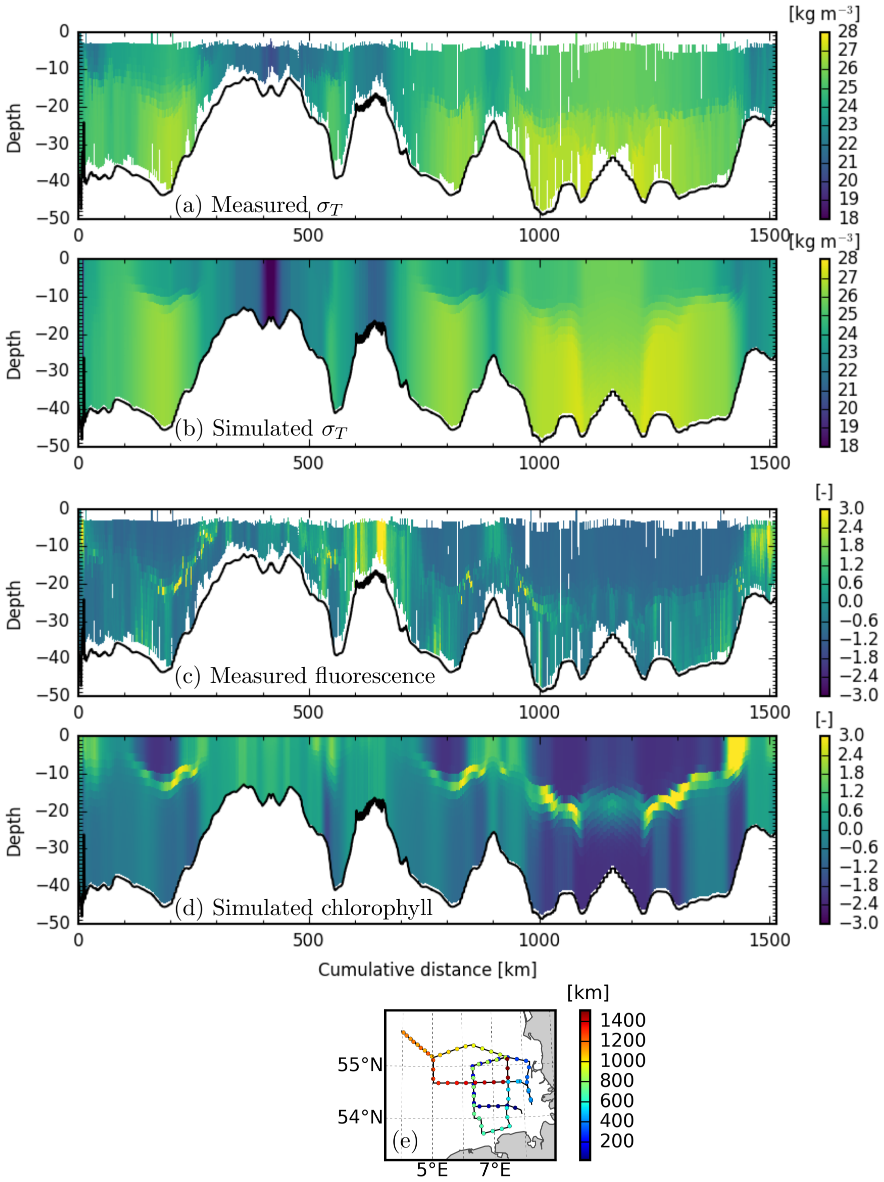

**Figure 9.** (a,b) $\sigma_T$, measured by Scanfish and estimated by the model (c,d) normalized anomalies of fluorescence measured by Scanfish and chlorophyll concentrations estimated by the model. Track of the cruise, which took place between 13-19 July 2010 is shown in (e).

stratified from April to September, with ~~maximum intensity and areal coverage in July. The areal extent and seasonality of stratification is in agreement with those reported by earlier studies (Schrum et al., 2003; van Leeuwen et al., 2015).~~ a maximum areal coverage and intensity (slightly above 8 K) in July.

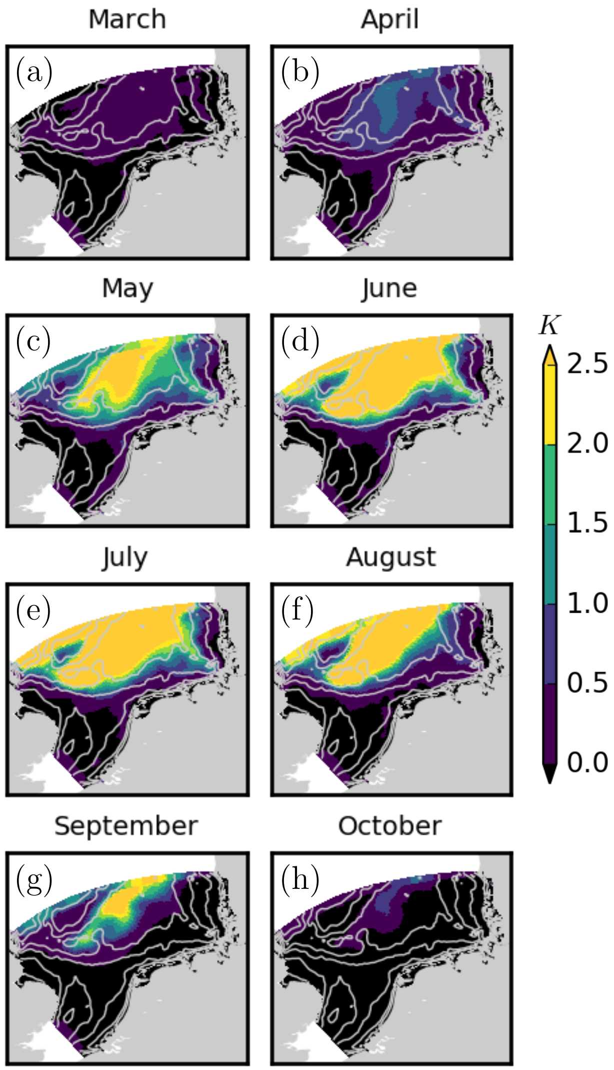

**Figure 10.** Average temperature difference [K] between the surface and bottom layers, averaged throughout 2000-2010 for each month. Gray lines show the isobaths.

~~Average winter concentrations of surface~~ Simulated climatological concentrations of DIN and DIP ~~for the entire simulation period display steep~~ display steep coastal gradients along the coasts of the German Bight (Fig. 11), ~~in line with observations (e.g., Brockmann et al., 1999). Given the riverine nutrient fluxes and uninterrupted nutrient supply from the bottom layers owed to the lack of stratification~~ both during the non-growing season (months 1-3 and 10-12) and the growing season (months 4-9). Within the ROFI (Region of Freshwater Influence, Simpson et al., 1993) of Rhine, nitrogen concentrations decrease about 5 fold (from $\geq 48$ mmolN m$^{-3}$ to 8-16 mmolN $^{-3}$) within a few grid cells, corresponding to about 10-15 km distance. In the

German Bight, non-growing season is similarly characterized by a thin stripe of high nutrient concentrations along the coast whereas during the growing season, especially phosphorus becomes depleted outside a confined zone of the Elbe plume. At the offshore areas, nutrient concentrations during the growing season are considerably lower than those during the non-growing season, driven by the phytoplankton growth, both directly by nutrient uptake and for the case of nitrogen also indirectly, by fueling denitrification in the sediment. The DIN:DIP ratio in the offshore regions is close to the Redfield molar ratio of 16:1 throughout the year reflecting oceanic conditions, while much higher at the coastal areas, particularly during the non-growing season, reflecting the high N:P content of the continental rivers (Radach and Pätsch, 2007). This transition from high coastal to low offshore N:P ratios is qualitatively consistent with observations (e.g., Burson et al., 2016).

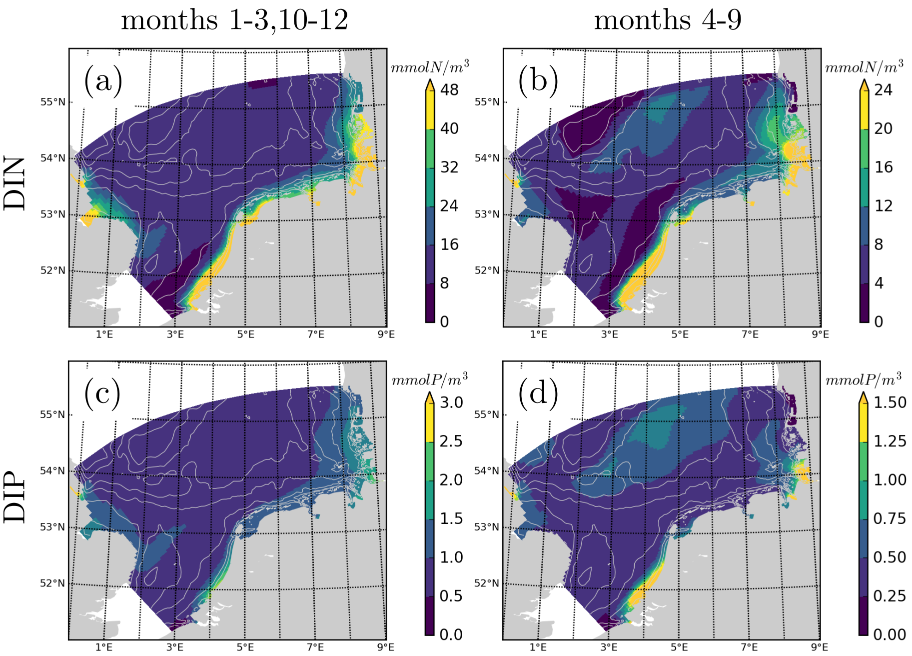

**Figure 11.** DIN (a,b) and DIP (c,d) concentrations at the surface layer, averaged over the non-growing (months 1-3 and 10-12, left) and growing seasons (months 4-9, right) for the entire simulation period (2000-2010). Concentrations at the bottom layer are almost identical for the months 1-3 and 10-12 and similar for the months 4-9. Gray lines show the isobaths. Note different color scales used for each panel, and that the scale used for DIN is 16 times that of DIP, such that identical coloring for DIN and DIP for the same season indicate a Redfield ratio of 16:1.

Both the satellite (ESA-CCI) images and our model estimates, averaged again for the non-growing and growing season, suggest steep coastal gradients in chlorophyll concentrations (Fig. 12) similar to the nutrient gradients shown above (Fig.~~10), it is not surprising that the surface nutrient concentrations are higher at the coasts, but the persistence of the phenomenon in the Wadden Sea regions that are not in close proximity to the riverine fluxes and~~ 11). The large scale agreement in coastal gradients result in high correlation coefficients (Fig. 12, Table 1). Normalized mean bias is small for the non-growing season but relatively high and positive (i.e., overestimation) for the growing season. Higher model estimates at the lower range (0-10 mgChl $m^{-3}$) is responsible for this positive bias, which is particularly the case during the first half of the growing season, where the bias is highest (Table 1).

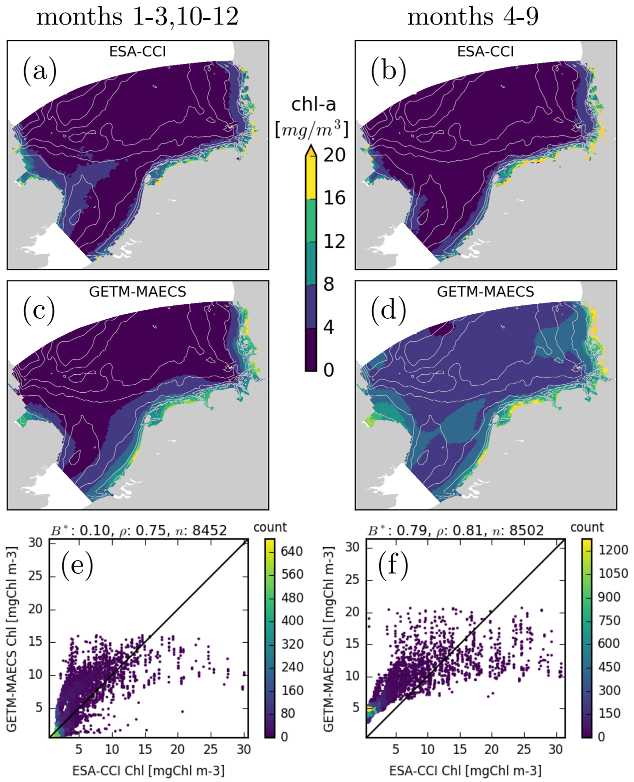

**Figure 12.** Comparison of satellite (ESA-CCI, a,b) and MAECS (c,d) estimates of surface chlorophyll concentrations averaged over 2008-2010 and for the non-growing (months 1-3 and 10-12, left) and growing seasons (months 4-9, right). 2-D histograms (e,f) show the number of occurrence of simulation-satellite data pairs. Gray lines in a-d show the isobaths. Normalized bias ($B^*$), Pearson correlation coefficients ($\rho$), and corresponding number of data points ($n$) are shown on top of scatter plots.

Our simulation results indicate significant spatio-temporal variability in Chl:C ratio, even when the seasonal averages are considered, i.e., omitting short-term variability (Fig. 13). Chl:C ratio is in general higher at the coasts than at offshore. Higher Chl:C ratios during the non-growing (months 10-12 and 1-3) season similarly reflect light limitation due to low amounts of incoming short wave radiation at the water surface. The simulated spatio-temporal differences in Chl:C ratios reach to about three fold between different seasons of the year and between offshore and coastal areas. The latter suggests that the differential acclimative state of phytoplankton cells amplify the steepness of ~~these gradients are not intuitively predictable. Steep cross-shore nutrient gradientswere partially explained by an interplay between density gradients and tidal mixing: during tidal flooding, high-salinity, therefore denser off-shore water sinks below the low-salinity, therefore lighter coastal water, thereby pushing the nutrient-rich bottom waters towards the coast (Ebenhöh, 2004; Burchard et al., 2008; Flöser et al., 2011; Hofmeister et~~

~~The relevant physical processes,i.e. tidal assymmetries in currents and mixing under coastal density gradients,and the accumulation of nutrients~~ the chlorophyll gradients across the coastal transition shown in Fig. 12.

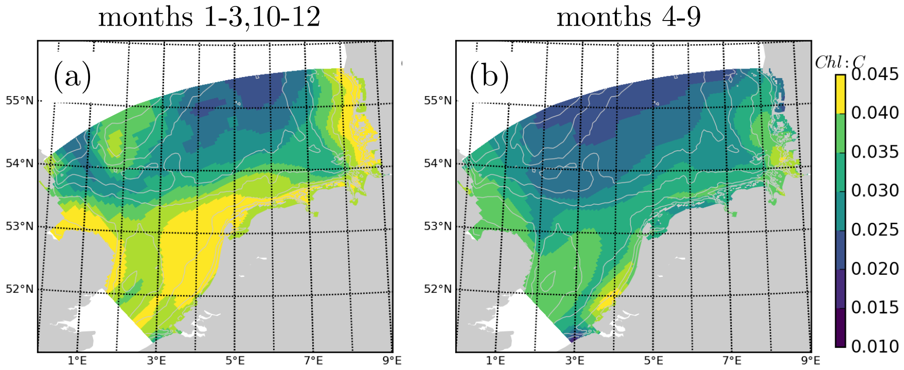

**Figure 13.** Chlorophyll:C ratio in phytoplankton, averaged over the non-growing (a) and growing season (b) of 2010. Gray lines in a-d show the isobaths.

For gaining a better understanding of the relevance of acclimation for capturing the coastal gradients, we considered a simplified, non-acclimative version of the model in which the resource utilization traits were fixed (see Appendix B3 for a detailed description), and two alternative parameterizations regarding the allocations to the light harvesting, nutrient acquisition and carboxylation machineries (which are state variables in the full model): first one with equal (balanced) allocation coefficients (=0.333), and a second one by assigning the spatio-temporal averages of the state variables integrated by the full (reference) model. Results of these two parameterizations were almost identical, so hereafter we will refer to the 'fixed' model in short, without specifying the particular parameterization.

The annual average coastal phytoplankton concentrations estimated by the acclimative model are much higher than those estimated by the fixed model, with no significant difference between the surface and water column averaged values (Fig. 14,a,b). In the offshore areas, the estimates of the acclimative model are higher than those of the fixed model at the surface (Fig. 14,a), but slightly lower when water column averages are considered (Fig. 14,b), indicating that the phytoplankton growth occurs mostly at the bottom layers in ~~off-shore waters are represented in the current model framework, so thatthis residual density-driven circulation mechanism is likely to be responsible for the emergence of steep nutrient gradients shown in~~ the fixed–trait model, which is consistent with the daily vertical profiles in the fixed–trait model (Fig. B4c). Importantly, these results suggest that, a coastal gradient in phytoplankton concentrations is predicted by a non-acclimative model, which is presumably driven by the nutrient gradients (Fig. 11~~. Productivity-enhanced aggregation of particulate organic matter with suspended sediments, and hence, higher sedimentation velocities within the coastal transition zone has recently been proposed to be another contributing factor for the maintenance of the coastal nutrient gradients (Maerz et al., 2016). This process has not been accounted for by our model, and representation of such a mechanism would necessitate explicit descriptions of mineral-POM interactions and variable sinking rate as a function of particle composition, structure and size (Maerz et al., 2011).~~

~~An exhaustive elaboration of the mechanisms for the maintenance of such gradients, their regional variability and steepness would be out of the scope of the current work, but constitutes a potential research goal for the future~~), but a much stronger gradient emerges when the acclimation processes are resolved. Specific to this example, towards the coast, phytoplankton adapt to the deteriorating light climate (Fig. B1) and increasing nutrient availability by investing more to the light harvesting machinery, as indicated by the increasing Chl:C ratios (Fig. 13), and thereby achieve higher coastal production rates than the case their physiology is fixed. As a result of increasing Chl:C ratios towards the coast, the chlorophyll concentrations display even a stronger gradient than that of the biomass: at the surface layer, increase of biomass concentrations towards the coast is about 3.5 fold (from about 10 to 35 mmolC/m$^3$), while that of the chlorophyll is about 7 fold (from about 2 to 14 mg/m$^3$) along the transect shown in Fig. 14).

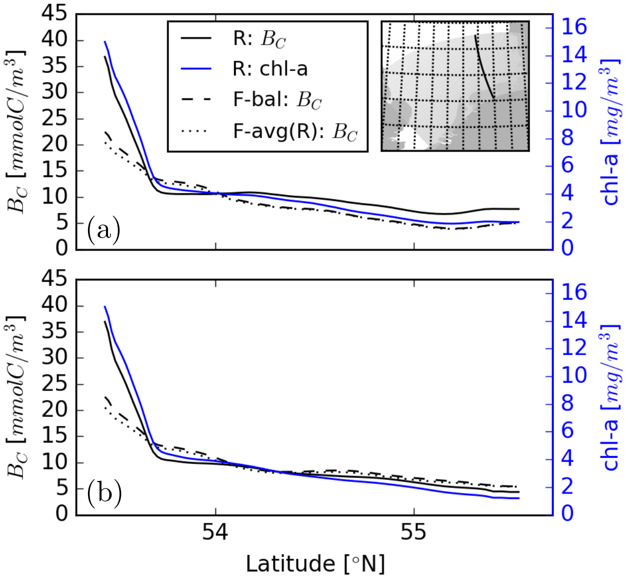

**Figure 14.** ~~Winter~~ Annual average phytoplankton carbon (~~January-February~~and for R, chlorophyll) ~~DIN~~ concentrations in 2010; (a) ~~and DIP~~ at the surface layer; (b) ~~concentrations~~ averaged over the ~~period 2000-2010~~ water column; obtained with R: reference (acclimative) model, F-bal: fixed-physiology model with balanced investments, F-avg(R): fixed-physiology model with allocation parameters as average trait values produced by R.

~~Interestingly, within the eastern portion of the model domain, the range of N:P ratios in DIM gradually decrease with bottom depth according to both the model estimates and ICES measurements~~

## 4 Discussion

In order to assess the performance of the new model system presented for the first time in this study, we employed several independent observation sources and types: FerryBox measurements to assess the horizontal distribution of salinity (Fig.

3); sparse in-situ measurements from the ICES dataset for an overall evaluation of the physical and biogeochemical model (Fig. 4, Fig. 8); measurements from 19 monitoring stations for evaluating the estimates for DIN, DIP and chlorophyll at specific locations (Fig. 5-7); Scanfish measurements for evaluating the vertical density and chlorophyll profiles (Fig. ~~12). Higher N:P ratios, which are mostly found at the shallower sites, i. e. , closer to the coast should be associated with the high N:P ratios at the continental rivers (Radach and Pätsch, 2007). Lower N:P ratios on the other hand, which, in a majority of cases, are recorded during the growth season , presumably results from a complex interplay between phytoplankton growth, sedimentation, denitrification and phosphorus absorption/desorption dynamics. The extent to which individual processes drive the regulation of water stoichiometry, and the implications of these changing external N:P ratios, e. g. , on the competition between different phytoplankton species, remain to be an open questions.~~ 9); and finally the satellite observations for evaluating the model skill regarding the horizontal distribution of climatological chlorophyll concentrations (Fig. 12) and attenuation of light (Fig. B1).

~~DIN:DIP ratio in water binned over 1 m bottom depth intervals according to ICES data (a,d) and matching MAECS results (b,e) at the surface (a-c) and bottom (d-f) layers, within the eastern portion of the model domain ($>$ 5°E, exact locations shown in c and f)~~ The physical model can provide a realistic description of the hydrodynamical processes foremost relevant for modeling the biogeochemistry of the system. Horizontal circulation patterns are captured as evidenced by the salinity distribution being in agreement with the observations (Fig. 3,4). Density structure of the system during summer, driven by a complex interplay between the salinity gradients, heat fluxes at the surface and tidal stirring is realistically captured, although the pycnocline depth seems to be underestimated (Fig. 9). Accordingly, temperature estimations match well with the observations, although there are cases where the stratification events are not reproduced by the model (Fig. 4), most of which are found to be within the western portion of the model domain. The areal extent and seasonality of stratification (Fig. 10) is in agreement with those reported by earlier studies (Schrum et al., 2003; van Leeuwen et al., 2015). For nutrient concentrations relative bias of $\leq$12% and correlation coefficients between 0.58-0.72 correspond to a high and moderate-high model skill, respectively (Table 1). For the pointwise comparisons of chlorophyll, model skill was moderate for the sparse measurements included in the ICES database, and for the stations in the German Bight (Table 1) but mostly low for the stations within the Western portion of the model domain. Comparison of climatological averages of the simulated chlorophyll with those of the satellite observations resulted in high correlations for all seasons, and low to moderate-low bias, except during the early growing season (Table 1.

~~Both the satellite (ESA-CCI)images and our model estimates, averaged over the years 2008-2010 for~~

The model captures the subsurface chlorophyll maxima occuring in the deeper parts of the model domain (Fig. 9). The phenomena has been previously documented in the southern North Sea (Weston et al., 2005; Fernand et al., 2013). Former 3-D modeling studies, such as that of van Leeuwen et al. (2013), apart from capturing the presence of a deep chlorophyll maximum, did not reproduce the rich variability revealed by the observations. Our comparative analysis shows that the formation and maintenance of such structures are critically dependent on the parametrization of the sinking rate of phytoplankton (Fig. B4a) and underwater light climate (Fig. B4b). Sinking speed of phytoplankton in the MAECS is inversely related to the nutrient quota of the cells, which mimics the internal buoyancy regulation ability of algae depending on internal nutrient reserves (see

Appendix A1) but also indirectly emulates chemotactic migration as typical for dinoflagellates (Durham and Stocker, 2012). This quota dependency of sinking results in considerable spatial variability, and significant differences between different seasons of the year (Fig. B3). The critical dependence of the formation and maintenance of vertical chlorophyll structures on the functional representation of sinking underlines the relevance of a consistent description of the intracellular regulation of nutrient storages. The latter, in turn, is determined by the metabolic needs, such as the intensity of light limitation, hence, investments to the synthesis of pigmentory material (Wirtz and Kerimoglu, 2016). Indeed, the ~~two halves of the growing season, suggest much higher concentrations within a thin coastal stripe relative to the off-shore concentrations~~ non-acclimative (fixed-trait) version of the model (Appendix B3) predicts qualitatively different vertical profiles of phytoplankton biomass (Fig. B4c), although the sinking parameterization in that simplified version is identical to that in the fully acclimative version. The non-acclimative model version might be tuned to match the observed vertical distributions of phytoplankton, however, this would probably be at the cost of compromised performance in some other respects, such as the horizontal gradients, or timing and amplitude of chlorophyll blooms. ~~The large scale agreement in coastal gradients result in high correlation coefficients, especially during summer (Fig.13). For the first half of the growing season, the higher range of~~

We conclude from the extensive model performance assessment that the model reproduces the main physical and biogeochemical characteristics of the southern North Sea especially within the German Bight, where the model resolution is finest (Fig. 1), and the influence of fluxes at the open boundaries is relatively small, given the predominantly counter-clockwise circulation pattern (Becker et al., 1992). The process of performance assessment also helped identifying the possibilities for further model refinement. For instance, a comparison with the satellite observations revealed that the light attenuation in the offshore areas is overestimated by the model, primarily because of the contributions by the climatological SPM forcing (Fig. B1). A likely consequence of the overestimated attenuation is an underestimation of the depth of primary production (e.g., Fig.B4b), and this may, in turn, explain the overestimated chlorophyll concentrations in the offshore areas during the growing season (Fig. 12b,d). Another source of error regarding the SPM-caused turbidity is that, at specific coastal sites, like at the Noordwijk-10 station, the measured suspended particulate material (SPM) concentrations show considerable inter-annual variations that can obviously be not represented by the climatological SPM forcing (Fig. B2), which may explain the particularly low correlation coefficient (0.14) obtained at this station for chlorophyll. A better representation of the SPM-caused turbidity might be achieved by an explicit description of the SPM dynamics (e.g., as in van der Molen et al., 2016). Coupling the biogeochemical model with such an SPM model would then also allow the description of the two-way interactions, i.e., not only light limitation (Tian et al., 2009), but also by the acceleration of sinking of SPM by the production of transparent exopolymer particles (Schartau et al., 2007; Maerz et al., 2016). At the stations within the ROFIs of major rivers, such as the Norderelbe and S. Amrum (Fig. 5) and Noordwijk–2&–10 (Fig. 6), the skill scores are relatively low (Table 1). These stations, especially the ~~modelled chlorophyll values exceed those of the ESA-CCI (Fig.13)~~Noordwijk–2 and –10 are located where the concentrations change dramatically within 10-15 km (e.g, Fig. 11). Accordingly, a slight error by the physical model in predicting the salinity front, e.g., because of an inadequate representation of the tidal dynamics, might result in considerable deviation of the estimated concentration of biogeochemical variables from the measurements. Relatively coarser model resolution at around the Dutch coast might therefore explain the consistently lower skill scores obtained at the Dutch stations. Identifying such potential inadequacies of the physical model requires further investigation, such as an assessment of the tidal constituents at the tidal gauges (e.g., Gräwe et al., 2016). Another potential source of error for the mismatches within the ROFIs is the potential flaws in the description of riverine loadings, such as assuming that the non-dissolved fractions of the total nitrogen and total phosphorus being entirely in labile form (Sect. 2.2.3). Although the earlier replenishment of phosphorus relative to nitrogen in the coastal sites is often reproduced (e.g., Sylt, Noordwijk-2, ~~which seems to be caused by underestimation by the satellite product, suggested by the fact that *in-situ* concentrations frequently reach well over 50 mg/m$^3$~~ Noordwijk-10, Terschelling-4), some delays occur in stations like Norderney, which probably reflects the oversimplification of the benthic processes with respect to the description of oxygen-driven iron-phosphorus complexation kinetics (Appendix A2), which has been suggested to be the main driver for the phenomena in the coastal areas (Jensen et al., 1995; van Beusekom et al., 1999; Grunwald et al., 2010).

The model predicts steep coastal gradients in nutrient concentrations (Fig. 11), in line with observations (e.g., Brockmann et al., 1999; Hy Maintenance of these gradients during winter is explained by the limited horizontal mixing due to the density gradients caused by the freshwater influx from the land (Simpson et al., 1993; Hydes et al., 2004), and trapping of this nutrient-rich freshwater at the coast due to the along-shore currents in the study system driven by predominantly westerly winds and the coriolis forcing (Becker et al., 1992; Simpson et al., 1993). During the warmer seasons when the offshore waters are stratified, owed to the presence of horizontal salinity gradients, a mechanism similar to the estuarine circulation (Simpson et al., 1990) was suggested to further promote these gradients along the Wadden Sea, also in regions far from river inputs (Burchard et al., 2008; Flöser et al., 2011; Hof Coastal waters remaining to be nutrient-replete during the growing season lead to high phytoplankton concentrations (Fig. 12) despite the higher turbidities at the coastal ~~stations in the German Bight~~ waters (Fig. ~~5). These lateral gradients in chlorophyll concentrations overlap with the nutrient (Fig.11), hence, productivity gradients (not shown) .~~ B1).

~~Comparison of satellite (ESA-CCI, a,b) and MAECS (c,d) estimates of surface chlorophyll concentrations averaged over 2008-2010 and for different seasonal intervals of the year. 2-D histograms (e,f) show the number of occurrence of simulation-satellite data pairs.~~

~~According to our simulation results of the year 2010, average~~

Comparison of the present model with earlier attempts is neither in the scope of this study, nor is possible without a dedicated benchmarking effort, using standardized forcing data and skill performance assessment datasets and methodology (e.g., as in Friedrichs et al., 2007). Even a qualitative comparison is difficult, given that spatial and temporal binning of the data, frequently employed in model validation (like in our Fig. 12), can dramatically impact the skill scores, and that pointwise comparisons with sparse observation datasets (like in our Fig. 4 and 8) are rarely performed (de Mora et al., 2013). However, skill of the presented model in estimating the chlorophyll concentrations in the SNS can argued to be at least comparable to those of the recent modelling applications for a relevant region (e.g., Edwards et al., 2012; de Mora et al., 2013; Ciavatta et al., 2016; Ford e This is noteworthy, given that phytoplankton is represented by a single species in our model, whereas in other modelling approaches, several species or groups are resolved. Inclusion of multiple functional types is motivated by the spatial and seasonal variability in the phytoplankton composition observed in the field: coastal areas of the SNS are dominated by diatoms, throughout the year in some sites (e.g., Alvarez-Fernandez and Riegman, 2014), and during spring in some others, later to be replaced by *Phaeocystis* during summer (e.g., van Beusekom et al., 2009), whereas the offshore areas are often dominated by dinoflagellates especially during summer (Freund et al., 2012; Wollschläger et al., 2015). These phytoplankton groups differ from each other by a number of traits, including the physiological traits that determine their ability to access the (mineral and light) resources and build biomass. For instance, in an experimental work, two diatom species were shown to have on average more than three fold higher Chl:C ~~ratio displays considerable spatio-temporal variability, even when the seasonal averages are considered, i. e. , omitting short-term variability (Fig.14) .~~ ratios than those of two dinoflagellate species (Chan, 1980), making them therefore more tolerant to the light-limited conditions of the turbid, coastal waters. In the presented approach, the cellular composition of the single, but acclimative phytoplankton group dynamically approaches towards (for some traits, instantaneously adopt) the physiological state of the ideal resource competitor in a given environment, which, in nature, happens through various processes from the plastic response of the individual cells to the species sorting at the community level. In a traditional, functional plankton type (PFT) model on the other hand, the species with most suitable traits will become the most dominant among others, while the proximity of the physiological traits to the theoretical optima, thus the overall productivity will be determined by the resolution of physiological traits as represented by the defined clones. The worst case is when there is only one, non-acclimative group, as illustrated in our experiment: at the turbid but nutrient–rich coastal areas, prioritization of the light harvesting over the nutrient acquisition machinery, as evidenced by the higher Chl:C ~~ratio is in general higher at the coasts than at off-shore. This pattern~~ ratios predicted by the acclimative model (Fig. 13), leads to better fitness, thus higher phytoplankton concentrations in comparison to the non-acclimative equivalents (Fig. 14). Moreover, because of the high Chl:C ratios at the coastal areas (Fig. 13), chlorophyll concentrations display even steeper gradients than the phytoplankton concentrations (Fig. 14). The transitional Chl:C pattern suggested by our model has been previously identified based on monitoring data by Alvarez-Fernandez and Riegman (2014)~~, and reflects the photoacclimative response to stronger light limitation at the coasts, manifested by both higher organic matter (not shown, but see Fig.13 for chlorophyll concentrations) and SPM concentrations. Higher~~. The Chl:C ratios ranging between 0.01-0.1 gChl/gC at the coastal stations and 0.002-0.02 gChl/gC at the offshore stations reported by Alvarez-Fernandez and Riegman (2014) envelope our estimated seasonal average values of 0.045 and 0.015 within the respective regions. According to the simulation results, Chl:C ratios ~~during~~ differ considerably also between the non-growing ~~(months 10-12 and 1-3) seasonsimilarly reflects light limitation~~ and growing season, with higher values during winter, due to low ~~amounts of incoming short wave radiation at the water surface and increased turbidity due to stronger vertical mixing near the coast~~light availability. A similar seasonal amplitude in ~~CHL~~Chl:C has been found by Llewellyn et al. (2005) for the English Channel ~~. Slightly higher Chl:C ratios during the first half of the growing season compared to the second half are likely due to lower nutrient concentrations during the second half, which results in larger investments in nutrient harvesting in the expense of light-harvesting machinery (see, e.g., Geider et al., 1997; Pahlow, 2005; Wirtz and Kerimoglu, 2016). The modeled spatio-temporal differences in Chl:C ratios reach to about three fold between different seasons of the year and between off-shore and coastal areas. The latter indicates that the differential acclimative state of phytoplankton cells amplify the steepness of the chlorophyll gradients across the coastal transition shown in Fig. 13, which, as mentioned above, seem to be driven mainly by nutrient gradients. This is significant, and calls for further attention, especially given that many modelling schemes applied at ecosystem-scales do not consider photoacclimation processes. As Behrenfeld et al. (2015) recently pointed out from a global perspective, satellite-based~~

~~primary productivity estimates can be misleading when they do not take the variability in Chl:C into account . Our results suggest that this caveat holds for the coastal ocean, characterized by relatively high production rates~~with higher ratios during winter.

As mentioned above, physiological composition is not the only relevant trait for determining the community composition in the study system. Diatoms are fast growers and defended against the efficient microzooplankton grazers, but this comes at the cost of silicate requirement for their growth (Loebl et al., 2009) and higher sedimentation losses (Riegman et al., 1993). *Phaeocystis* are slow growers, but by forming large colonies, they are well defended against zooplankton (Peperzak et al., 1998). Finally, the dinoflagellates, also despite being slow growers, are mobile (Durham and Stocker, 2012) and mostly have access to alternative nutrient sources through their phagotrophic abilities (Löder et al., 2012). Representation of zooplankton with a single group may also be an oversimplification, as the microzooplankton and mesozooplankton have considerably different growth rates (Hansen et al., 1997) and functional responses to prey availabilities (Kiørboe, 2011). Moreover, effects of temperature on mesozooplankton occurs through phenological shifts (e.g., Greve et al., 2004) that might have a determining role on the maximum chlorophyll concentrations (van Beusekom et al., 2009), which can probably be only partially reflected by the simple Q10 rule we applied for grazing rates (Appendix A1). None of these ecophysiological aspects were taken into account in our model, and this may explain some of the discrepancies between the simulated and observed chlorophyll concentrations. In future work, inclusion of few other phytoplankton groups –each being acclimative, and one additional zooplankton group is foreseen. While the consideration of other phytoplankton traits should be straightforward, inclusion of phagotrophy as an additional physiological allocation trait represented by a state variable is possible (e.g., as in Chakraborty et al., 2017), but would require re-derivation of the model equations.

~~Chlorophyll:C ratio in phytoplankton, averaged over non-growing (a) and two halves of the growing season (b,c) of 2010.~~

## 5 Conclusions

In this study, we described the implementation of a coupled physical-biogeochemical model to the Southern North Sea (SNS) and analyzed the model results in comparison to a large collection of *in-situ* and remote sensing data. The model system accounts for key coastal processes, such as the forcing by local atmospheric conditions, riverine loadings of inorganic and organic material, atmospheric nitrogen deposition, spatio-temporal variations in the underwater light climate, major benthic processes and nutrient concentrations at open boundaries, and importantly, it hosts a novel model of phytoplankton growth, which replaces otherwise heuristic formulations of photosynthesis and nutrient uptake with mechanistically sound ones (Wirtz and Kerimoglu, 2016). Based on comparisons with a number of data sources, we conclude that the model system can produce a realistic decadal hindcast of the ~~SNS~~ German Bight for the period 2000-2010, in terms of both the temporal and spatial distribution of key ecosystem variables, as well as a large area of validity, i.e., both in coastal and ~~off-shore~~ offshore regions of the German Bight.

~~We emphasize that even the phytoplankton concentrations are generally well captured by our model, considering the systematic difficulties in reproducing chlorophyll concentrations by ecosystem models in general (see, e.g., Radach and Moll, 2006).~~

~~This is noteworthy, given that phytoplankton is represented by a single species in our model, whereas in reality the phytoplankton composition displays systematic shifts throughout the season: the early spring composition is usually dominated by diatoms while other species or groups usually become more abundant later in the year, such as *Phaeocystis* at coastal regions (eg., van Beusekom et a dinoflagellates off-shore (Freund et al., 2012; Wollschläger et al., 2015). We argue that the ability of our model to capture both the spring and summer is, to a great extent, owed to the fact that photoacclimation and optimality in nutrient uptake processes were accounted for. In reality, environmental change, e.g., improvement of light conditions and depletion of nutrient concentrations from spring to summer, promotes the species which have more suitable traits, e.g., regarding light and nutrient utilization.~~ In 3-D model applications so far, photoacclimation of phytoplankton has been either ignored altogether, or it was accounted for in a heuristic sense, where the change in Chl:C ratio is described based on an empirical relationships (Blackford et al., 2004; Fennel et al., 2006). In our model, adaptation of the phytoplankton community to the light and nutrient environment is represented by dynamically changing and instantaneously optimized trait values as described extensively by ~~(Wirtz and Kerimoglu, 2016). Other potentially relevant selection factors, such as the changes in the community structure of heterotrophic grazers (Alvarez-Fernandez et al., 2012; Löder et al., 2012; Beaugrand et al., 2014) or limitation of diatoms by silicate (Loebl et al., 2009) are omitted in this study, and remain to be future research goals, along with other model refinements like improving the descriptions of the benthic processes and benthic-pelagic exchange, light climate as a function of SPM dynamics and composition of riverine nutrient fluxes.~~

Wirtz and Kerimoglu (2016). Our findings suggest that the steep chlorophyll gradients across the coastal transition zone is mainly driven by the nutrient gradients, but amplified ~~by the~~ first by the acclimative capacity, then further by higher Chl:C ratios at the coastal waters. The large variations in simulated Chl:C ratios within the SNS, both in a space and time, indicate that ~~ignorance of~~ ignoring photoacclimation can lead to potentially flawed estimates for primary production or phytoplankton biomass as was recently pointed out by Arteaga et al. (2014) and Behrenfeld et al. (2015), ~~who used photoacclimation schemes to derive~~ based on the variability of Chl:C ratios at global scales. Here we show that ~~such considerations apply also at coastal environments~~ this warning applies especially in the coastal environments characterized by steep resource gradients, which may be critical, given the increasing recognition of the role of coastal-shelf systems in the global carbon and nutrient cycling (Fennel, 2010; Bauer et al., 2013).

## Appendix A: Detailed Model Description

### A1 Pelagic Module

Local source-sink terms for all dynamic variables, functional description of processes and relationships between quantities and parameters used for the pelagic module are provided in ~~Tab.~~ Table A1–A3.

Importantly, the biogeochemical model resolves photoacclimation of phytoplankton, described by dynamical partitioning of resources to light harvesting pigments (Eq. A7), enzymes involved in carboxylation reactions (Eq. A8) and nutrient uptake sites (i.e., $f_{LH} + f_C + f_V = 1$) as in Wirtz and Pahlow (2010). Uptake of each nutrient is optimally regulated (as expressed by $a_i$ in Eq. A16~~–~~-A17), and following Pahlow (2005); Smith et al. (2009), optimality along the affinity-intracellular transport trade-off ($A_i = f_i^A \cdot A_i^*$ and $V_{max,i} = (1 - f_i^A) \cdot V_{max,i}^*$, see Table A3 for the definition of parameters). As a second novelty, the growth model uniquely describes the interdependence between limiting nutrients to be variable between full inter-dependence (as in product rule) and no-interdependence (as in Liebig's law of minimum) as a function of nitrogen quota (See Eq. A13). For a detailed explanation of the phytoplankton growth model and solution of differential expressions in Eq. A7,A8 and A17 refer to Wirtz and Kerimoglu (2016). For enabling the spatial transport of the 'property variables' of phytoplankton such as $Q_i$, $f_{\mathrm{LH}}$ and $f_{\mathrm{LH}}$, they have been transformed to bulk variables by multiplying with the phytoplankton carbon biomass, i.e., $B_{\mathrm{C}}$. Parameterization of the phytoplankton model, except $\theta_C$, fall within the range of ~~values used for the species considered~~ parameter values used by Wirtz and Kerimoglu (2016). The exact values of the parameters were established by manual tuning, given that important phytoplankton species such as various diatom and dinoflagellate species, and *Phaeocystis* sp. that dominate the phytoplankton composition in the SNS (eg., Wiltshire et al., 2010) have not been studied formerly within the presented model framework.

Phytoplankton losses are due to aggregation and zooplankton grazing (see below). Specific aggregation loss rate (Eq. A19) is described as a function of DOC that mimics transparent exopolymer particles (Schartau et al., 2007) to account for particle stickiness, multiplied by the sum of phytoplankton biomass and of POM reflecting density dependent interaction, which is equivalent to a quadratic loss term. Zooplankton dynamics are described only in terms of their carbon content, assuming stoichiometric homeostasis (Sterner and Elser, 2002). Grazing is described by a Holling Type-3 function of prey concentration (Eq. A20). A lumped loss term accounts for the respiratory losses and exudation of N and P in dissolved inorganic form (Eq. A21), which are adjusted depending on the balance between the stoichiometry of zooplankton and that of the ingested food for maintaining the homeostasis (Eq. A22). ~~Effect of the~~ The effect of organisms at higher trophic levels, mainly by fish and gelatinous zooplankton are mimicked by a density-dependent mortality of zooplankton, modified by a function of total attenuation of Photosynthetically Available Radiation (PAR) (Eq. A23) to account for higher predation pressure exerted by fish at the ~~off-shore~~ offshore regions of the North Sea, which amounts to about two times that in the coastal regions according to the estimates based on trawl surveys (Maar et al., 2014).

~~Settling velocity of POM, expressed by $w_{POM}$ is prescribed as a constant value, whereas that of phytoplankton, $w_B$ is assumed to be modified by their nutrient (quota) status. As decreased internal nutrient quotas likely affect the cells ability to regulate buoyancy and lead to faster migration towards deeper, potentially nutrient rich waters (Boyd and Gradmann, 2002), we assume that maximum sinking rates realized at fully depleted quotas approach to a small background value with increasing quotas as has been observed especially for, but not limited to, diatoms (Smayda and Boleyn, 1965; Bienfang and Harrison, 1984).~~

~~Finally, all~~ All kinetic rates were modified for ambient water temperature, T (K) using the Q10 rule parameterized specifically for autotrophs and small heterotrophs (=bacteria for hydrolysis and remineralization) and for zooplankton.

## A2 Benthic Module

The benthic module provides simplistic descriptions of the degradation of N and P from POM to DIM, their fluxes across the benthic-pelagic interface, removal of N due to denitrification and accounts for the sorption dynamics of P.

**Table A1.** Source-sink terms of the dynamic variables of the pelagic module. The index $i$ represents the elements C, N, P. By definition, $Q_\mathrm{C} = Q_\mathrm{C}^Z$=1, $Q_i$=$B_i$/$B_\mathrm{C}$. Dynamics of Dissolved Inorganic Carbon (DIC) is not resolved, thus (Eq. A4) not integrated for $i$=C. Description of processes or functional relationships (capital letters) and of parameters (small letters) are provided in Tables A2 and A3, respectively.

| | | | |
|---|---|---|---|
| Autotrophic biomass | $s(B_\mathrm{C})$ | $= (V_\mathrm{C} - \sum_i V_i \zeta_i - L_A) \cdot B_\mathrm{C} - G \cdot Z_\mathrm{C}$ | (A1) |
| Internal quota | $s(Q_i)$ | $= V_i - V_\mathrm{C} Q_i$ | (A2) |
| Zooplankton | $s(Z_\mathrm{C})$ | $= (\gamma G - M - L_Z) \cdot Z_\mathrm{C}$ | (A3) |
| Dissolved inorganics | $s(\mathrm{DIM}_i)$ | $= L_Z Z_\mathrm{C} Q_i^Z + r_\mathrm{DOM}\, \mathrm{DOM}_i - V_i\, B_\mathrm{C}$ | (A4) |
| Dissolved organics | $s(\mathrm{DOM}_i)$ | $= r_\mathrm{POM}\, \mathrm{POM}_i - r_\mathrm{DOM} \mathrm{DOM}_i$ | (A5) |
| Particulate organics | $s(\mathrm{POM}_i)$ | $= L_A B_\mathrm{C} Q_i + (1-\gamma) G Z_\mathrm{C} Q_i + M Z_\mathrm{C} Q_i^Z - r_\mathrm{POM} \mathrm{POM}_i$ | (A6) |
| Carboxylation (Rub) | $s(f_\mathrm{C})$ | $= \delta_\mathrm{C} \cdot \left( \frac{\partial V_\mathrm{C}}{\partial f_\mathrm{C}} + \sum_i \frac{\partial V_\mathrm{C}}{Q_i} \frac{\mathrm{d}Q_i}{\mathrm{d}f_\mathrm{C}} \right)$ | (A7) |
| Pigmentation (Chl) | $s(f_\mathrm{LH})$ | $= \delta_\mathrm{LH} \cdot \left( \frac{\partial V_\mathrm{C}}{\partial f_\mathrm{LH}} + \sum_i \frac{\partial V_\mathrm{C}}{\partial Q_i} \frac{\mathrm{d}Q_i}{\mathrm{d}f_\mathrm{LH}} \right)$ | (A8) |

POM degrades into DIM in one step, described as a first order reaction, the rate of which is modified for temperature using the Q10 rule. POM flux into the sediments by settling of material from the water fuels the benthic POM (bPOM) (Eq.A4). On the other hand, diffusive flux of DIM is possibly bi-directional, depending on the concentration gradient between water and soil (Eq. A4). Inorganic phosphorus (denoted as TIP,(Eq. A4) is assumed to exist in two states: sorbed and dissolved state. Fraction of the sorbed state is given by a function of dissolved oxygen (DO), to account for the production and adsorption of Fe-P complexes in oxic conditions and their desorption at anoxic conditions (Eq. A4). Given the observed inverse relationship between temperature and oxygen concentrations in sediments ~~(eg., Jensen et al., 1995)~~(e.g., Jensen et al., 1995), DO is heuristically estimated as a function of temperature ($T$) to capture the seasonal hypoxia events. Resulting functional relationships between the sorbed fraction of TIP, T and DO are shown in Fig. A1(a-b). Following the simplistic approach used for the ECOHAM model (Pätsch and Kühn, 2008), denitrification rate is estimated from the degradation rate (Eq. A4) using empirically derived ratios and stoichiometric conversions, considering in addition the limitation imposed by the available DIN and inhibition by DO (Soetaert et al., 1996). Resulting functional relationships between denitrification, T and DO are shown in Fig. A1(c-d).

**Table A2.** Process descriptions and functional relationships. The index $i$ represents the elements C, N and P. The index $j$ represents groups with different Q10 values. Description of parameters (small letters) are provided in ~~Tab.~~ Table A3.

| | | | |
|---|---|---|---|
| Carbon uptake | $V_{\mathrm{C}}$ | $= P \cdot g_n\left(\mathcal{C}_n\left(q_{\mathrm{N}}, \mathcal{C}_n\left(q_{\mathrm{P}}, q_{\mathrm{C}}\right)\right)\right) - \sum_i \zeta_i V_i$ | (A9) |
| Light lim. primary prod. | $P$ | $= f_{\mathrm{C}}\, P_{\mathrm{max}} \cdot \left(1 - \mathrm{e}^{-\alpha\theta \mathrm{PAR}/P_{\mathrm{max}}}\right)$ | (A10) |
| Chlorophyll conc. in chloroplasts | $\theta$ | $= \theta_{\mathrm{C}} \frac{f_{\mathrm{LH}}}{q_{\mathrm{N}}\, f_{\mathrm{C}}}$ | (A11) |
| Relative resource availability | $q_i$ | $= \frac{Q_i - Q_i^0}{Q_i^* - Q_i^0}$ | (A12) |
| Co-limitation function | $\mathcal{C}_n(q_i, q_j)$ | $= q_i \cdot g_n\left(\frac{q_j}{q_i}\right) \cdot \left(1 + \frac{q_i q_j}{n} + log(4^{-1/n} + 0.5/n)\right)$ | (A13) |
| Queuing function | $g_n(r)$ | $= \frac{r - r^{1+n}}{1 - r^{1+n}}$ | (A14) |
| Degree of independence | $n$ | $= n^* \cdot (1 + q_{\mathrm{N}})$ | (A15) |
| Nutrient uptake | $V_i$ | $= f_{\mathrm{V}}\, a_i \cdot \left(V_{\mathrm{max},i}^{-1} + (A_i \mathrm{DIM}_i)^{-1}\right)^{-1}$ | (A16) |
| Uptake activity | $a_i$ | $= \left(1 + \mathrm{e}^{-\tau_{\mathrm{V}} \frac{\mathrm{d}V_{\mathrm{C}}}{\mathrm{d}a_i}}\right)^{-1}$ | (A17) |
| Flexibility ($X$ =C, LH) | $\delta_X$ | ~~$= (f_X - f^{\mathrm{min}}) \cdot (1 - f^{\mathrm{min}} - f_{\mathrm{C}} - f_{\mathrm{LH}})$~~ $= f_X \cdot (1 - f_X)$ | (A18) |
| Losses due to aggregation | $L_A$ | $= L_A^* \cdot \left(\frac{a_{DOC}\mathrm{DOM_C}}{1 + a_{DOC}\mathrm{DOM_C}}\right) \cdot \left(B_{\mathrm{N}} + \mathrm{POM_N}\right)$ | (A19) |
| Grazing | $G$ | $= G_{max} \frac{B_{\mathrm{C}}^2}{K_G^2 + B_{\mathrm{C}}^2}$ | (A20) |
| Zooplankton loss | $L_Z$ | $= m_r Q_i^Z - S +$ max(0,$\gamma G(Q_i - Q_i^Z)$) | (A21) |
| Zooplankton homeostatic adjustment | $S$ | $=$ if $(m_r Q_i^Z + \gamma G(Q_i - Q_i^Z)) < 0$: $(1-\gamma)GQ_i$; else:0 | (A22) |
| Zooplankton mortality | $M_i$ | $= m_f \cdot \left(1 + \Delta_f \cdot \left(1 - \left(1 + \mathrm{e}^{s_k \cdot (k_{tot}^* - k_{tot})}\right)^{-1}\right)\right) \cdot Z_{\mathrm{C}}$ | (A23) |
| Total PAR attenuation | $k_{tot}$ | $= -\frac{z}{\eta_2} - \int_z^0 \sum_i k_{c,i} c_i(z')dz'$ | (A24) |
| Phytoplankton sinking | $w_B$ | $= w_B^0 + w_B^* \mathrm{e}^{-s_w q_N q_P}$ | (A25) |
| Temperature dependence | $F_T^j$ | $= Q10_j^{(T - T_{\mathrm{ref}}/10)}$ | (A26) |

**Table A3.** Parameters of the pelagic module. Codes for sources: c: calibrated; a: assumed; l: typical literature value; d: by definition; 1:Wirtz and Kerimoglu (2016); 2:Hansen et al. (1997, for copepods); 3:Oubelkheir et al. (2005); 4:Stedmon et al. (2001); 5:Maar et al. (2014)

| Symbol | Description | Value | Unit | Source |
|---|---|---|---|---|
| Parameters relevant to phytoplankton | | | | |
| $\alpha$ | Light absorption coefficient | 0.2 | $m^2$ mmolC(µE gCHL)$^{-1}$ | 1,c |
| $A_{\mathrm{P}}^*$ | Affinity to $PO_4$ | 0.15 | $m^3$(mmolC d)$^{-1}$ | 1,c |
| $A_{\mathrm{N}}^*$ | Affinity to inorganic N | 0.4 | $m^3$(mmolC d)$^{-1}$ | 1 |
| $P_{\mathrm{max}}^*$ | Potential photosynthesis rate | 9.0 | $d^{-1}$ | 1,c |
| $\theta_{\mathrm{C}}$ | CHL-a/C ratio in chloroplasts | 1.0 | gChl molC$^{-1}$ | c |
| $Q_{\mathrm{N}}^0$ | Subsistence quota for N | 0.035 | molN molC$^{-1}$ | 1,c |
| $Q_{\mathrm{P}}^0$ | Subsistence quota for P | 0.0 | molP molC$^{-1}$ | 1 |
| $Q_{\mathrm{N}}^*$ | Reference N quota | 0.17 | molN molC$^{-1}$ | 1,c |
| $Q_{\mathrm{P}}^*$ | Reference P quota | 0.0055 | molP molC$^{-1}$ | 1 |
| $n^*$ | specific independence | 4.0 | - | 1,c |
| $V_{\mathrm{max,N}}^0$ | Potential N uptake rate | 1.0 | molN (mmolC d)$^{-1}$ | 1,c |
| $V_{\mathrm{max,P}}^0$ | Potential P uptake rate | 0.1 | molP (mmolC d)$^{-1}$ | 1,c |
| $\zeta_N$ | C cost of N assimilation | 4.0 | molC molN$^{-1}$ | 1,c |
| $\zeta_P$ | C cost of P assimilation | 24.0 | molC molP$^{-1}$ | 1,c |
| $\tau_{\mathrm{v}}$ | Relaxation time scale for $a_i$ | 10 | d | 1 |
| ~~$f^{\mathrm{min}}$ Minimum allocation 0.02- 1~~ $w_B^*$ | Maximum quota-dependent sinking rate | 3.0 | m $d^{-1}$ | c |
| $w_B^0$ | Background sinking rate | 0.2 | m $d^{-1}$ | c |
| $s_w$ | Scaling coefficient for sinking function | 4.0 | - | c |
| $L_A^*$ | Maximum aggregation rate | 0.003 | molC molN$^{-1}$ | c |
| $a_{DOC}$ | DOC specific aggregation coefficient | 0.1 | mmolC $m^{-3}$ | c |
| $Q10_B$ | Q10 coefficient for autotrophs and bacteria | 1.5 | - | 1 |

(continued on the next page)

(continues from the previous page)

| Symbol | Description | Value | Unit | Source |
|---|---|---|---|---|
| Parameters relevant to zooplankton | | | | |
| $Q_N^Z$ | N:C ratio | 0.25 | molN molC$^{-1}$ | 1 |
| $Q_P^Z$ | P:C ratio | 0.02 | molP molC$^{-1}$ | 1 |
| $G_{max}$ | Max. grazing rate | 1.2 | d$^{-1}$ | 2 |
| $\gamma$ | Assimilation efficiency | 0.35 | - | 2 |
| $K_G$ | Half saturation constant for grazing | 20.0 | mmolC m$^{-3}$ | 2 |
| $m_r$ | Basal respiration rate | 0.02 | d$^{-1}$ | 1 |
| $m_f$ | Base mortality rate | 0.02 | m$^3$ (mmolC d) $^{-1}$ | c |
| $\Delta_f$ | Maximum incremental mortality factor | 1.0 | - | 5 |
| $k_{tot}^*$ | Critical total PAR attenuation | 0.4 | m$^2$ mmolC$^{-1}$ | c |
| $s_k$ | Scaling coefficient for mortality function | 10.0 | mmolC m$^{-2}$ | c |
| $Q10_Z$ | Q10 coefficient for zooplankton | 2.0 | - | 1 |
| Other biogeochemical parameters | | | | |
| $T_{\text{ref}}$ | Reference temperature for kinetic rates | 288 | K | d |
| $w_{POM}$ | Sinking rate of POM | 6.0 | m d$^{-1}$ | c |
| $r_{POM}$ | Hydrolysis rate | 0.03 | d$^{-1}$ | c |
| $r_{DOM}$ | Remineralization rate | 0.03 | d$^{-1}$ | c |
| $k_B$ | Attenuation coefficient for phytoplankton | 0.015 | m$^2$ mmolC$^{-1}$ | 3 |
| $k_{POC}$ | Attenuation coefficient for POC | 0.01 | m$^2$ mmolC$^{-1}$ | 3 |
| $k_{DOC}$ | Attenuation coefficient for DOC | 0.0025 | m$^2$ mmolC$^{-1}$ | 4 |

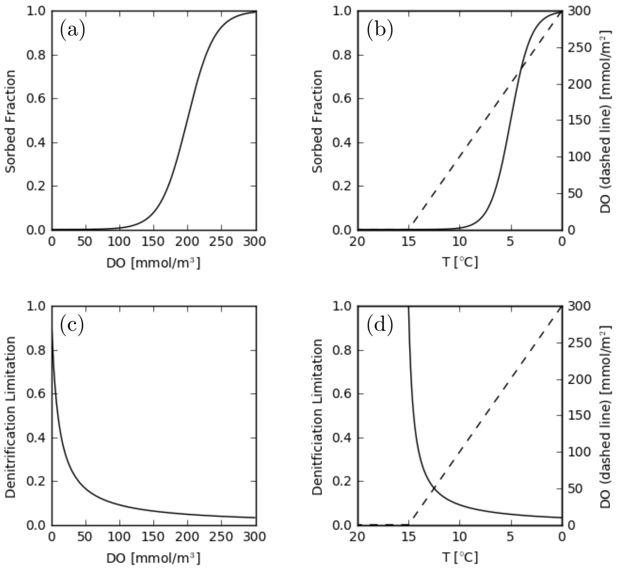

**Figure A1.** Fraction of sorbed fraction of benthic phosphorus as functions of DO (a) and T (b), regulation of benthic denitrification rate as functions of DO (c) and T (d), and DO as a function of T (b,d).

**Table A4.** Source-sink terms of the dynamic variables, and functional relationships of the benthic module. sDIM$_{\mathrm{X}}$=sDIX and sPOM$_{\mathrm{X}}$=sPOX, where X={N,P}. Description of parameters (small letters) are provided in ~~Tab.~~TableA5

| | | | |
|---|---|---|---|
| Dynamics: | | | |
| Benthic POM | $s(\mathrm{bPOM}_i)$ | $= E_{\mathrm{POM}} - R_{\mathrm{i}}$ | |
| Benthic TIP | $s(\mathrm{bTIP})$ | $= E_{\mathrm{DIP}} + R_{\mathrm{P}}$ | |
| Benthic DIN | $s(\mathrm{bDIN})$ | $= E_{\mathrm{DIN}} + R_{\mathrm{N}} - \Upsilon$ | |
| Functional relationships: | | | |
| Benthic Remineralization rate | $R_{\mathrm{i}}$ | $= r_B \cdot \mathrm{sPOM_i}$ | (A27) |
| POM exchange with water | $E_{\mathrm{POX}}$ | $= \psi_{POM} * POM$ | (A28) |
| DIM exchange with water | $E_{\mathrm{DIX}}$ | $= D_{DIM} \cdot \frac{\mathrm{DIM}-\mathrm{bDIM}}{\Delta_Z}$ | (A29) |
| Fraction of inorganic P in dissolved phase | bDIP | $= 1 - \mathrm{bAP}$ | (A30) |
| Fraction of inorganic P in adsorbed phase | bAP | $= \left(1 + \mathrm{e}^{s_a \cdot (\mathrm{bDO}^* - \mathrm{bDO})}\right)^{-1}$ | (A31) |
| Denitrification | $\Upsilon$ | $= c_{O:N} c_{N:O} R_{\mathrm{N}} \cdot \left(\frac{\mathrm{bDIN}}{K_{\Upsilon,DIN} + \mathrm{bDIN}}\right) \cdot \left(1 - \frac{\mathrm{bDO}}{K_{\Upsilon,DO} + \mathrm{bDO}}\right)$ | (A32) |
| Benthic dissolved oxygen | bDO | $= 300.0 - c_{DO} * T$ | (A33) |
| Temperature dependence | $F_T^b$ | $= Q10_b^{(T - T_{\mathrm{ref}}/10.0)}$ | (A34) |

**Table A5.** Parameters of the benthic module. Codes for sources: c:calibrated; a:assumed; l: typical literature value; 1:Soetaert et al. (1996); 2:Seitzinger and Giblin (1996)

| Symbol | Description | Value | Unit | Source |
|---|---|---|---|---|
| $r_b$ | Benthic degradation rate | 0.05 | $\mathrm{d}^{-1}$ | c |
| $\psi_{POM}$ | Sinking velocity of POM across the benthic-pelagic interface | 3.0 | $\mathrm{d}^{-1}$ | c |
| $D_{DIM}$ | Diffusivity of DIM across the benthic-pelagic interface | 5e-4 | $\mathrm{m}^2\ \mathrm{d}^{-1}$ | l |
| $\Delta_Z$ | Thickness of the boundary layer | 0.2 | m | a |
| $c_{DO}$ | DO-T coefficient | 20 | $\mathrm{mmolO\ K}^{-1}$ | c |
| $K_{\Upsilon,DO}$ | Half saturation for DO inhibition of denitrification | 10 | $\mathrm{mmolO\ m}^{-2}$ | 1 |
| $K_{\Upsilon,DIN}$ | Half saturation for DIN limitation of denitrification | 30 | $\mathrm{mmolO\ m}^{-2}$ | 1 |
| $c_{O:N}$ | Consumed oxygen per degraded nitrogen | 6.625 | $\mathrm{molO\ molN}^{-3}$ | a |
| $c_{N:O}$ | Denitrified N per consumed oxygen | 0.116 | $\mathrm{molN\ molO}^{-3}$ | 2 |
| $s_a$ | Scaling coefficient for DO-sorption relationship | 0.05 | $\mathrm{m}^3\ \mathrm{mmolC}^{-1}$ | c |
| bDO$^*$ | Critical benthic DO concentration for P-soprtion | 200 | $\mathrm{molO\ m}^{-3}$ | c |
| $Q10_b$ | Q10 coefficient for benthic reactions | 2.0 | - | l |

# Appendix B: Additional Analyses

## B1 Realism of Light Climate

Main driver of the spatio-temporal variations of the light climate in the southern North Sea is recognized to be the suspended particulate material (SPM) concentrations (e.g., Tian et al., 2009). In this study, light attenuation caused by SPM was provided as a 2-D forcing field of monthly climatologies (as required by GETM), which was extracted for 5 m depth from an original 3-D climatological (daily) dataset constructed by a statistical regression approach (Heath et al., 2002) and used in ECOHAM (e.g., Große et al., 2016). Here we aim to gain insight into the realism of the light climate represented by the model, in particular with respect to the turbidity caused by SPM, as the rest of the turbidity is mainly caused by the simulated variables, in particular phytoplankton, realism of which is discussed extensively in the main text (e.g., Fig. 8, 9, 12).

Along a transect following the model grid with a principal east-west axis, the qualitative pattern of the total attenuation estimated by the model at the surface layer agrees with that estimated by a satellite product, both averaged for 2008-2010 (Fig. B1), high towards the British coast at the western border, even higher at the German coast at the eastern border, and low in between. However, the variability in the attenuation estimated by the model is dampened than that by the satellite product, in particular, in the form of an overestimation of the offshore values. Some of this mismatch might be owed to the difference between the wavelengths at which the attenuation is provided by the model (average between 400-700 nm) and satellite product (490 nm), but this is not expected to be the major reason. Therefore, we conclude that the turbidity in the offshore regions is overestimated by the model. We further note that about 80% of the total attenuation at these offshore regions is due to SPM used as forcing (Fig. B1).

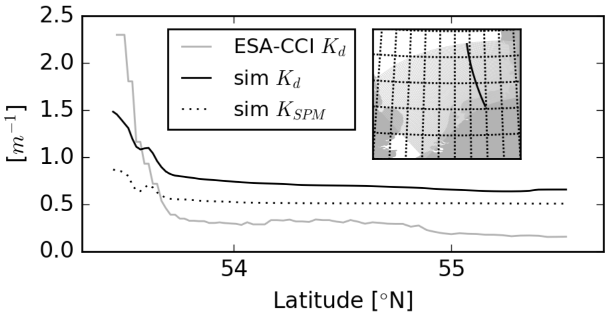

**Figure B1.** Total light attenuation along the transect shown in the inset as estimated by the satellite product (ESA-CCI $K_d$, solid gray line) and by the model at the surface layer (sim $K_d$, solid black line). Light attenuation caused only by SPM used as model forcing is shown separately (sim $K_{SPM}$, solid dotted line). All values represent averages between 2008-2010. The satellite estimates are from 490 nm wavelength and the model estimates represent the average within the PAR (400-700 nm) spectrum.

SPM concentrations, hence turbidity, within the regions located at the transition between the low-turbidity offshore waters to high-turbidity coastal waters (e.g., between 8-9 °E in Fig. B1,) display a considerable amount of sub-annual and inter-annual variability, driven by a combination of processes like riverine discharges, salinity fronts and sediment resuspension (e.g., Tian et al., 2009; S

This is exemplified by the SPM concentrations in 2008 and 2009 measured at the Noordwijk-10 station (Fig. B2). Such variations in SPM-caused turbidity are, by definition, not captured by the monthly climatology data, and in turn, leading to mismatches in the simulated phytoplankton, for instance in the form of timing errors (Fig.6).

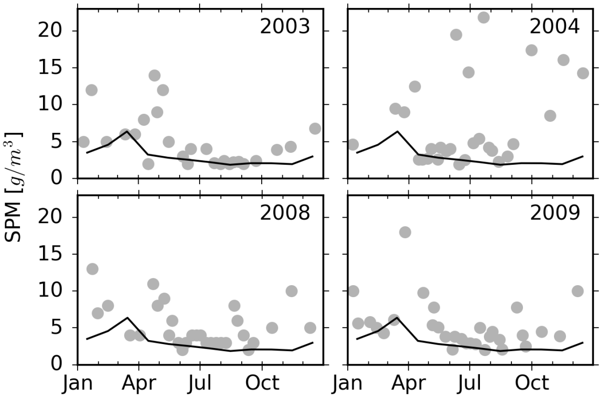

**Figure B2.** SPM concentrations measured (gray dots) and the monthly climatologies used as model forcing (black line) at Noordwijk-10 station (location shown in Fig. 6).

## B2 Phytoplankton Sinking Rates and Vertical Chlorophyll Profiles

Average phytoplankton sinking rates estimated by the model at the surface layers vary considerably across seasons, with higher sinking rates at the offshore areas during summer than in the rest of the year (Fig. B3). Sinking rates at the bottom layer are lower than at the surface, both during spring and summer (Fig. B3). These patterns are driven by the nutrient quota dependence of sinking rates (Eq. A25), and low nutrient quotas at the surface layers in the stratified offshore ares during summer (Fig. 10), caused by depletion of nutrients at the surface layers (Fig. 11). Because of the continuous supply of nutrients from the sediments, phytoplankton at the bottom layer maintain high nutrient quotas throughout the year, and have therefore lower sinking rates. Range of observed mean sinking rates (-0.92-1.14 m/d) in the Rhine ROFI (Peperzak et al., 2003) is roughly consistent with those estimated by the model. Estimated sinking rates being higher during summer than in spring, and at the surface than at the bottom layer seem to be also roughly consistent with the observations made at the Yangtze River estuary (Guo et al., 2016, Fig.6). However, both in the Yangzte River estuary and in the Rhine ROFI, some observations indicate higher sinking rates at the deeper layers during spring (Peperzak et al., 2003; Guo et al., 2016). This is explained by the species-specific differences in sinking rates (e.g., sinking rates of Diatoms being higher than Dinoflagellates and *Phaeocystis*), and differences in community composition at the surface (dominated by dinoflagellates or *Phaeocystis*) and bottom layers (dominated by diatoms), therefore, cannot be captured by the presented single species model.

The vertical distribution of chlorophyll qualitatively depends on the formulation of phytoplankton light availability, sinking and the resource utilization traits of phytoplankton. To demonstrate this, we considered alternative parameterizations regarding

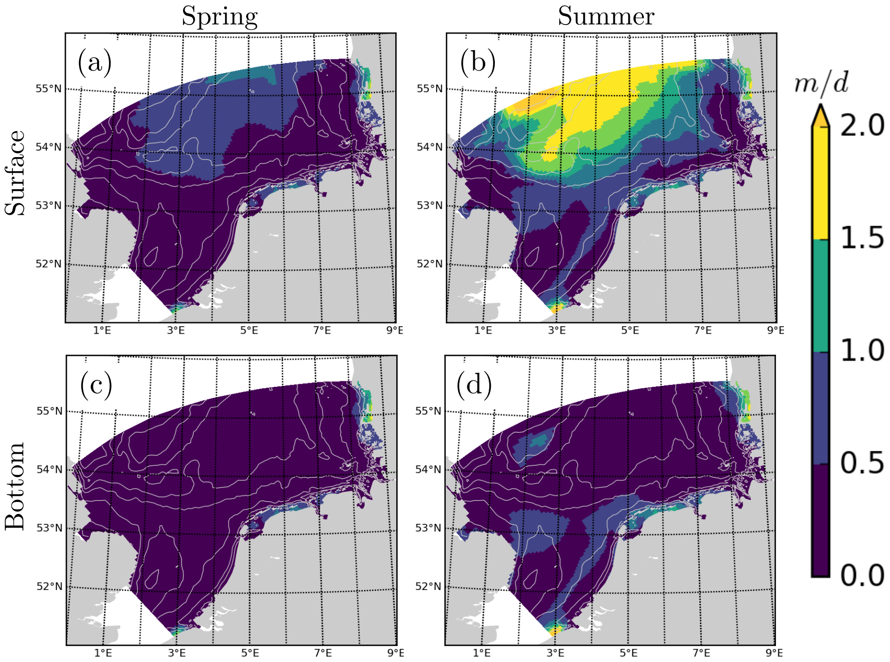

**Figure B3.** Phytoplankton sinking rates (a,b) at the surface layer and (c,d) at the bottom layer, averaged over spring (months 3-5, left) and summer (months 6-8, right) of 2010.

the sinking of phytoplankton and light climate and a non-acclimative model version where the physiology of phytoplankton is fixed (see section B3 for a detailed description), and compare the resulting chlorophyll profiles with the original (reference) model run for 3 example days and at a deep spot inside the German Bight (Fig. B4). The vicinity of this time interval and location (55°N, 5°E) was characterized by an occurrence of a thin chlorophyll layer according to the Scanfish data, as captured quite realistically by the reference run (Fig. 9).

The model run with constant and low sinking rate also resulted in deep chlorophyll maxima for the first 2 days (Fig. B4a), which is, however not concentrated at the thermocline as in the reference run (Fig. 9), but rather close to the surface with a wider vertical distribution, and on the third day a monotonic profile with the higher values homogeneously distributed within the upper mixed layer. The model with constant and high sinking rate on the other hand, resulted in profiles monotonically increasing towards the bottom, with overall low concentrations (Fig. B4a). The model run that assumed a spatially constant, low background attenuation values characteristic of clear ocean waters resulted in a sharp increase in chlorophyll concentrations at around 15 meters depth as in the case of the reference run (Fig. B4b), but then the concentrations do not decrease towards the bottom significantly, unlike in the case of the reference run. Higher specific attenuation coefficients resulted in distinct deep chlorophyll maxima in the first 2 days, although about 5 m closer to the surface, and on the 3rd day homogeneous distribution within the upper mixed layer, again unlike in the case of the reference run (Fig. B4b). Finally with the simplified model with fixed physiologies for two different parameterizations regarding the allocation to the light harvesting, nutrient acquisition and carboxylation machineries, phytoplankton ends up always being concentrated at the bottom layers (Fig. B4c).

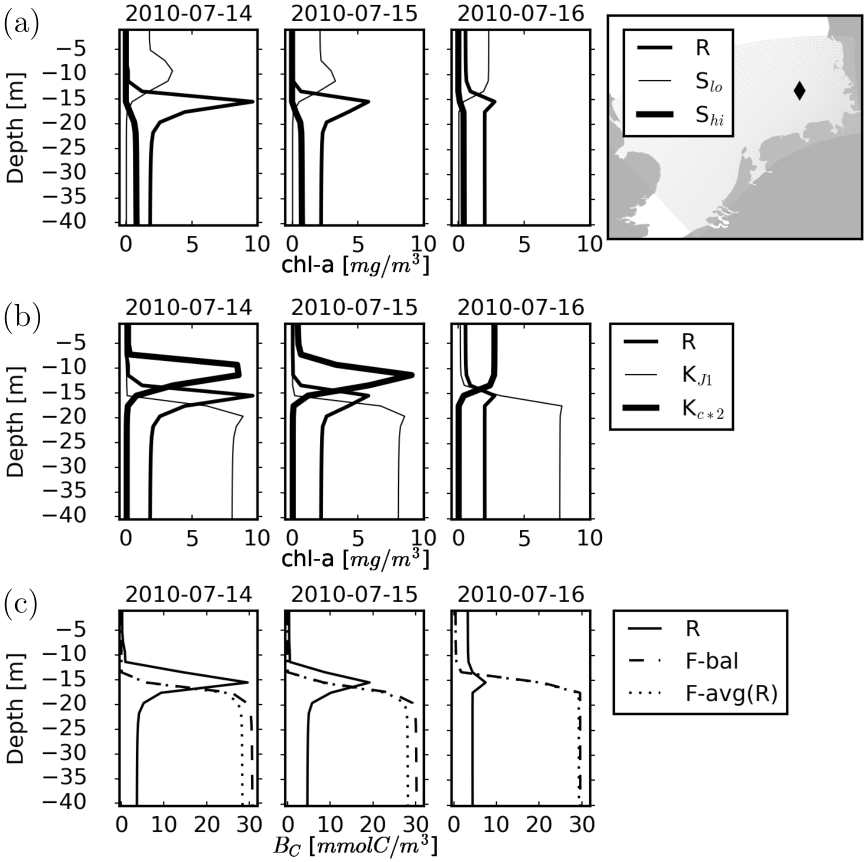

**Figure B4.** Vertical distribution of the simulated phytoplankton chlorophyll(a-b) and carbon (c) for 3 example days in July 2010 at an example spot (55°N, 5°E, shown with the diamond symbol in the inset map) for various model realizations, regarding; **a)** phytoplankton sinking, where R: the reference model (with $w_B^0$=0.2 and $w_B^*$= 3.0 m/d as in Table A3); $S_{lo}$ and $S_{hi}$: phytoplankton sinking rate set to constant ($w_B^*$= 0.0 m/d), and respectively, low ($w_B^0$=0.2) and high ($w_B^0$=3.0) values; **b)** the light climate, where R: the reference model with the light attenuation within the blue-green spectrum (as described by the length scale coefficient $eta_2$ in Eq.2) determined by a background SPM-caused turbidity used as model forcing (see section 2.2.3) and shading by the modeled variables (with specific attenuation coefficients listed in Table A3); $K_{J1}$: low attenuation achieved by setting a small (=23m) background value for $eta_2$ (characterizing clear-water conditions Paulson and Simpson, 1977) and keeping the specific attenuation coefficients as in R; $K_{c*2}$: high attenuation achieved by setting the specific attenuation coefficients twice their original values and keeping the SPM-caused turbidity as in R; **c)** resource utilization traits of phytoplankton, here as represented by R: the reference model with dynamic and optimal allocation of resource utilization traits; and two non-acclimative model versions (explained in Appendix B3 and shown in Fig.14) F-bal: balanced allocations to light harvesting, nutrient acquisition and carboxylation; and F-avg(R): allocation coefficients calculated as the spatio-temporal averages from the reference run.

### B3 Non-acclimative Model

For gaining insight into the relevance of acclimation aspects of the model, we considered a simplified version of the model in which the adaptive and optimality based features of the model were excluded. For transforming the full model to an otherwise equivalent non-acclimative version:

1. Dynamic equations Eq.A7-A8 that describe the allocation of resources to light harvesting ($f_{\mathrm{LH}}$), carboxylation ($f_{\mathrm{C}}$) and nutrient acquisition (1-$f_{\mathrm{LH}}$-$f_{\mathrm{C}}$) traits were excluded.
2. Instead of being optimized, $f_i^A$ was fixed to a constant value of 0.5, implying equal investments into affinity and intracellular transport.
3. Uptake activity function, $a_i$ was replaced with a classical linear function of individual cellular quotas ($a_i = \frac{Q_i - Q_i^0}{Q_i^{max} - Q_i^0}$).

In this simplified, fixed-trait model, $f_{\mathrm{LH}}$ and $f_{\mathrm{C}}$, which are dynamic state variables in the full model, become parameters. We considered two conceptual assumptions for assigning their values: 1) balanced allocations to each cellular machinery (referred to as 'F-bal' in Fig. 14 and Fig. B4c), achieved by setting $f_{\mathrm{LH}}$=$f_{\mathrm{C}}$=0.333 2) assigning the domain-wide, volume-weighted averages obtained with the acclimative model for a specific time period (referred to as 'F-avg(R)' in Fig. 14 and Fig. B4c), which were, for the year 2010 (for which the results are compared), $f_{\mathrm{LH}}$=0.38 and $f_{\mathrm{C}}$=0.24 for the year 2010. The further two parameters, namely the upper bounds of nitrogen and phosphorus quotas, were set to $Q_N^{max} = 0.35$ and $Q_P^{max} = 0.04$ such that the resulting range of N:C and P:C ratios are similar to those obtained with the full model for the year 2010, for which the results are compared.

*Author contributions.* OK and KW designed and outlined the study. OK calibrated the model, ran the simulations, performed the majority of analyses and drafted the manuscript. OK and RH created the model setup and prepared model forcing. KW, RH and OK developed the biogeochemical model and wrote the model code. RH and OK prepared the salinity cruise plot. RR planned and carried out the Scanfish measurements in the German Bight. RR, JM and RH handled the Scanfish data and contributed to the preperation of the Scanfish plot. JM developed a SPM climatology for a former model version. All authors participated in revising the manuscript.

*Acknowledgements.* We gratefully acknowledge Markus Schartau (Helmholtz Centre for Ocean Research Kiel) for his contributions to the initial development of MAECS, Carsten Lemmen (HZG) for his help with setting up the supercomputing environment, Sonja van Leeuwen (Centre for Environment, Fisheries and Aquaculture Science) for providing data on riverine fluxes, S~~"ø~~önke Hohn (Leibniz Centre for Tropical Marine Research) and Annika Eisele (HZG) for their assistance in formatting and checking the river data, Fabian Große (University of Hamburg -UH) and Markus Kreus (UH) for providing the boundary conditions for the biogeochemical model and Johannes Pätsch (UH) for providing the SPM climatology. Justus van Beusekom (based on his work in AWI, now HZG), Karen H. Wiltshire (AWI), Annika Grage (NLWKN), Thorkild Petenati (LLUR), Sieglinde Weigelt-Krenz (BSH) are acknowledged for providing monitoring data. Justus van Beusekom (HZG), Fabian Große (UH), Ivan Kuznetsov (HZG), Hermann-Josef Lenhart (UH) and Corinna Schrum (HZG) are acknowledged for their helpful comments during various stages of this work. This is a contribution by the Helmholtz Society through the PACES program. OK, RH and KW were supported by the German Federal Ministry of Education and Research (BMBF) throgh the MOSSCO project. OK and KW were additionally supported by the German Research Foundation (DFG) through the priority program 1704 Dynatrait. The authors gratefully acknowledge the computing time granted by the John von Neumann Institute for Computing (NIC) and provided on the supercomputer JURECA (Jülich Supercomputing Centre, 2016) at Jülich Supercomputing Centre. Comments by three anonymous referees helped significantly improving the paper.

# References

Alvarez-Fernandez, S. and Riegman, R.: Chlorophyll in North Sea coastal and offshore waters does not reflect long term trends of phytoplankton biomass, Journal of Sea Research, 91, 35–44, doi:10.1016/j.seares.2014.04.005, 2014.

Alvarez-Fernandez, S., Lindeboom, H., and Meesters, E.: Temporal changes in plankton of the North Sea: Community shifts and environmental drivers, Marine Ecology Progress Series, 462, 21–38, doi:10.3354/meps09817, 2012.

Amann, T., Weiss, A., and Hartmann, J.: Carbon dynamics in the freshwater part of the Elbe estuary, Germany: Implications of improving water quality, Estuarine, Coastal and Shelf Science, 107, 112–121, doi:10.1016/j.ecss.2012.05.012, 2012.

Arteaga, L., Pahlow, M., and Oschlies, A.: Global patterns of phytoplankton nutrient and light colimitation inferred from an optimality-based model, Global Biogeochemical Cycles, 28, 648–661, doi:10.1002/2013GB004668, 2014.

Baschek, B., Schroeder, F., Brix, H., Riethmüller, R., Badewien, T. H., Breitbach, G., Brügge, B., Colijn, F., Doerffer, R., Eschenbach, C., Friedrich, J., Fischer, P., Garthe, S., Horstmann, J., Krasemann, H., Metfies, K., Ohle, N., Petersen, W., Pröfrock, D., Röttgers, R., Schlüter, M., Schulz, J., Schulz-Stellenfleth, J., Stanev, E., Winter, C., Wirtz, K., Wollschläger, J., Zielinski, O., and Ziemer, F.: The Coastal Observing System for Northern and Arctic Seas (COSYNA), Ocean Science Discussions, pp. 1–73, doi:10.5194/os-2016-31, 2016.

Bauer, J. E., Cai, W.-J., Raymond, P. A., Bianchi, T. S., Hopkinson, C. S., and Regnier, P. A. G.: The changing carbon cycle of the coastal ocean., Nature, 504, 61–70, doi:10.1038/nature12857, 2013.

Beaugrand, G., Harlay, X., and Edwards, M.: Detecting plankton shifts in the North Sea: A new abrupt ecosystem shift between 1996 and 2003, Marine Ecology Progress Series, 502, 85–104, doi:10.3354/meps10693, 2014.

Becker, G., Dick, S., and Dippner, J.: Hydrography of the German Bight, Marine Ecology Progress Series, 91, 9–18, 1992.

Behrenfeld, M. J., O'Malley, R. T., Boss, E. S., Westberry, T. K., Graff, J. R., Halsey, K. H., Milligan, A. J., Siegel, D. A., and Brown, M. B.: Revaluating ocean warming impacts on global phytoplankton, Nature Climate Change, 6, 1–27, doi:10.1038/nclimate2838, 2015.

Bienfang, P. and Harrison, P.: CO-variation of sinking rate and cell quota among nutrient replete marine phytoplankton, Marine Ecology Progress Series, 14, 297–300, 1984.

Blackford, J., Allen, J., and Gilbert, F.: Ecosystem dynamics at six contrasting sites: a generic modelling study, Journal of Marine Systems, 52, 191–215, doi:10.1016/j.jmarsys.2004.02.004, 2004.

Bonachela, J. A., Allison, S. D., Martiny, A. C., and Levin, S. A.: A model for variable phytoplankton stoichiometry based on cell protein regulation, Biogeosciences, 10, 4341–4356, doi:10.5194/bg-10-4341-2013, 2013.

Bonachela, J. A., Klausmeier, C. A., Edwards, K. F., Litchman, E., and Levin, S. A.: The role of phytoplankton diversity in the emergent oceanic stoichiometry, Journal of Plankton Research, 38, 1021–1035, doi:10.1093/plankt/fbv087, 2016.

Boyd, C. and Gradmann, D.: Impact of osmolytes on buoyancy of marine phytoplankton, Marine Biology, 141, 605–618, doi:10.1007/s00227-002-0872-z, 2002.

Brockmann, U., Raabe, T., Hesse, K., Viehweger, K., Rick, S., Starke, A., Fabiszisky, B., Topçu, D., and Heller, R.: Seasonal budgets of the nutrient elements N and P at the surface of the German Bight during winter 1996, spring 1995, and summer 1994, Deutsche Hydrographische Zeitschrift, 51, 267–291, doi:10.1007/bf02764177, 1999.

Brockmann, U. H.: Organic matter in the Elbe estuary, Netherlands Journal of Aquatic Ecology, 28, 371–381, doi:10.1007/BF02334207, 1994.

Bruggeman, J. and Bolding, K.: A general framework for aquatic biogeochemical models, Environmental Modelling & Software, 61, 249–265, doi:10.1016/j.envsoft.2014.04.002, 2014.

Burchard, H. and Bolding, K.: GETM: A general estuarine transport model, Tech. rep., Joint Research Centre, Ispra, Italy, 2002.

Burchard, H., Bolding, K., Kühn, W., Meister, A., Neumann, T., and Umlauf, L.: Description of a flexible and extendable physical-biogeochemical model system for the water column, Journal of Marine Systems, 61, 180–211, doi:10.1016/j.jmarsys.2005.04.011, 2006.

Burchard, H., Flöser, G., Staneva, J. V., Badewien, T. H., and Riethmüller, R.: Impact of Density Gradients on Net Sediment Transport into the Wadden Sea, Journal of Physical Oceanography, 38, 566–587, doi:10.1175/2007JPO3796.1, 2008.

Burson, A., Stomp, M., Akil, L., Brussaard, C. P. D., and Huisman, J.: Unbalanced reduction of nutrient loads has created an offshore gradient from phosphorus to nitrogen limitation in the North Sea, Limnology and Oceanography, 61, 869–888, doi:10.1002/lno.10257, 2016.

Chakraborty, S., Nielsen, L., and Andersen, K. H.: Trophic strategies of unicellular plankton, American Naturalist, 189, doi:10.1086/690764, 2017.

Chan, A.: Comparative physiological study of marine diatoms and dinoflagellates in relation to irradiance and cell size. II. Relationship between photosynthesis, growth and carbon/chlorophyll a Ratio, Journal of Phycology, 16, 428–432, 1980.

Ciavatta, S., Kay, S., Saux-Picart, S., Butenschön, M., and Allen, J.: Decadal reanalysis of biogeochemical indicators and fluxes in the North West European shelf-sea ecosystem, Journal of Geophysical Research: Oceans, 121, 1824–1845, doi:10.1002/2015JC011496, 2016.

Cloern, J. E., Foster, S. Q., and Kleckner, A. E.: Phytoplankton primary production in the world's estuarine-coastal ecosystems, Biogeosciences, 11, 2477–2501, doi:10.5194/bg-11-2477-2014, 2014.

Daewel, U. and Schrum, C.: Simulating long-term dynamics of the coupled North Sea and Baltic Sea ecosystem with ECOSMO II: Model description and validation, Journal of Marine Systems, 119-120, 30–49, doi:10.1016/j.jmarsys.2013.03.008, 2013.

Dähnke, K., Bahlmann, E., and Emeis, K.: A nitrate sink in estuaries? An assessment by means of stable nitrate isotopes in the Elbe estuary, Limnology and Oceanography, 53, 1504–1511, doi:10.4319/lo.2008.53.4.1504, 2008.

Daines, S. J., Clark, J. R., and Lenton, T. M.: Multiple environmental controls on phytoplankton growth strategies determine adaptive responses of the N : P ratio, Ecology Letters, 17, 414–425, doi:10.1111/ele.12239, 2014.

de Mora, L., Butenschön, M., and I., A. J.: How should sparse marine in situ measurements be compared to a continuous model: an example, Geoscientific Model Development, 6, 533–548, doi:10.5194/gmd-6-533-2013, 2013.

Durham, W. M. and Stocker, R.: Thin phytoplankton layers: characteristics, mechanisms, and consequences, Annual Review of Marine Science, 4, 177–207, doi:10.1146/annurev-marine-120710-100957, 2012.

Ebenhöh, W.: Shallowness may be a major factor generating nutrient gradients in the Wadden Sea, Ecological Modelling, 174, 241–252, doi:10.1016/j.ecolmodel.2003.07.011, 2004.

Edwards, K. P., Barciela, R., and Butenschön, M.: Validation of the NEMO-ERSEM operational ecosystem model for the North West European Continental Shelf, Ocean Science, 8, 983–1000, doi:10.5194/os-8-983-2012, 2012.

Emeis, K. C., van Beusekom, J., Callies, U., Ebinghaus, R., Kannen, A., Kraus, G., Kröncke, I., Lenhart, H., Lorkowski, I., Matthias, V., Möllmann, C., Pätsch, J., Scharfe, M., Thomas, H., Weisse, R., and Zorita, E.: The North Sea - A shelf sea in the Anthropocene, Journal of Marine Systems, 141, 18–33, doi:10.1016/j.jmarsys.2014.03.012, 2015.

Fennel, K.: The role of continental shelves in nitrogen and carbon cycling: Northwestern North Atlantic case study, Ocean Science, 6, 539–548, doi:10.5194/os-6-539-2010, 2010.

Fennel, K., Wilkin, J., Levin, J., Moisan, J., O'Reilly, J., and Haidvogel, D.: Nitrogen cycling in the Middle Atlantic Bight: Results from a three-dimensional model and implications for the North Atlantic nitrogen budget, Global Biogeochemical Cycles, 20, 1–14, doi:10.1029/2005GB002456, 2006.

Fernand, L., Weston, K., Morris, T., Greenwood, N., Brown, J., and Jickells, T.: The contribution of the deep chlorophyll maximum to primary production in a seasonally stratified shelf sea, the North Sea, Biogeochemistry, 113, 153–166, doi:10.1007/s10533-013-9831-7, 2013.

Flöser, G., Burchard, H., and Riethmüller, R.: Observational evidence for estuarine circulation in the German Wadden Sea, Continental Shelf Research, 31, 1633–1639, doi:http://dx.doi.org/10.1016/j.csr.2011.03.014, 2011.

Ford, D. A., van der Molen, J., Hyder, K., Bacon, J., Barciela, R., Creach, V., McEwan, R., Ruardij, P., and Forster, R.: Observing and modelling phytoplankton community structure in the North Sea: can ERSEM-type models simulate biodiversity?, Biogeosciences, 14, 1419–1444, doi:10.5194/bg-2016-304, http://www.biogeosciences-discuss.net/bg-2016-304/, 2017.

Freund, J. A., Grüner, N., Brüse, S., and Wiltshire, K. H.: Changes in the phytoplankton community at Helgoland, North Sea: lessons from single spot time series analyses, Marine Biology, 159, 2561–2571, doi:10.1007/s00227-012-2013-7, 2012.

Friedrichs, M. A. M., Dusenberry, J. A., Anderson, L. A., Armstrong, R. A., Chai, F., Christian, J. R., Doney, S. C., Dunne, J., Fujii, M., Hood, R., Moore, J. K., Schartau, M., Spitz, Y. H., and Wiggert, J. D.: Assessment of skill and portability in regional marine biogeochemical models: Role of multiple planktonic groups, Journal of Geophysical Research, 112, C08 001, doi:10.1029/2006JC003852, 2007.

Geider, R., MacIntyre, H., and Kana, T.: Dynamic model of phytoplankton growth and acclimation: responses of the balanced growth rate and the chlorophyll a:carbon ratio to light, nutrient-limitation and temperature, Marine Ecology Progress Series, 148, 187–200, 1997.

Geyer, B.: High-resolution atmospheric reconstruction for Europe 1948–2012: coastDat2, Earth System Science Data, 6, 147–164, doi:doi:10.5194/essd-6-147-2014, 2014.

Grant, M., Jackson, T., Chuprin, A., Sathyendranath, S., Zühlke, M., Dingle, J., Storm, T., Boettcher, M., and Fomferra, N.: OC-CCI v2.0 Product User Guide 2.0.5, Tech. rep., European Space Agency, Frascati, Italy, 2015.

Grant, M., Jackson, T., Chuprin, A., Sathyendranath, S., Zühlke, M., Dingle, J., Storm, T., Boettcher, M., and Fomferra, N.: Product user guide, Ocean Color Climate Change Initiative (OC_CCI)—Phase two, Tech. Rep. D3.4 PUG 3.1.0, Tech. rep., European Space Agency, Frascati, Italy, 2017.

Gräwe, U., Flöser, G., Gerkema, T., Duran-Matute, M., Badewien, T., Schulz, E., and Burchard, H.: A numerical model for the entire Wadden Sea: skill assessment and analysis of hydrodynamics, Journal of Geophysical Research: Oceans, 121, 5231–2551, doi:10.1002/2016JC011655, 2016.

Greve, W., Reiners, F., Nast, J., and Hoffmann, S.: Helgoland Roads meso- and macrozooplankton time-series 1974 to 2004: lessons from 30 years of single spot, high frequency sampling at the only off-shore island of the North Sea, Helgoland Marine Research, 58, 274–288, doi:10.1007/s10152-004-0191-5, 2004.

Gröger, M., Maier-Reimer, E., Mikolajewicz, U., Moll, A., and Sein, D.: NW European shelf under climate warming: implications for open ocean – shelf exchange, primary production, and carbon absorption, Biogeosciences, 10, 3767–3792, doi:10.5194/bg-10-3767-2013, 2013.

Große, F., Greenwood, N., Kreus, M., Lenhart, H. J., Machoczek, D., Pätsch, J., Salt, L. A., and Thomas, H.: Looking beyond stratification: a model-based analysis of the biological drivers of oxygen depletion in the North Sea, Biogeosciences, 13, 2511–2535, doi:10.5194/bgd-12-12543-2015, 2016.

Grunwald, M., Dellwig, O., Kohlmeier, C., Kowalski, N., Beck, M., Badewien, T. H., Kotzur, S., Liebezeit, G., and Brumsack, H.-J.: Nutrient dynamics in a back barrier tidal basin of the Southern North Sea: Time-series, model simulations, and budget estimates, Journal of Sea Research, 64, 199–212, doi:10.1016/j.seares.2010.02.008, 2010.

Guo, S., Sun, J., Zhao, Q., Feng, Y., Huang, D., and Liu, S.: Sinking rates of phytoplankton in the Changjiang (Yangtze River) estuary: A comparative study between *Prorocentrum dentatum* and *Skeletonema dorhnii* bloom, Journal of Marine Systems, 154, 5–14, doi:10.1016/j.jmarsys.2015.07.003, http://dx.doi.org/10.1016/j.jmarsys.2015.07.003, 2016.

Hansen, P., Bjørnsen, P., and Hansen, B.: Zooplankton grazing and growth: Scaling within the 2-2,000 $\mu$m body size range, Limnology and Oceanography, 42, 687–704, 1997.

Heath, M. R., Edwards, A. C., Patsch, J., and Turrell, W.: Modelling the behaviour of nutrient in the coastal waters of Scotland, Tech. rep., Scottish Executive Central Research Unit,, Edinburgh, 2002.

Hetzel, Y., Pattiaratchi, C., Lowe, R., and Hofmeister, R.: Wind and tidal mixing controls on stratification and dense water outflows in a large hypersaline bay, Journal of Geophysical Research: Oceans, 120, 6034–6056, doi:10.1002/2015JC010733, 2015.

Hofmeister, R., Bolding, K., Hetland, R. D., Schernewski, G., Siegel, H., and Burchard, H.: The dynamics of cooling water discharge in a shallow, non-tidal embayment, Continental Shelf Research, 71, 68–77, doi:10.1016/j.csr.2013.10.006, 2013.

Hofmeister, R., Flöser, G., and Schartau, M.: Estuary-type circulation as a factor sustaining horizontal nutrient gradients in freshwater-influenced coastal systems, Geo-Marine Letters, doi:10.1007/s00367-016-0469-z, 2016.

Holt, J. and Umlauf, L.: Modelling the tidal mixing fronts and seasonal stratification of the Northwest European Continental shelf, Continental Shelf Research, 28, 887–903, doi:10.1016/j.csr.2008.01.012, 2008.

Hydes, D. J., Gall, A. C. L., and Proctor, R.: The balance of supply of nutrients and demands of biological production and denitrification in a temperate latitude shelf sea — a treatment of the southern North Sea as an extended estuary, Marine Chemistry, 68, 117–131, 1999.

Hydes, D. J., Gowen, R. J., Holliday, N. P., Shammon, T., and Mills, D.: External and internal control of winter concentrations of nutrients (N, P and Si) in north-west European shelf seas, Estuarine, Coastal and Shelf Science, 59, 151–161, doi:10.1016/j.ecss.2003.08.004, 2004.

Jensen, H. S., Mortensen, P. B., Andersen, F. O., Rasmussen, E., and Jensen, A.: Phosphorus cycling in a coastal marine sediment, Aarhus Bay, Denmark, Limnology and Oceanography, 40, 908–917, 1995.

Jolliff, J., Kindle, J., Shulman, I., Penta, B., Friedrichs, M., Helber, R., and Arnone, R.: Summary diagrams for coupled hydrodynamic-ecosystem model skill assessment, Journal of Marine Systems, 76, 64–82, doi:10.1016/j.jmarsys.2008.05.014, 2009.

Jülich Supercomputing Centre: JURECA: General-purpose supercomputer at Jülich Supercomputing Centre, Journal of large-scale research facilities, 2, doi:10.17815/jlsrf-2-121, 2016.

Kiørboe, T.: How zooplankton feed: mechanisms, traits and trade-offs., Biological Reviews of the Cambridge Philosophical Society, 86, 311–39, doi:10.1111/j.1469-185X.2010.00148.x, http://www.ncbi.nlm.nih.gov/pubmed/20682007, 2011.

Klausmeier, C., Litchman, E., Daufresne, T., and Levin, S.: Optimal nitrogen-to-phosphorus stoichiometry of phytoplankton, Nature, 429, 171–174, doi:1.1029/2001GL014649, 2004.

Lemmen, C., Hofmeister, R., Klingbeil, K., Nasermoaddeli, M. H., Kerimoglu, O., Burchard, H., K?sters, F., and Wirtz, K. W.: Modular System for Shelves and Coasts (MOSSCO v1.0) - a flexible and multi-component framework for coupled coastal ocean ecosystem modelling, Geoscientific Model Development Discussions, 138, 30, doi:10.5194/gmd-2017-138, http://arxiv.org/abs/1706.04224http://www.geosci-model-dev-discuss.net/gmd-2017-138/, 2017.

Litchman, E., Pinto, P. D. T., Klausmeier, C. A., Thomas, M. K., and Yoshiyama, K.: Linking traits to species diversity and community structure in phytoplankton, Hydrolobiologia, 653, 15–28, doi:10.1007/s10750-010-0341-5, 2010.

Llewellyn, C. A., Fishwick, J. R., and Blackford, J. C.: Phytoplankton community assemblage in the English Channel : a comparison using chlorophyll a derived from HPLC-CHEMTAX and carbon derived from microscopy cell counts, Journal of Plankton Research, 27, 103–119, doi:10.1093/plankt/fbh158, 2005.

Löder, M., Kraberg, A., Aberle, N., Peters, S., and Wiltshire, K.: Dinoflagellates and ciliates at Helgoland Roads, North Sea, Helgoland Marine Research, 66, 11–23, doi:10.1007/s10152-010-0242-z, 2012.

Loebl, M., Dolch, T., and van Beusekom, J. E. E.: Annual dynamics of pelagic primary production and respiration in a shallow coastal basin, Journal of Sea Research, 58, 269 – 282, doi:10.1016/j.seares.2007.06.003, 2007.

Loebl, M., Colijn, F., van Beusekom, J. E. E., Baretta-Bekker, J. G., Lancelot, C., Philippart, C. J. M., Rousseau, V., and Wiltshire, K. H.: Recent patterns in potential phytoplankton limitation along the Northwest European continental coast, Journal of Sea Research, 61, 34–43, doi:10.1016/j.seares.2008.10.002, 2009.

Los, F. J., Villars, M. T., and van der Tol, M. W. M.: A 3-dimensional primary production model (BLOOM/GEM) and its applications to the (southern) North Sea (coupled physical–chemical–ecological model), Journal of Marine Systems, 74, 259–294, doi:10.1016/j.jmarsys.2008.01.002, 2008.

Maar, M., Rindorf, A., Møller, E. F., Christensen, A., Madsen, K. S., and van Deurs, M.: Zooplankton mortality in 3D ecosystem modelling considering variable spatial–temporal fish consumptions in the North Sea, Progress in Oceanography, 124, 78–91, doi:10.1016/j.pocean.2014.03.002, 2014.

Maerz, J., Verney, R., Wirtz, K. W., and Feudel, U.: Modeling flocculation processes: Intercomparison of a size class-based model and a distribution-based model, Continental Shelf Research, 31, 84–93, doi:10.1016/j.csr.2010.05.011, 2011.

Maerz, J., Hofmeister, R., van der Lee, E. M., Gräwe, U., Riethmüller, R., and Wirtz, K. W.: Maximum sinking velocities of suspended particulate matter in a coastal transition zone, Biogeosciences, 13, 4863–4876, doi:10.5194/bg-13-4863-2016, 2016.

Meyer, E. M., Pohlmann, T., and Weisse, R.: Thermodynamic variability and change in the North Sea (1948–2007) derived from a multidecadal hindcast, Journal of Marine Systems, 86, 35–44, doi:10.1016/j.jmarsys.2011.02.001, 2011.

Morel, F.: Kinetics of nutrient uptake and growth in phytoplankton, Journal of Phycology, 23, 137–150, 1987.

Oubelkheir, K., Sciandra, A., and Babin, M.: Bio-optical and biogeochemical properties of different trophic regimes in oceanic waters, Limnology and Oceanography, 50, 1795–1809, 2005.

Pahlow, M.: Linking chlorophyll – nutrient dynamics to the Redfield N : C ratio with a model of optimal phytoplankton growth, Marine Ecology Progress Series, 287, 33–43, 2005.

Pahlow, M. and Oschlies, A.: Chain model of phytoplankton P, N and light colimitation, Marine Ecology Progress Series, 376, 69–83, doi:10.3354/meps07748, 2009.

Pätsch, J. and Kühn, W.: Nitrogen and carbon cycling in the North Sea and exchange with the North Atlantic—A model study. Part I. Nitrogen budget and fluxes, Continental Shelf Research, 28, 767–787, doi:10.1016/j.csr.2007.12.013, 2008.

Pätsch, J. and Lenhart, H.: Daily Loads of Nutrients, Total Alkalinity, Dissolved Inorganic Carbon and Dissolved Organic Carbon of the European Continental Rivers for the Years 1977-2009, Tech. rep., 2011.

Paulson, C. and Simpson, J.: Irradience measurements in the upper ocean, Journal of Physical Oceanography, 7, 952–956, 1977.

Peperzak, L., Coljin, F., Gieskes, W., and JCH, P.: Development of the diatom-Phaeocystis spring bloom in the Dutch coastal zone of the North Sea: the silicon depletion versus the daily irradiance threshold hypothesis, Journal of Plankton Research, 20, 517–537, 1998.

Peperzak, L., Coljin, F., Koeman, F., Gieskes, W., and Joordens, J.: Phytoplankton sinking rates in the Rhine region of freshwater influence, Journal of Plankton Research, 25, 365–383, 2003.

Petersen, W.: FerryBox systems: State-of-the-art in Europe and future development, Journal of Marine Systems, 140, 4–12, doi:10.1016/j.jmarsys.2014.07.003, 2014.

Postma, H.: Transport and accumulation of suspended matter in the Dutch Wadden Sea, Netherlands Journal of Sea Research, 1, 148–180, doi:10.1016/0077-7579(61)90004-7, 1961.

Puls, W., Heinrich, H., and Mayerj, B.: Suspended Particulate Matter Budget for the German Bight, Marine Pollution Bulletin, 34, 398–409, 1997.

Radach, G. and Moll, A.: Review of three-dimensional ecological modeling related to the North Sea shelf system. Part II: Model validation and data needs, Oceanography and Marine Biology, Annual Review, 44, 1–60, 2006.

Radach, G. and Pätsch, J.: Variability of Continental Riverine Freshwater and Nutrient Inputs into the North Sea for the Years 1977 – 2000 and Its Consequences for the Assessment of Eutrophication, Estuaries and Coasts, 30, 66–81, 2007.

Riegman, R., Kuipers, B. R., Noordeloos, A. A. M., and Witte, H. J.: Size-differential control of phytoplankton and the structure of plankton communities*, Control, 31, 255–265, 1993.

Schartau, M., Engel, A., Schröter, J., Thoms, S., Völker, C., and Wolf-Gladrow, D.: Modelling carbon overconsumption and the formation of extracellular particulate organic carbon, Biogeosciences, 4, 13–67, doi:10.5194/bgd-4-13-2007, 2007.

Schrum, C., Siegismund, F., and St. John, M.: Decadal variations in the stratification and circulation patterns of the North Sea. Are the 1990s unusual?, ICES Marine Science Symposia, 219, 121–131, 2003.

Seitzinger, S. P. and Giblin, A. E.: Estimating denitrification in North Atlantic continental shelf sediments, Biogeochemistry, 35, 235–260, 1996.

Simpson, J., Brown, J., Matthews, J., and Allen, G.: Tidal Straining, Density Currents, and Stirring in the Control of Estuarine Stratification, Estuaries, 13, 125–132, 1990.

Simpson, J., Bos, W., Schirmer, F., Souza, A., Rippeth, T., Jones, S., and Hydes, D.: Periodic stratification in the Rhine ROFI in the North Sea, Oceanologica Acta, 16, 23–32, 1993.

Skogen, M. D. and Mathisen, L. R.: Long-term effects of reduced nutrient inputs to the North Sea, Estuarine, Coastal and Shelf Science, 82, 433–442, doi:10.1016/j.ecss.2009.02.006, http://dx.doi.org/10.1016/j.ecss.2009.02.006, 2009.

Smayda, T. J. and Boleyn, B. J.: Experimental observations on the flotation of marine diatoms. 1. *Thalassiosira cf. nana*, *Thalassiosira rotula* and *Nitzchia seriata*, Limnology and Oceanography, 10, 499–509, doi:10.4319/lo.1965.10.4.0499, 1965.

Smith, S. L., Yamanaka, Y., Pahlow, M., and Oschlies, A.: Optimal uptake kinetics: physiological acclimation explains the pattern of nitrate uptake by phytoplankton in the ocean, Marine Ecology Progress Series, 384, 1–12, doi:10.3354/meps08022, 2009.

Smith, S. L., Pahlow, M., Merico, A., and Wirtz, K. W.: Optimality-based modeling of planktonic organisms, Limnology and Oceanography, 56, 2080–2094, doi:10.4319/lo.2011.56.6.2080, 2011.

Soetaert, K., J., H. P. M., and Middelburg, J. J.: A model of early diagenetic processes from the shelf to abyssal depths, Geochimica et Cosmochimica Acta, 60, 1019–1040, 1996.

Stedmon, C., Markager, S., and Kaas, H.: The optics of chromophoric dissolved organic matter (CDOM) in the Greenland Sea: An algorithm for differentiation between marine and terrestrially derived organic matter, Limnology and Oceanography, 46, 2087–2093, 2001.

Sterner, R. and Elser, J.: Ecological stoichiometry: The biology of elements from molecules to the biosphere, Princeton University Press, Princeton, NJ, 2002.

Stips, A., Bolding, K., Pohlmann, T., and Burchard, H.: Simulating the temporal and spatial dynamics of the North Sea using the new model GETM (general estuarine transport model), Ocean Dynamics, 54, 266–283, doi:10.1007/s10236-003-0077-0, 2004.

Su, J., Tian, T., Krasemann, H., Schartau, M., and Wirtz, K.: Response patterns of phytoplankton growth to variations in resuspension in the German Bight revealed by daily MERIS data in 2003 and 2004, Oceanologia, 57, 328–341, doi:10.1016/j.oceano.2015.06.001, 2015.

Tian, T., Merico, A., Su, J., Staneva, J., Wiltshire, K. H., and Wirtz, K. W.: Importance of resuspended sediment dynamics for the phytoplankton spring bloom in a coastal marine ecosystem, Journal of Sea Research, 62, 214–228, 2009.

van Beusekom, J., Brockmann, U., Hesse, K.-J., Hickel, W., Poremba, K., and Tillmann, U.: The importance of sediments in the transformation and turnover of nutrients and organic matter in the Wadden Sea and German Bight, Deutsche Hydrographische Zeitschrift, 51, 245–266, doi:10.1007/BF02764176, 1999.

van Beusekom, J. E. and de Jonge, V. N.: Long-term changes in Wadden Sea nutrient cycles: importance of organic matter import from the North Sea, Hydrobiologia, 475/476, 185–194, 2002.

van Beusekom, J. E., Loebl, M., and Martens, P.: Distant riverine nutrient supply and local temperature drive the long-term phytoplankton development in a temperate coastal basin, Journal of Sea Research, 61, 26–33, doi:10.1016/j.seares.2008.06.005, 2009.

van der Molen, J., Ruardij, P., and Greenwood, N.: Potential environmental impact of tidal energy extraction in the Pentland Firth at large spatial scales: results of a biogeochemical model, Biogeosciences, 13, 2593–2609, doi:10.5194/bg-13-2593-2016, 2016.

van Leeuwen, S., Tett, P., Mills, D., and van der Molen, J.: Stratified and nonstratified areas in the North Sea: Long-term variability and biological and policy implications Sonja, Journal of Geophysical Research: Oceans, 120, 4670–4686, doi:10.1002/2014JC010485, 2015.

van Leeuwen, S. M., van der Molen, J., Ruardij, P., Fernand, L., and Jickells, T.: Modelling the contribution of deep chlorophyll maxima to annual primary production in the North Sea, Biogeochemistry, 113, 137–152, doi:10.1007/s10533-012-9704-5, 2013.

Vichi, M., Pinardi, N., and Masina, S.: A generalized model of pelagic biogeochemistry for the global ocean ecosystem. Part I: Theory, Journal of Marine Systems, 64, 89–109, doi:10.1016/j.jmarsys.2006.03.006, 2007.

Weisse, R., Bisling, P., Gaslikova, L., Geyer, B., Groll, N., Hortamani, M., Matthias, V., Maneke, M., Meinke, I., Meyer, E. M. I., Schwichtenberg, F., Stempinski, F., Wiese, F., and Wöckner-Kluwe, K.: Climate services for marine applications in Europe, Earth Perspectives, 2, 1–14, doi:10.1186/s40322-015-0029-0, 2015.

Weston, K., Fernand, L., Mills, D. K., Delahunty, R., and Brown, J.: Primary production in the deep chlorophyll maximum of the central North Sea, Journal of Plankton Research, 27, 909–922, doi:10.1093/plankt/fbi064, 2005.

Wiltshire, K. H., Malzahn, A. M., Wirtz, K. W., Greve, W., Janisch, S., Mangelsdorf, P., Manly, B. F. J., and Boersma, M.: Resilience of North Sea phytoplankton spring bloom dynamics: An analysis of long-term data at Helgoland Roads, Limnology and Oceanography, 53, 1294–1302, doi:10.4319/lo.2008.53.4.1294, 2008.

Wiltshire, K. H., Kraberg, A., Bartsch, I., Boersma, M., Franke, H.-D., Freund, J., Gebühr, C., Gerdts, G., Stockmann, K., and Wichels, A.: Helgoland Roads, North Sea: 45 Years of Change, Estuaries and Coasts, 33, 295–310, doi:10.1007/s12237-009-9228-y, 2010.

Wirtz, K. W. and Kerimoglu, O.: Optimality and variable co-limitation controls autotrophic stoichiometry, Frontiers in Ecology and Evolution, doi:10.3389/fevo.2016.00131, 2016.

Wirtz, K. W. and Pahlow, M.: Dynamic chlorophyll and nitrogen:carbon regulation in algae optimizes instantaneous growth rate, Marine Ecology Progress Series, 402, 81–96, doi:10.3354/meps08333, 2010.

Wollschläger, J., Wiltshire, K. H., Petersen, W., and Metfies, K.: Analysis of phytoplankton distribution and community structure in the German Bight with respect to the different size classes, Journal of Sea Research, 99, 83–96, doi:10.1016/j.seares.2015.02.005, 2015.